Title
Gene expression of cell types present in the vascular wall during the initiation and progression of atherosclerosis

Author
Erbilgin, Ayca

Publication Date
2012

Peer reviewed|Thesis/dissertation

UNIVERSITY OF CALIFORNIA

Los Angeles

Gene expression of cell types present in the vascular wall during the initiation and progression of atherosclerosis

A dissertation submitted in partial satisfaction of the requirements for the degree Doctor of Philosophy in Microbiology, Immunology, and Molecular Genetics

by

Ayca Erbilgin

2012

ABSTRACT OF THE DISSERTATION

Gene expression of cell types present in the vascular wall during the initiation and progression of atherosclerosis

by

Ayca Erbilgin

Doctor of Philosophy in Microbiology, Immunology, and Molecular Genetics

University of California, Los Angeles, 2012

Professor Aldons J. Lusis, Chair

A key element of atherosclerosis, the primary cause of coronary artery disease (CAD), is chronic inflammation of the vessel wall. Identifying the gene expression of the cells present in the vessel wall during atherogenesis can clarify these events and provide new research possibilities. The work presented here characterizes a putative transcription factor that contributes to atherosclerosis, identifies candidate genes involved in the activation of endothelial cells, and defines the expression patterns of CAD GWAS candidate genes in mouse vascular cells.

Zhx2, a putative transcription factor, was identified as a gene controlling plasma lipid levels using congenic mice and fine-mapping. Liver-specific Zhx2 transgenic mice on a Zhx-null background exhibited a corrected plasma lipid profile, confirming Zhx2 as the gene controlling the plasma lipid phenotype. Male Zhx2-null mice had

atherosclerotic lesions nine times smaller than mice with a wild-type Zhx2 allele, a large effect that could not be fully explained by their plasma lipid profiles. Treatment of macrophages with the pro-inflammatory factor LPS elicited a strong increase in Zhx2 transcript, suggesting involvement in the inflammatory response. A bone marrow transplant of Zhx2-null hematopoietic stem cells into Zhx2 wild-type mice resulted in a more than 4-fold reduction in atherosclerotic lesion size, supporting a role for Zhx2 in the chronic immune response accompanying atherosclerosis.

Endothelial cells are a central component in the initiation and progression of atherosclerosis, and the study of their expression profile could provide valuable data. Since the cell culture of mouse aortic endothelial cells (MAECs) has been challenging, we identified an alternate method for the isolation of RNA from these cells. Microarray analysis of these transcripts identified 14 differentially expressed genes in pre-lesioned MAECs, eight of which have not been previously described in atherosclerosis. This method has also made it feasible to collect RNA samples from distinct cell types present in the vessel wall during atherosclerosis. Recent genome wide association studies on CAD have identified loci representing 56 candidate genes. We used quantitative PCR to identify the expression levels of these genes in each atherosclerotic cell type and report the results.

The dissertation of Ayca Erbilgin is approved.

Judith A Berliner

Kenneth Alan Bradley

Genhong Cheng

Aldons J Lusis, Committee Chair

University of California, Los Angeles

2012

My dissertation is dedicated to

my grandfather Ibrahim, who devoted his life to education

my grandmother Hayriye, who sacrificed for future generations

my brother Onur, who keeps me to the highest standard

my father Bulent, who gave me the love of learning

my mother Suheyla, who taught me to love myself

my husband Emrah, who supports me in all my ambitions

Bu doktora tezini:

hayatını eğitime adamış Dedem İbrahim Erbilgin'e;

çocuklarının geleceği için çekinmeden yaptığı fedakarliklar için Anneannem Hayriye Yücetürk'e

bana en üstün değleri hatırlatan kardeşim Onur Erbilgin'e

bana oğrenme aşkını asilayan Babam Bülent Erbilgin'e

kendim ile barişik olmayı oğreten Annem Süheyla Yücetürk'e

Hedeflerime ulaşmamda bana herzaman destek olan eşim Emrah Köstem'e adıyorum...

and

my teachers

I-Heng McComb

Dr Robert Goldberg

Dr Judith Berliner

Dr Jake Lusis

without whom I could not have come this far

TABLE OF CONTENTS

Abstract of the Dissertation	ii
Dedication	v
List of Figures	viii
List of Tables	xi
Acknowledgements	xiii
Vita	xv
Publications	xvi
Chapter 1. Introduction	1
References	9
Chapter 2. Identification of Zhx2 as a novel regulator of plasma lipid metabolism	13
References	20

Chapter 3. The role of Zhx2 in atherosclerosis 22

References 63

Chapter 4. Genomic analysis of atherosclerosis initiation

in the major vascular cell types in mice 68

References 112

Chapter 5. Concluding Remarks 119

References 126

LIST OF FIGURES

Chapter 2

Figure 2-1. Genotypes and phenotypes of subcongenic strains 16

Figure 2-2. Expression analysis of genes within critical subcongenic region 17

Figure 2-3. Plasma lipid levels in liver-specific transgenic Zhx2 mice 18

Figure 2-4. Quantitative PCR analysis of selected genes in livers of sub13, BALB/cJ, and Zhx2 transgenic mice 19

Figure 2-5. Analysis of mRNA expression during murine liver development in sub13 and BALB/cJ strains 20

Chapter 3

Figure 3-1. Atherosclerotic lesions in male Zhx2 null vs wild-type mice 43

Figure 3-2. Atherosclerotic lesions in female Zhx2 null vs wild-type mice 44

Figure 3-3. Absence of Zhx2 reduces aneurysm and aortic calcification 45

Figure 3-4. Blood plasma levels in male Zhx2 null vs wild-type mice 47

Figure 3-5. Blood plasma levels in female Zhx2 null vs wild-type mice 48

Figure 3-6. Zhx2 levels in LPS-treated macrophages 49

Figure 3-7. Zhx2 expression across 64 inbred mouse strains 51

Figure 3-8. Venn diagram of LPS-induced genes in macrophages from Zhx2 null vs wild-type 54

Figure 3-9. Bone marrow transplants in Zhx2 wild-type mice change HSC genotype 54

Figure 3-10. Atherosclerotic lesions in Zhx2 wild-type bone marrow recipients 55

Figure 3-11. Plasma lipid levels for bone marrow recipients 56

Chapter 4

Figure 4-1. Cells isolated from the intima of healthy mouse aortas are endothelial cells 98

Figure 4-2. Treatment of whole aortas with pro-inflammatory factors prior to MAEC isolation 99

Figure 4-3. Differential gene expression of pre-lesioned MAECs compared to healthy MAECs 101

Figure 4-4. Experimental outline of cell collection for GWAS gene expression studies 102

Figure 4-5. Overview of differential gene expression 103

Supplemental Figure 4-1. Overview of MAEC isolation and treatment procedure. 104

Supplemental Figure 4-2. Amplification of MAEC RNA does not impact relative gene expression levels 104

Supplemental Figure 4-3. Staining for lesions in ApoE -/- mice at 4 and 24 weeks 105

LIST OF TABLES

Chapter 3

Table 3-1. Differentially expressed genes in livers from Ldlr -/- Zhx2 null vs wild-type mice 57

Table 3-2. eQTL hotspot in LPS-treated macrophages 58

Table 3-3. Fold-changes in Zhx2 wild-type vs null mice 58

Table 3-4. LPS-induced genes that differ between Zhx2 genotypes 59

Supplemental Table 3-1. Gene ontology results for Zhx2 null vs wild-type macrophages 60

Supplemental Table 3-2. Fold-changes above 5-fold in response to LPS in Zhx2 null and wild-type macrophages 62

Chapter 4

Table 4-1. Number of genes differentially expressed from healthy to pre-lesioned MAECs 105

Table 4-2. Top differentially expressed genes in MAECs 106

Table 4-3. Gene transcript presence of 56 GWAS genes 107

Table 4-4. Fold-change of GWAS candidate genes from healthy to diseased cell types 108

Supplemental Table 4-1. RT-qPCR primer sequences 109

Supplemental Table 4-2. levels of adipose, leukocyte, and

macrophage cell markers in MAEC preps 111

ACKNOWLEDGMENTS

I would like to acknowledge Jake Lusis for introducing me to the field of genetics during the winter quarter of 2002, and again for giving me a chance to work with him when I returned to UCLA for graduate school in 2006. His enthusiasm and love for science has kept me motivated throughout my time as a graduate student, and as a result I am very excited for my future as a scientist.

I would also like to acknowledge Judith Berliner for her dedication and encouragement during my graduate work. She is a wonderful source of support and a role model.

In addition, I would like to acknowledge many members of the Lusis lab, who have helped with scientific guidance and moral support: Casey Romanoski, for being my first and best friend in the lab; Brian Bennett, for helping me through the rocky first few years as a graduate student; Mete Civelek, for helping me through the rocky last few years as a graduate student; Luz Orozco, for teaching me everything I know about macrophages; and Brian Parks for support during the dark days of mouse work. I would also like to thank Xuping Wang and Judy Wu for their help with atherosclerosis data; Nam Che, for help with cell culture; Lawrence Castellani and Sharda Charugundia, for their help with lipid analyses; and Rosa Chen, for administrative help.

I would also like to thank those outside of the Lusis lab, namely Michael Weinstein, who gave me immeasurable amounts of help on bone marrow transplants, and Peter Gargalovic, who continues to work with me on the Zhx2 project. Lastly, I would like to thank my husband Emrah Kostem for helping me with all things R.

In Chapter 2, I have included a reproduction of the manuscript “Quantitative trait locus mapping and identification of Zhx2 as a novel regulator of plasma lipid metabolism”. Gargalovic, P.S., et al., Circulation Cardiovascular genetics, 2010. 3(1): p. 60-7. I have been granted permission by the publisher to include this manuscript (license number 2902240530995).

Chapter 4 is a version of a submitted manuscript “Genomic analysis of atherosclerosis initiation in the major vascular cell types in mice”, Ayca Erbilgin, Nathan Siemers, Paul Kayne, Wen-pin Yang, Judith Berliner, Aldons J. Lusis. AE, JB, and AJL designed research, AE performed research and wrote the paper, NS, PK, and WY performed microarray analysis.

I received funding from the UCLA Cellular and Molecular Biology training grant from 2007-2010 (Ruth L. Kirschstein National Research Service Award GM007185) and American Heart Association predoctoral fellowship from 2010 to 2012.

VITA

2003	B. S., Molecular, Cell, and Developmental Biology University of California, Los Angeles
2003 - 2005	Research Associate I, ParAllele Biosciences, South San Francisco
2005 - 2006	Research Assistant II, Affymetrix, South San Francisco
2006 - present	Graduate Student Researcher Department of Microbiology, Immunology, and Molecular Genetics University of California, Los Angeles
2007 - 2010	NIH Ruth L. Kirschstein National Research Service Award GM07185 “The construction of vascular endothelial cell co-expression networks”
2008	Teaching Assistant, Human Genetics 156 Department of Human Genetics, University of California Los Angeles
2009	Teaching Assistant, Honors Collegium 70A: Genetic Engineering in Medicine, Agriculture, and Law Dr. Bob Goldberg, University of California Los Angeles
2010 - present	AHA WSA Spring 2010 Predoctoral Fellowship 10PRE3420032 “Using network analysis to identify genetic components of atherosclerosis in mouse aortic endothelial cells”

Publications:

1. Gargalovic, PS, Erbilgin A, Kohannim O, Pagnon J, Wang X, Castellani L, LeBeouf R, Peterson ML, Spear BT, Lusis AJ. Quantitative Trait Locus Mapping and Identification of Zhx2 as a Novel Regulator of Plasma Lipid Metabolism. Circ Cardiovasc Genet. published online Dec 30, 2009.

2. Ireland J, Carlton VE, Falkowski M, Moorhead M, Tran K, Useche F, Hardenbol P, Erbilgin A, Fitzgerald R, Willis TD, Faham M. Large-scale characterization of public database SNPs causing non-synonymous changes in three ethnic groups. Hum Genet. 2006 Mar;119(1-2):75-83.

3. Hardenbol P, Yu F, Belmont J, Mackenzie J, Bruckner C, Brundage T, Boudreau A, Chow S, Eberle J, Erbilgin A, Falkowski M, Fitzgerald R, Ghose S, Iartchouk O, Jain M, Karlin-Neumann G, Lu X, Miao X, Moore B, Moorhead M, Namsaraev E, Pasternak S, Prakash E, Tran K, Wang Z, Jones HB, Davis RW, Willis TD, Gibbs RA. Highly multiplexed molecular inversion probe genotyping: over 10,000 targeted SNPs genotyped in a single tube assay. Genome Res. 2005 Feb;15(2):269-75.

Presentations:

1. "A methodology for the isolation of mouse aortic endothelial cells and analysis of their expression profiles under various in vivo and in vitro conditions", April 2011, Arteriosclerosis, Thrombosis and Vascular Biology Scientific Sessions, poster presentation.

2. “The role of Zhx2 in atherosclerosis, plasma lipid metabolism, and developmental regulation”, October 2009, American Society of Human Genetics conference, poster presentation.

3. “HO-1 and the Inflammatory Response in Aortic Endothelial Cells”, June 2008, 6th International Conference on Pathways, Networks, and Systems Medicine, poster presentation.

Chapter 1

Introduction

Cardiovascular diseases are the leading cause of death in the western world [1]; in 2008, coronary artery disease (CAD) caused the death of approximately one in every six deaths in the United States [2]. The leading cause of CAD is atherosclerosis, a thickening of the artery wall due to the accumulation of lipids, fibrous elements, and cell migration and death [1]. This process eventually leads to the formation of an atherosclerotic plaque, which narrows the blood vessel lumen, and upon rupture can cause acute coronary syndrome, myocardial infarction, or stroke. Susceptibility to CAD varies greatly among the human population; as a complex disease, many environmental and genetic factors are involved in disease susceptibility [3]. The factors leading to the initiation and progression of atherosclerosis are complex and involve the interaction of many biological systems. The two major areas of current research in this field center around plasma lipid metabolism, a process that can control the levels of cholesterol in the blood and cells [4], and the chronic inflammation that drives atherogenesis [5]. Pharmacological tools such as statins [6] affect plasma lipid levels and are widely used, but these drugs have limitations [7]. The use of anti-inflammatory therapeutics for atherosclerosis is a promising approach; unfortunately pharmaceuticals based on manipulating the immune response have not yet become available for patient treatment [7]. Many aspects of the molecular events that occur as a part of the chronic inflammatory response in atherosclerosis remain unclear. As our knowledge of these events increases, the potential for developing therapies targeting the chronic inflammation in atherosclerosis will become more feasible.

The immune response in atherosclerosis

Atherosclerosis is initiated by the diffusion of lipids carried by low-density lipoprotein (LDL) particles through the endothelium [8, 9]. In the intima they form oxidized LDL (oxLDL) and minimally modified LDL (mmLDL), which contain oxidized phospholipids such as oxidized 1-palmitoyl-2-arachnidonoyl-sn-glycero-3-phosphorylcholine (oxPAPC) [10]. These modifications lead to the recruitment of leukocytes, such as monocytes and T-cells, by endothelial cells. Once monocytes migrate into the intimal layer, they differentiate into macrophages and take up oxLDL particles and other lipoproteins, becoming cholesterol-loaded and form foam cells. This process instigates chronic inflammation, which leads to increased activation of leukocytes and endothelial cells. The accumulation of these cells, along with smooth muscle cells that have migrated from the medial layer of the artery, additional cells of the immune system such as mast and dendritic cells, fibrous elements, and a necrotic core consisting of dead cells and cholesterol, forms an atherosclerotic plaque [11]. Thrombosis occurs when the fibrous cap of an advanced lesion weakens and ruptures.

Genome-wide association studies

Recent advances in technology have made it possible to perform genome-wide association studies (GWAS) on complex diseases such as CAD [12-15]. Most GWAS studies on CAD employ a case-control strategy, in which DNA from patients diagnosed with phenotypes of the disease are compared to DNA from healthy control patients. Genomic variants called single nucleotide polymorphisms (SNPs) are genotyped genome-wide for each subject, then associations are calculated between each SNP and presence of the disease [16]. GWAS meta-analyses published in 2011 reported data

from almost 40,000 coronary disease cases in humans; to date, 35 loci have been robustly mapped for CAD using GWAS methods [17]. Although GWAS have identified novel candidate genes for CAD, these studies offer no additional data regarding the contribution of the genes towards disease. Follow-up studies are needed to i) confirm the gene(s) represented by the associated genetic variants, ii) determine the biological system(s) in which the gene acts to affect disease, and iii) identify the mechanism of gene activity. Mice are a well-studied model organism for cardiovascular diseases, and allow for experimental methods that would be difficult or impossible in human subjects [18, 19], and provide a useful tool in interpreting the GWAS results.

Zinc fingers and homeoboxes 2: a putative transcription factor with a role in atherosclerosis

Late in 2011, a GWAS studying coronary intima-media thickness, a measure of subclinical atherosclerosis, identified a SNP near Zinc-fingers and homeoboxes 2 (Zhx2) as the most significantly associated SNP with the disease **[20]**. This gene has been studied in the Lusis lab as a transcription factor potentially affecting plasma lipid levels and atherosclerosis since 1999. Our lab initially identified the *Hyplip2* locus on mouse chromosome 15 as controlling lipoprotein lipid levels using an F2 cross between the inbred mouse strains MRL, which is susceptible to atherosclerosis and has a high plasma lipid profile, and BALB/cJ, which is resistant to atherosclerosis and has low plasma lipid levels **[21]**. A congenic mouse was constructed that encompassed the chromosome 15 region corresponding to the high lipid phenotype from the susceptible MRL strain on a BALB/cJ background **[22]** . When these congenic mice were placed on

an atherogenic diet and compared to BALB/cJ mice a strong increase in atherosclerotic lesion size was seen, suggesting this chromosome 15 region affected atherosclerosis in addition to plasma lipid levels. In Chapter 2, I discuss the identification and confirmation of the gene underlying this region as the putative transcription factor Zhx2. Gene expression levels were used to initially identify Zhx2 as the causal gene in this region, and this hypothesis was confirmed through the use of a Zhx2-transgenic mouse **[23]**.

Studies on the role of Zhx2 in atherosclerosis are discussed in Chapter 3. We observed a striking atherogenic affect of Zhx2, as male Zhx2-null mice on an LDLR-null background and western diet exhibited 9-fold smaller atherosclerotic lesions compared to wild-type mice. Cholesterol levels from these mice were not quite as dramatic, suggesting Zhx2 may affect additional systems. The observation that Zhx2 is induced in macrophages by lipopolysaccharide (LPS), a pro-inflammatory molecule, indicates that Zhx2 may act on the inflammatory response to impact atherosclerosis. A bone marrow transplant of Zhx2-null hematopoietic stem cells into Zhx2 wild-type mice resulted in an over four-fold reduction of atherosclerotic lesions, supporting the hypothesis that Zhx2 mediates atherosclerosis through cells of the immune system. Although microarray expression analysis of Zhx2-null versus wild-type macrophages revealed potential targets of Zhx2 regulation, additional studies will be needed to identify DNA targets of Zhx2. We believe that Zhx2 could regulate a novel genetic pathway that controls inflammation, therefore affecting atherosclerosis.

Isolation and analysis of the gene expression of mouse aortic endothelial cells

The endothelium serves as a barrier between the intima and the blood, which transports LDL particles and leukocytes. The various changes in endothelial cell function during the early stages of atherogenesis are critical for disease progression. Relevant endothelial dysfunctions include permeability differences that allow for the passage of LDL into the vessel wall, cell activation that leads to the recruitment of leukocytes and mediates chronic inflammation, and structural changes in the endothelial layer [1]. The study of the transcriptional perturbations that accompany endothelial dysfunction would allow for better understanding of the molecular events that control these changes, and would provide candidates for therapeutic targets.

A common experimental method for the study of single cell types is to generate and grow cell cultures; this allows for an abundance of cells and easier experimental planning. Unfortunately, cells cultured *in vitro* lack the interactions with other cells and tissues, and sometimes result in cell modifications that may not represent the *in vivo* behavior of the cell type. Previous studies in our lab have utilized human aortic endothelial cell (HAEC) cultures to great success [24-26], but acquiring the same quality of cell cultures from mice has been much more challenging. Mouse aortic endothelial cells (MAECs) de-differentiate as they are cultured and do not adequately represent an *in vivo* endothelial cell, so other methods need to be used in order to gather endothelial-specific transcription from mouse aortas.

In Chapter 4, I describe a previously published method to isolate the intimal layer of the mouse aorta [27], and my characterization of the preps acquired as consisting of endothelial cells. This method was adapted to allow for the treatment of the aorta with pro-inflammatory agents such as oxLDL, oxPAPC, and LPS prior to isolation of MAEC

RNA. As a very small amount of RNA is isolated from one mouse aorta, I applied an RNA amplification method that allows for the microarray and high-throughput RT-qPCR analysis of these samples. I employed these methods to identify transcripts that are differentially expressed in MAECs taken from pre-lesioned aortas as compared to healthy aortas, many of which have not previously been described in this context.

A survey of CAD GWAS candidate gene expression in atherosclerotic cell types of the aorta

The MAEC RNA isolation method described in Chapter 4 allows for the separation of the aortic intima from the media, resulting in preps consisting of discrete cell types. These represent two of the main cell types found in atherosclerotic lesions: endothelial cells and smooth muscle cells. Another key component of lesions, foam cells, can be collected from LDLR -/- mice on a western diet [28]. Intimal cells gathered from atherosclerotic mice that have aortic lesions represent the heterogeneous composition of cell types present in atheromas. This data set, consisting of three separate cell types present in atherosclerosis and the one representing the whole lesion, can be used to survey the expression patterns of candidate genes.

As previously mentioned, GWAS have resulted in the identification of many loci associated with CAD, representing nearly 60 genes. As GWAS do not provide mechanistic data regarding the possible role of these genes in disease, further experiments are necessary. In Chapter 4, I present a complete assessment of the transcriptional presence of the 56 GWAS candidate genes that have mouse homologs in the four atherosclerotic cell types I have collected. I found that 50 of these genes are

expressed in at least one of the cell types tested; expression of the other six is not detectable in cells present in vascular lesions. Furthermore, I determined that 31 of these GWAS candidate genes are differentially expressed between healthy and diseased cell types, indicating a role for these genes in atherosclerosis mediated through that cell type. These results can be used for planning studies on individual candidate genes, and provide additional information regarding the function of many GWAS candidate genes.

In summary, my dissertation work addresses the questions surrounding the inflammatory response that occurs in the vessel wall during atherosclerosis using genetics in mouse models of CAD. I characterized a putative transcription factor that contributes to atherosclerosis, identified candidate genes involved in the activation of endothelial cells during the early stages of atherosclerosis, and observed the expression patterns of CAD GWAS candidate genes in mice in order to elucidate future pathways for their study.

Bibliography

1. Weber, C. and H. Noels, *Atherosclerosis: current pathogenesis and therapeutic options.* Nature medicine, 2011. **17**(11): p. 1410-22.
2. Roger, V.L., et al., *Executive summary: heart disease and stroke statistics--2012 update: a report from the American Heart Association.* Circulation, 2012. **125**(1): p. 188-97.
3. Maclellan, W.R., Y. Wang, and A.J. Lusis, *Systems-based approaches to cardiovascular disease.* Nature reviews. Cardiology, 2012.
4. Hegele, R.A., *Plasma lipoproteins: genetic influences and clinical implications.* Nature reviews. Genetics, 2009. **10**(2): p. 109-21.
5. Rader, D.J. and A. Daugherty, *Translating molecular discoveries into new therapies for atherosclerosis.* Nature, 2008. **451**(7181): p. 904-13.
6. LaRosa, J.C., J. He, and S. Vupputuri, *Effect of statins on risk of coronary disease: a meta-analysis of randomized controlled trials.* JAMA : the journal of the American Medical Association, 1999. **282**(24): p. 2340-6.
7. Charo, I.F. and R. Taub, *Anti-inflammatory therapeutics for the treatment of atherosclerosis.* Nature reviews. Drug discovery, 2011. **10**(5): p. 365-76.
8. Hansson, G.K. and A. Hermansson, *The immune system in atherosclerosis.* Nature immunology, 2011. **12**(3): p. 204-12.
9. Hansson, G.K. and P. Libby, *The immune response in atherosclerosis: a double-edged sword.* Nature reviews. Immunology, 2006. **6**(7): p. 508-19.
10. Berliner, J.A. and A.D. Watson, *A role for oxidized phospholipids in atherosclerosis.* The New England journal of medicine, 2005. **353**(1): p. 9-11.

11. Lusis, A.J., *Atherosclerosis.* Nature, 2000. **407**(6801): p. 233-41.

12. Schunkert, H., et al., *Large-scale association analysis identifies 13 new susceptibility loci for coronary artery disease.* Nature genetics, 2011. **43**(4): p. 333-8.

13. *A genome-wide association study in Europeans and South Asians identifies five new loci for coronary artery disease.* Nature genetics, 2011. **43**(4): p. 339-44.

14. Kathiresan, S., et al., *Genome-wide association of early-onset myocardial infarction with single nucleotide polymorphisms and copy number variants.* Nature genetics, 2009. **41**(3): p. 334-41.

15. Samani, N.J., et al., *Genomewide association analysis of coronary artery disease.* The New England journal of medicine, 2007. **357**(5): p. 443-53.

16. Hirschhorn, J.N. and M.J. Daly, *Genome-wide association studies for common diseases and complex traits.* Nature reviews. Genetics, 2005. **6**(2): p. 95-108.

17. Peden, J.F. and M. Farrall, *Thirty-five common variants for coronary artery disease: the fruits of much collaborative labour.* Human molecular genetics, 2011. **20**(R2): p. R198-205.

18. Stylianou, I.M., et al., *Genetic basis of atherosclerosis: insights from mice and humans.* Circulation research, 2012. **110**(2): p. 337-55.

19. Daugherty, A., *Mouse models of atherosclerosis.* The American journal of the medical sciences, 2002. **323**(1): p. 3-10.

20. Bis, J.C., et al., *Meta-analysis of genome-wide association studies from the CHARGE consortium identifies common variants associated with carotid intima media thickness and plaque.* Nature genetics, 2011.

21. Gu, L., M.W. Johnson, and A.J. Lusis, *Quantitative trait locus analysis of plasma lipoprotein levels in an autoimmune mouse model : interactions between lipoprotein metabolism, autoimmune disease, and atherogenesis.* Arteriosclerosis, Thrombosis, and Vascular Biology, 1999. **19**(2): p. 442-53.

22. Wang, X., et al., *Hyplip2, a new gene for combined hyperlipidemia and increased atherosclerosis.* Arteriosclerosis, Thrombosis, and Vascular Biology, 2004. **24**(10): p. 1928-34.

23. Gargalovic, P.S., et al., *Quantitative trait locus mapping and identification of Zhx2 as a novel regulator of plasma lipid metabolism.* Circulation. Cardiovascular genetics, 2010. **3**(1): p. 60-7.

24. Romanoski, C.E., et al., *Network for activation of human endothelial cells by oxidized phospholipids: a critical role of heme oxygenase 1.* Circulation research, 2011. **109**(5): p. e27-41.

25. Romanoski, C.E., et al., *Systems genetics analysis of gene-by-environment interactions in human cells.* American journal of human genetics, 2010. **86**(3): p. 399-410.

26. Gargalovic, P.S., et al., *Identification of inflammatory gene modules based on variations of human endothelial cell responses to oxidized lipids.* Proceedings of the National Academy of Sciences of the United States of America, 2006. **103**(34): p. 12741-6.

27. Jongstra-Bilen, J., et al., *Low-grade chronic inflammation in regions of the normal mouse arterial intima predisposed to atherosclerosis.* The Journal of experimental medicine, 2006. **203**(9): p. 2073-83.

28. Li, A.C., et al., *Differential inhibition of macrophage foam-cell formation and atherosclerosis in mice by PPARalpha, beta/delta, and gamma.* The Journal of clinical investigation, 2004. **114**(11): p. 1564-76.

Chapter 2

Identification of Zhx2 as a novel regulator of plasma lipid metabolism

Quantitative Trait Locus Mapping and Identification of Zhx2 as a Novel Regulator of Plasma Lipid Metabolism

Peter S. Gargalovic, PhD; Ayça Erbilgin, BS; Omid Kohannim, BS; Joanne Pagnon, MS; Xuping Wang, MD; Lawrence Castellani, PhD; Renee LeBoeuf, PhD; Martha L. Peterson, PhD; Brett T. Spear, PhD; Aldons J. Lusis, PhD

Background—We previously mapped a quantitative trait locus on chromosome 15 in mice contributing to high-density lipoprotein cholesterol and triglyceride levels and now report the identification of the underlying gene.

Methods and Results—We first fine-mapped the locus by studying a series of congenic strains derived from the parental strains BALB/cJ and MRL/MpJ. Analysis of gene expression and sequencing followed by transgenic complementation led to the identification of zinc fingers and homeoboxes 2 (Zhx2), a transcription factor previously implicated in the developmental regulation of α-fetoprotein. Reduced expression of the protein in BALB/cJ mice resulted in altered hepatic transcript levels for several genes involved in lipoprotein metabolism. Most notably, the Zhx2 mutation resulted in a failure to suppress expression of lipoprotein lipase, a gene normally silenced in the adult liver, and this was normalized in BALB/cJ mice carrying the Zhx2 transgene.

Conclusions—We identified the gene underlying the chromosome 15 quantitative trait locus, and our results show that Zhx2 functions as a novel developmental regulator of key genes influencing lipoprotein metabolism. **(*Circ Cardiovasc Genet*. 2010;3:60-67.)**

Key Words: genetics ■ lipoproteins ■ atherosclerosis ■ genes ■ mapping

Despite several large-scale genome-wide association studies, the genetic factors contributing to lipoprotein metabolism remain poorly understood. Thus, the loci identified thus far explain <20% of the hereditary component of lipoprotein levels, except for lipoprotein(a).[1–5] This is explained in part by complex gene-by-environment interactions, rare variations, and population heterogeneity.[6] Moreover, some of the novel loci contain multiple genes or genes with no known connections to lipoprotein metabolism, and establishing their functions based on human studies will be difficult.[7]

Clinical Perspective on p 67

A complementary approach to understand the biology and genetics of lipoprotein metabolism is to study natural variations in experimental organisms such as mice and rats.[8] Although the common variations contributing to interindividual differences for complex traits are unlikely to be conserved between species, one would expect a level of conservation of the pathways involved. Unfortunately, efforts to identify genes for complex traits in mice and rats have rarely been successful.[9] A major problem has been the lack of mapping resolution in quantitative trait locus (QTL) analyses.[10] We report here the dissection of a QTL for lipoprotein levels in mice with a strategy based on the analysis of congenic and subcongenic strains, followed by screening for structural and regulatory gene variations.

We previously mapped a locus on chromosome 15 (Chr.15, named *Hyplip 2*) contributing to complex variations in total cholesterol, high-density lipoprotein cholesterol, and triglyceride levels in a genetic cross between strains BALB/cJ and MRL/MpJ (MRL).[11] To validate the QTL mapping results, the Chr.15 region from MRL was introgressed onto the background of BALB/cJ strain. Analysis of the congenic strain, named CON15, confirmed the QTL findings and revealed a striking influence of the locus on susceptibility to diet-induced atherosclerosis.[12] Further biomedical studies of the congenic strain showed that the variation influenced clearance of triglyceride-rich lipoproteins rather than their production.[13]

Received August 22, 2009; accepted December 14, 2009.

From the Departments of Medicine (P.S.G., A.E., O.K., J.P., X.W., L.C., A.J.L.), Microbiology, Immunology, and Molecular Genetics (P.S.G., O.K., J.P., X.W., L.C., A.J.L.), and Human Genetics (P.S.G., O.K., J.P., X.W., L.C., A.J.L.), University of California, Los Angeles, Calif; Department of Pathobiology (R.L.), University of Washington, Seattle, Wash; and Department of Microbiology, Immunology, and Molecular Genetics (M.L.P., B.T.S.), University of Kentucky, Ky.

Dr Gargalovic's current affiliation is Research & Development, Bristol-Myers Squibb Company, Princeton, NJ.

Ayça Erbilgin and Omid Kohannim contributed equally to this work.

The online-only Data Supplement is available at http://circgenetics.ahajournals.org/cgi/content/full/CIRCGENETICS.109.902320.

Correspondence to Aldons J. Lusis, PhD, Division of Cardiology, Department of Medicine, University of California, 470-123 CHS, Los Angeles, CA 90095-1679. E-mail jlusis@mednet.ucla.edu

Circ Cardiovasc Genet **is available at http://circgenetics.ahajournals.org** **DOI: 10.1161/CIRCGENETICS.109.902320**

In this study, the congenic strain, encompassing >100 Mbp, was narrowed to ≈5 Mbp by analysis of subcongenic strains. Examination of the genes residing in the region by sequencing and quantification of transcript levels identified a strong candidate, the zinc fingers and homeoboxes 2 (Zhx2) transcription factor, previously shown to contribute to the developmental regulation of α-fetoprotein.[14] We confirmed that Zhx2 variation was indeed responsible for the lipoprotein alterations in mice by using transgenic complementation and showed that a major impact is altered expression of lipoprotein lipase (Lpl), an enzyme central to the metabolism of triglyceride-rich lipoproteins.

Methods

Animals and Diets

Strain BALB/cJ mice were obtained from the Jackson Laboratory (Bar Harbor, Me). Strain BALB/cH was obtained from Harlan (Indianapolis, Ind). CON15 was constructed as described previously.[12] Mice were fed a standard rodent chow diet containing 4% fat (Ralston-Purina Co., St. Louis, Mo.).

Developmental Curves

BALB/cJ and Sub13 mice were euthanized at birth and 5, 14, and 60 days after birth. The livers were removed and immediately frozen in liquid nitrogen. Five livers were taken for each time point from each strain. RNA was extracted with use of the Qiagen RNeasy kit, and cDNA was synthesized with use of the Applied Biosystems cDNA kit. Expression levels were assessed by quantitative real-time polymerase chain reaction (PCR).

Liver-Specific Zhx2 Transgenic Mice

A liver-specific transthyretin promoter/enhancer cassette identical to that used in a previously published study[14] was used to generate Zhx2 transgenic mice. Three independent founders were crossed to BALBc/J. All 3 transgenic founders expressed Zhx2 at a very similar level and corrected the elevated α-fetoprotein phenotype. Offspring of 1 representative founder were transferred to the University of California, Los Angeles Animal Facility, and used for further breeding and lipid analysis. To generate mice for data collection, these mice were first bred among themselves, and progeny containing the transgene were backcrossed to BALB/cJ mice. Mice were bled under isoflurane anesthesia after overnight fasting at 8 weeks of age after having been fed a chow diet. Blood was collected through the retro-orbital vein into EDTA anticoagulant as previously described.[12] Plasma total cholesterol, high-density lipoprotein cholesterol, and triglyceride levels were measured with enzymatic assays. Transgenic livers for quantitative PCR analysis were also collected at 8 weeks of age from a separate cohort of mice and immediately flash-frozen in liquid nitrogen. RNA was extracted by using the RNeasy kit (Qiagen).

Subcongenic Mapping and Genotyping

In brief, the subcongenic strains were isolated by identifying recombinations within the Chr.15 locus. Parental CON15 mice heterozygous at the Chr.15 locus were intercrossed, and progeny were genotyped at the selected polymorphic microsatellite markers (Research Genetics) by PCR. Near the area of the critical region, a dense series of polymorphic markers (≈1 Mbp) apart were typed (between D15Mit26 and D15Mit101) to pinpoint the recombination break point. Recombinant strains were expanded, and progeny were analyzed for plasma lipid levels. For each subcongenic strain, a minimum of 20 mice were examined. The BALB/cJ mice used for analyses were offspring of a CON15 intercross lacking the MRL allele, to minimize the genetic background variation. The Zhx2 mutation was genotyped by using primers that mapped within the first intron of Zhx2 and that flanked the retrovirus insertion site.[14] The resulting 342-bp DNA was amplified in an undisrupted wild-type allele, while the presence of insertion lacked the PCR product. Each DNA sample was also amplified with control PCR primers that mapped within the third exon of Zhx2 (776-bp product; supplemental Table I).

Plasma Lipid Analysis

After overnight fasting, mice under isoflurane anesthesia were subjected to blood collection through the retro-orbital vein into EDTA anticoagulant as described.[15] Mice were bled at 8 to10 weeks of age. Plasma total cholesterol, high-density lipoprotein cholesterol, and triglyceride levels were measured by enzymatic assays.[15]

Real-Time Quantitative PCR Analysis

Two-month-old males from BALB/cJ, Sub6, or Sub13 strains maintained on a chow diet were fasted overnight and euthanized, and livers were removed. Total RNA was isolated from mouse tissues with RNAlater (Ambion) and RNeasy isolation kit (Qiagen) incorporating on-column DNase treatment according to the manufacturer's instructions. Three micrograms of total RNA was reverse-transcribed with the use of random hexamers and Superscript-III reverse transcriptase (Invitrogen). Quantitative real-time PCR was performed as described previously.[16] cDNA sequences for the analyzed genes were obtained from a gene bank and primers were designed with the use of PrimerQuest software (IDT Technologies). For each gene, all available mRNA sequences in the GenBank were analyzed to identify common regions, which were then used for primer selection to ensure targeting of all gene splice variants. Sequences of primers can be found in supplemental Table II. Each individual mouse cDNA was analyzed separately by the relative standard curve method. A standard curve was first constructed for each transcript, including actin (used as endogenous control) by pooling aliquots of sample cDNAs and preparing serial dilutions. Relative expression values of each gene in individual samples were then obtained from the constructed standard curve and corrected for actin expression. The final data are expressed as the mean difference in gene expression level for the indicated strain relative to BALB/cJ littermates (set to 1) ±1 SD.

Expression Arrays

BALB/cJ males (n=4) and Sub13 males (n=4) maintained on a chow diet at 2 months of age were fasted overnight and euthanized, and livers were removed. Tissues were stored at −80°C in RNAlater (Ambion), and RNA was isolated with the RNeasy isolation kit (Qiagen) incorporating on-column DNase treatment according to the manufacturer's instructions. RNA from 8 samples was analyzed on an Agilent 2100 Bioanalyzer (Agilent) to assess the RNA integrity and hybridized to Illumina MouseRef-8 Expression BeadChip according to manufacturer instructions. Data were processed with BeadStudio software (Illumina), and probes were selected on the basis of the threshold of ≥95% probability of positive signal detection. To select differentially expressed genes between the 2 strains, we used expression array analysis software GeneSifter.Net (VizXlabs, Seattle, Wash) with cutoff criteria $P<0.05$ (Student's t test with Benjamini and Hochberg correction for the false-discovery rate) and absolute mean value fold change ≥1.5. Gene expression differences passing these criteria were expressed as the mean fold change between the compared strains (supplemental Table III).

Sequencing

PrimerQuest software (IDT Technologies) was used to design PCR primers spanning coding exons (genomic DNA) or in some cases, cDNA of genes within the critical region (supplemental Table I). Sub6 and BALB/cJ liver-derived cDNA was isolated as described previously. Genomic DNA was isolated with the Qiagen DNeasy kit. Amplified PCR products were sequenced on an Applied Biosystems 3730 instrument (Laragen Inc) and sequences were aligned with Vector NTI software (Invitrogen).

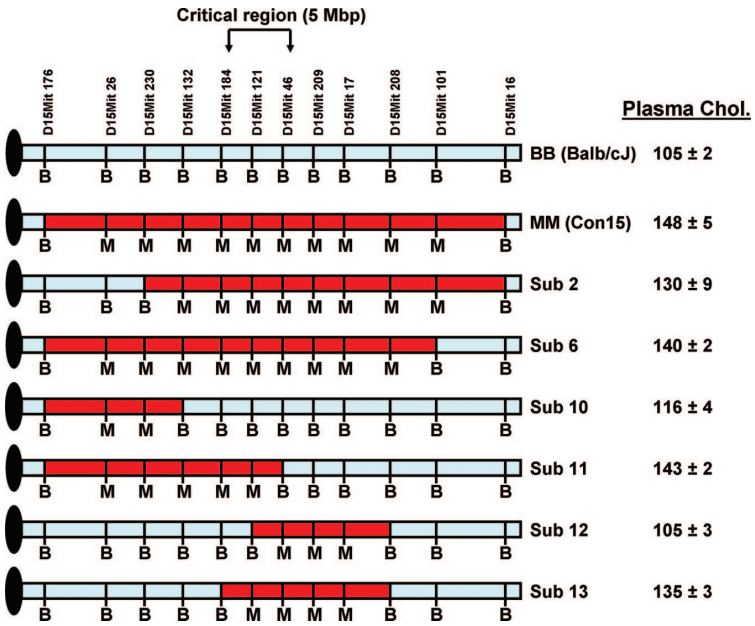

Figure 1. Genotype of selected subcongenic strains. Genotypes of derived subcongenic strains and parental CON15 strain at the polymorphic microsatellite markers used for genotyping (M indicates MRL/MpJ allele; B, BALB/cJ allele). Segregation of genotypes with male plasma cholesterol levels (depicted as mean±SEM in mg/dL) was used to narrow the *Hyplip2* locus within the 5-Mbp critical region bordered by markers D15Mit184 and D15Mit46.

Statistical Analysis

Data are presented as mean±SEM. The ANOVA *t* test was performed with Statview (Abacus Concepts, Inc) to compare differences between groups in lipid and gene expression levels. Differences were considered statistically significant at $P<0.05$. Because the traits tested were not independent of 1 another, a multiple-comparison adjustment was not performed; but with the exceptions of triglyceride levels in males and total cholesterol levels in females, the results remained significant after Bonferroni correction (supplemental Table IV). Previous studies demonstrated that the lipoprotein traits tested are normally distributed, with the exception of triglycerides. Both parametric and nonparameteric values can be found in supplemental Table IV.

Results

Subcongenic Strain Generation and Fine-Mapping of the Chr. 15 Locus

We have previously demonstrated the feasibility of subdividing the CON15 region (100 Mbp) into 2 smaller segments by using the subcongenic breeding strategy.[12] Given this early success, we further subdivided the CON15 region by generating a total of 13 recombinant subcongenic strains, differing in the length and position of the MRL segment. Male and female progeny of each subcongenic strain were analyzed for plasma cholesterol and triglyceride levels and compared with CON15 and BALB/cJ counterparts. Five strains (Sub6, Sub10, Sub11, Sub12, and Sub13) proved to be most informative (Figure 1; supplemental Table V). Because of large nongenetic variations in plasma triglyceride levels, fasted plasma cholesterol levels in males were used as the main phenotype to narrow the locus. The Sub6, Sub11, and Sub13 strains had significantly elevated plasma cholesterol (30% to 40%) compared with BALB/cJ, similar to the CON15 strain. In contrast, strains Sub10 and Sub12 exhibited plasma cholesterol levels similar to those in BALB/cJ and significantly lower than those in CON15. This was true for heterozygous and homozygous animals carrying the MRL alleles at the subcongenic locus, consistent with a dominant pattern of inheritance (supplemental Table V). Cholesterol levels in females showed somewhat smaller differences, intermediate between CON15 and BALB/cJ strains. Based on the segregation of plasma cholesterol levels with individual strain genotypes, the original locus could be reduced to ≈5 Mbp region spanning markers D15Mit184 (24 cM) and D15Mit46 (26 cM) (Figure 1).

Expression Analysis and Sequencing of Genes Within the Critical 5-Mbp Region and Identification of Zhx2 as a Hyplip2 Candidate

At this stage, further subdivision of the locus was not practically feasible. To identify the candidates, we chose a systematic 2-prong approach, combining gene expression profiling and sequence analysis. We reasoned that the underlying genetic variation would either have a pronounced effect on mRNA expression or result in modification of the protein coding sequence. Based on external databases (RefSeq, UniProt, and GenBank), the 5-Mbp critical region harbors 30 genes (supplemental Table VI). We used quantitative PCR to analyze expression of all 30 genes and associated transcript variants in livers of BALB/cJ and Sub6 strains (Figure 2A). Liver was selected because of its key role in modulation of plasma lipid metabolism. These experiments were initiated before isolation of the Sub13 strain, therefore leading to the choice of strain Sub6. Of 30 genes, 28 were detectable in the liver, of which the majority showed remarkably similar expression in the 2 strains. Two genes exhibited a >2-fold difference between the 2 strains: Zhx2 expression was strikingly reduced in BALB/cJ mice (38-fold), and BC030396 expression (coding for hypothetical protein MGC14128) was also reduced in BALB/cJ mice (3-fold), but its expression in

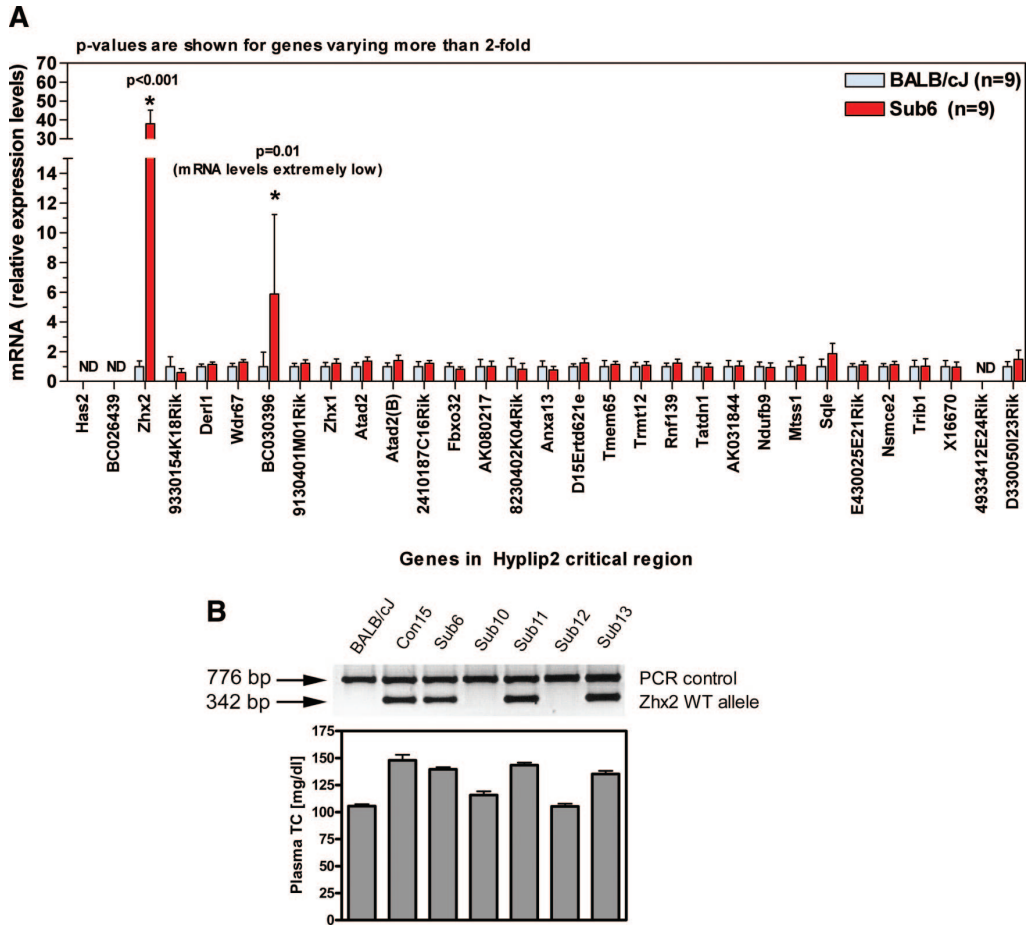

Figure 2. Expression analysis of genes within the critical region and identification of Zhx2 as a *Hyplip2* candidate. A, Liver expression of genes located within the critical region (between markers D15Mit184 and D15Mit46) was analyzed by quantitative PCR in BALB/cJ and Sub6 males as described in Methods section. Results are expressed as the mean differences in expression levels of each gene in the Sub6 strain relative to BALB/cJ strain (set to 1) ±1 SD. *Significantly different mean expression value from control ($P<0.05$). ND indicates genes below detectable levels. Liver mRNA levels of the BC030396 gene in both strains were very low and bordering detection limits of quantitative PCR. *P* values are shown only for genes with mean expression values differing by >2-fold. B, Retroviral insertion in Zhx2 gene segregates with plasma cholesterol levels in CON15 and subcongenic strains. DNA isolated from individual strains was subjected to genotyping for the presence of retrovirus insertion in Zhx2. As indicated in Methods section, the presence of a 342-bp product indicates the wild-type allele, whereas absence of the 342-bp product indicates presence of a homozygous mutant allele. As a PCR quality control, the region within the third exon of the Zhx2 gene was also amplified (776-bp product). Plasma cholesterol levels in BALB/cJ, Con15, and subcongenic strains (male mice) are shown below the Zhx2 genotypes. For subcongenic strains, heterozygous and homozygous male cholesterol values were combined and expressed as mean±SEM.

the liver was very low, approaching the limits of detection. Even at relatively high RNA (cDNA) input=30 ng, the average fluorescence threshold cycle (Ct) value for BC030396 in the quantitative PCR reaction was >35, nearing single-copy quantities and difficult to precisely quantify. On comparison, the average Ct values for Zhx2 were 26 and 32 in Sub6 and BALB/cJ strains, respectively. Sequencing of coding exons and exon/intron boundaries of genes present in the critical region led to the identification of several single-nucleotide polymorphisms. However, none of the identified single-nucleotide polymorphisms resulted in amino acid alterations and were absent in the exon/intron splice junctions (supplemental Table VI). Thus, Zhx2 became our primary candidate because of the very large difference in mRNA levels between the 2 strains.

During the course of this work, Perincheri et al[14] showed that the BALB/cJ strain contains an endogenous retroviral insertion in the first intron of the Zhx2 gene, greatly reducing levels of correctly spliced mRNA and functional protein. This recessive mutation results in a failure to fully repress postnatal expression of the α-fetoprotein and H19 genes in the livers of the BALB/cJ strain. We designed genotyping primers that flank the retrovirus insertion site of the Zhx2 gene. As predicted from the individual strain genotypes (Figure 1), the Zhx2 mutant allele (lack of the 342-bp product) was present in the BALB/cJ, Sub10, and Sub12 strains and absent in the

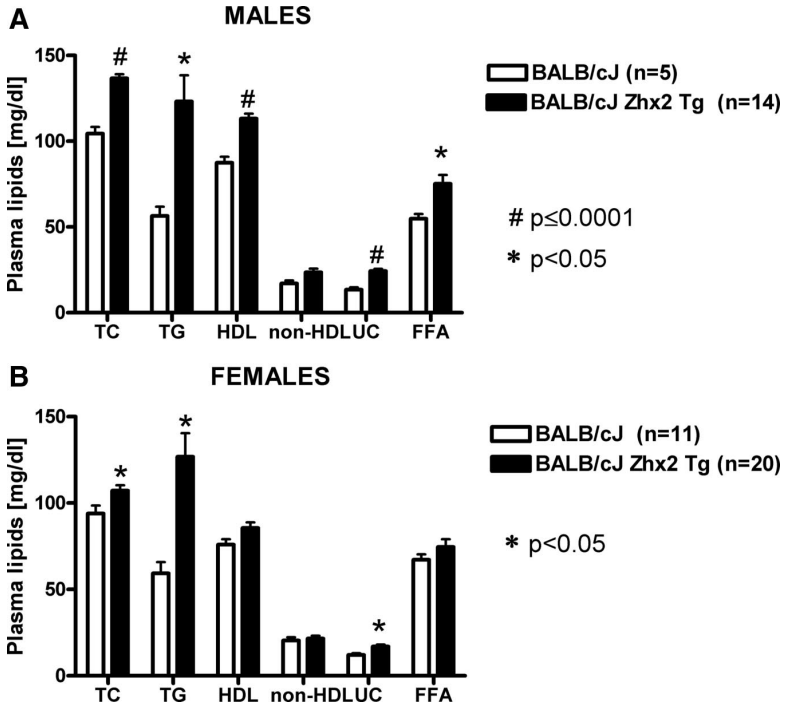

Figure 3. Liver-specific transgenic expression of Zhx2 in BALB/cJ mice increases plasma cholesterol and triglycerides. Liver-specific Zhx2 transgenic mice were repeatedly backcrossed to BALB/cJ, and mice homozygous for endogenous BALB/cJ Zhx2 allele were selected. These mice containing the Zhx2 transgene were then mated with BALB/cJ mice to generate littermates with and without the transgene. Plasma lipid levels were measured in 8-week-old fasted mice. Values are expressed as mean±SEM.

CON15, Sub6, Sub11, and Sub13 strains. Thus, the Zhx2 mutation segregated with reduced plasma cholesterol levels in subcongenic strains (Figure 2B).

Validation of Zhx2 as the Causal Gene

The Zhx2 mutation found in the BALB/cJ strain does not occur in other closely related strains, such as BALB/cH or BALB/cBy.[14,17] Consistent with a role for Zhx2 in plasma lipid levels, we observed that cholesterol levels in BALB/cH mice (130±3 mg/dL) were significantly higher than in BALB/cJ mice (103±2 mg/dL) but very similar to those in Sub13 mice (133±4 mg/dL; supplemental Figure I).

To validate the hypothesis that Zhx2 was the gene responsible for the phenotypic differences between BALB/cJ and MRL strains, we used a transgenic complementation approach. The Zhx2 coding region was subcloned into an expression vector driven by liver-selective transthyretin promoter to generate transgenic mice. Transgenic founder mice were backcrossed to the BALB/cJ background until homozygous for the Chr.15 BALB/cJ allele and further crossed to BALB/cJ mice to generate offspring littermates, with and without the transgene, which were then used for phenotyping (Figure 3). Both male and female Zhx2 transgenic mice exhibited significantly elevated plasma cholesterol and triglyceride levels, in essence identical with those in the CON15 strain and very similar to those in the subcongenic strains carrying the MRL allele. These data were consistent with the level of Zhx2 expression in transgenic mice, which was very similar to endogenously expressed gene (Figure 4). When compared with BALB/cJ mice, Zhx2 expression was 34-fold higher in transgenic mice and 49- and 38-fold higher in Sub13 and Sub6 strains, respectively. These data thus confirmed that the Zhx2 mutation underlies the Chr. 15 QTL.

Gene Expression Profiling and Identification of Lpl as a Gene Regulated by Zhx2

The Zhx2 gene was cloned recently as a member of the *ZHX* gene family, functioning as a transcriptional repressor and binding partner of nuclear transcription factor Y alpha (NF-YA) in vitro.[18,19] In vivo and in vitro studies indicate that Zhx2 functions as a postnatal repressor of the fetal liver genes α-fetoprotein, H19, and Glypican 3.[14,20,21] It is therefore highly plausible that Zhx2 also influences lipid metabolism by regulation of downstream gene targets. To help understand the underlying mechanism, we compared global gene expression in livers of the BALB/cJ and Sub13 strains. Because the Sub13 strain is on a BALB/cJ background and Zhx2 is the only gene exhibiting detected variation at the locus, strain differences should originate almost exclusively from the Zhx2 allele variant. We found 1084 differentially expressed genes, several of which are known to be involved in liver and plasma lipid metabolism (supplemental Table VII). Earlier metabolic studies in CON15 and BALB/cJ strains revealed that reduced triglyceride levels in BALB/cJ are caused by enhanced lipoprotein lipase (LPl)-mediated lipolysis and plasma clearance of triglyceride-rich plasma lipoproteins.[13] The Lpl gene was among the genes exhibiting elevated expression in the BALB/cJ livers. To confirm the expression profiling data, the Lpl expression was further evaluated by quantitative PCR. Lpl was significantly elevated in BALB/cJ strain (3 to 5 fold) when compared with Sub13 strain (Figure 4A), and its expression was suppressed in BALB/cJ strain expressing the Zhx2 liver transgene (Figure 4B). We also

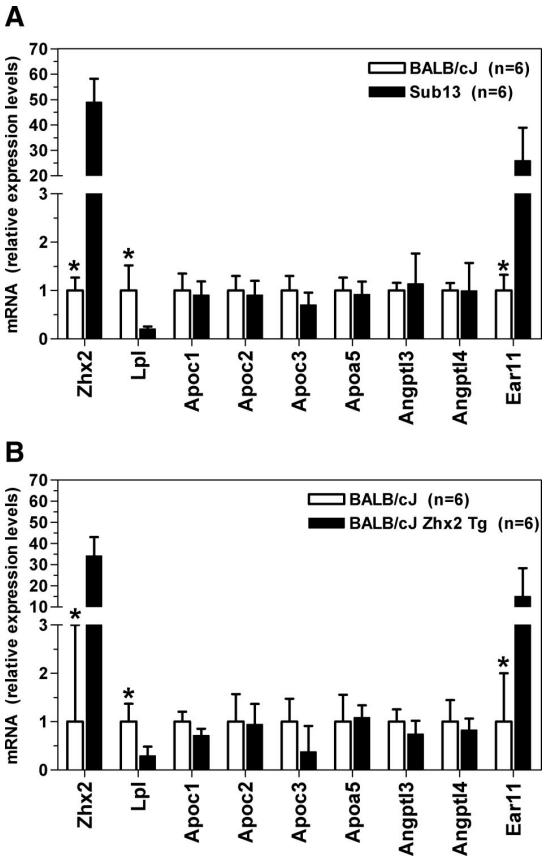

Figure 4. Quantitative PCR analysis of selected genes in livers of Sub13, BALB/cJ, and Zhx2 transgenic strains. BALB/cJ, Sub13 ,and littermate mice±Zhx2 transgene were fasted overnight and euthanized, and expression of selected genes was analyzed as described in Methods section. In addition to selected genes modulating plasma lipid metabolism, expression of Zhx2 and Ear11 (the most highly differentially expressed gene on the expression array; see supplemental Table VII) was also measured. Results are expressed as the mean differences in expression levels for the indicated strains relative to BALB/cJ littermates (set to 1) ±1 SD. *Significantly different mean expression value from control ($P<0.05$).

measured expression of other genes known to be involved in modulation of lipase activity, including Apoc1, Apoc2, Apoc3, Apoa5, Angptl3, and Angptl4, and these were not significantly affected (Figure 4). These findings indicate that Zhx2 acts as a suppressor of Lpl expression in the liver. Although low levels of Zhx2 resulted in increased expression of Lpl and most other differentially regulated genes, some genes such as Ear11 exhibited the opposite pattern (Figure 4).

To further examine the effects of Zhx2 on developmental regulation, we monitored expression levels of Lpl and Ear11 in liver during development, beginning at birth. Low levels of functional Zhx2 in BALB/cJ mice led to an increase in Lpl levels compared with Sub13 mice throughout early development, indicating that Zhx2 acts to repress Lpl (Figure 5A and 5B). These results are similar to the effects of Zhx2 on α-fetoprotein and H19. Interestingly, a different developmental expression pattern was observed in the case of Ear11, a member of the eosinophil-associated ribonuclease family. Although this gene may be repressed by Zhx2 immediately after birth, low levels of Zhx2 result in dramatically downregulated expression of Earl1 at 14 and 60 days (Figure 5C). Thus, the function of Zhx2 seems to be highly context dependent.

Discussion

Using a mouse QTL mapping strategy, we identified the Zhx2 transcription factor as a novel modulator of cholesterol and triglyceride metabolism. Our results indicate that Zhx2 plays a role in the developmental regulation of genes involved in lipid metabolism, although the mechanism by which lipids are affected is unclear.

One striking example of the molecular impact of Zhx2 deficiency that we identified is the repression of Lpl expression during postnatal development. Interestingly, Lpl is normally not expressed in adult liver.[22] Studies in rats have shown that Lpl expression is high during the fetal period but rapidly extinguished shortly after birth.[23] In fact, the expression pattern of the Lpl gene in hepatocarcinoma cell lines exhibits certain similarities to α-fetoprotein, and Lpl expression can be elevated in mice bearing liver tumors.[24,25] In addition, the proximal promoter of the Lpl gene contains NF-YA binding sites known to play important roles in regulation of Lpl expression.[26,27] Therefore, the altered plasma lipid phenotype could be a consequence, in part, of changes in Zhx2-mediated regulation of Lpl expression. Indeed, many apolipoproteins (eg, ApoA-I, ApoA-IV, ApoE, ApoB, and ApoC) and lipoprotein enzymes (eg, LPL, lecithin:cholesterol acyltransferase, and hepatic lipase) exhibit substantial temporal and tissue-specific alterations in gene expression during the fetal and neonatal periods.[22,28–30] Zhx2 has not been shown to bind DNA directly, and the mechanism by which it modulates Lpl expression is also not clear. One possible mechanism could involve indirect interaction by binding to 1 of its DNA binding partners, such as Zhx3.[31] We did not observe transcriptional differences among strains at Zhx3 (quantitative PCR P value=0.59) or at Zhx1 (Figure 2A). Although neither Zhx1 nor Zhx3 variations contributed to lipid metabolism in the MRL×BALB/cJ cross, differences in Zhx3 were associated with high-density lipoprotein cholesterol levels in a CAST/Ei×C57BL/6J intercross (M. Mehrabian, Ph.D., and A.J. Lusis, Ph.D., unpublished data, 2009).

As yet, there have been few examples of the successful identification of genes contributing to QTL for complex traits in mice. Our strategy of narrowing the QTL by using subcongenic strains followed by expression screening and sequencing was effective but laborious. It is noteworthy that Chr.15 QTL in the original cross between MRL and BALB/cJ was large (log of the odds score=11.6), as QTL with very modest effects would clearly be much more difficult to identify with our strategy.[11] We previously showed that the Chr.15 congenic interval had a very large impact on atherosclerosis, much larger than would be expected from the relatively modest changes in lipoprotein levels.[12] Preliminary studies on a low-density lipoprotein receptor-null background

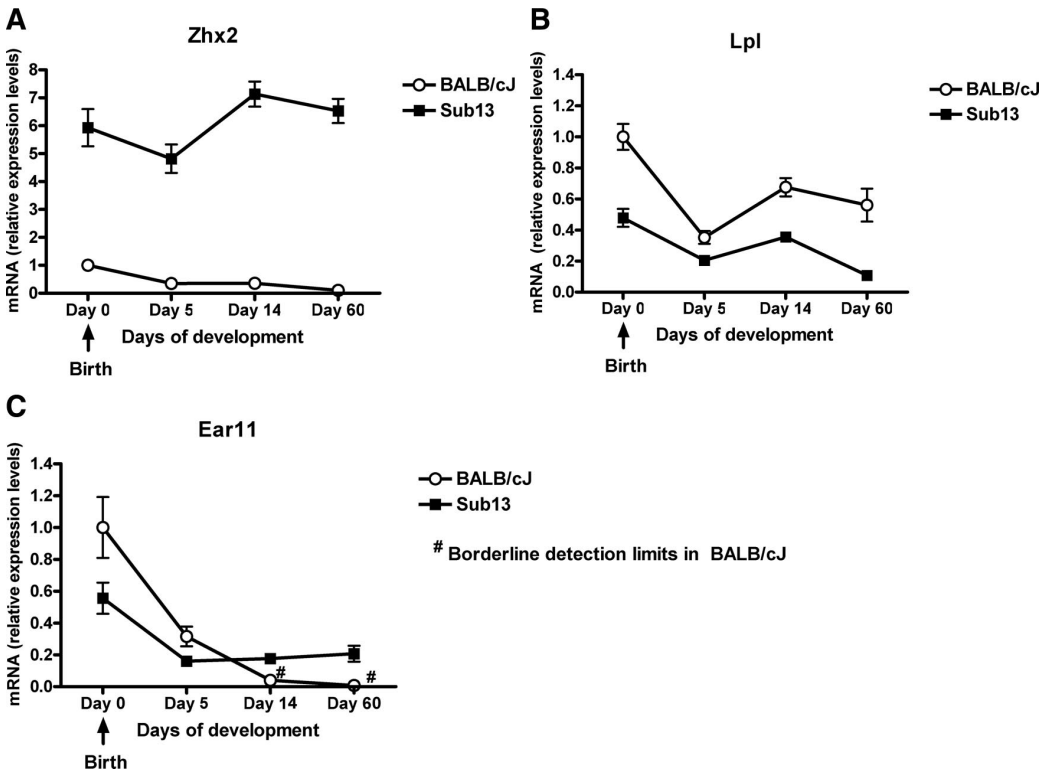

Figure 5. Analysis of mRNA expression levels during murine liver development in Sub13 and BALB/cJ strains. BALB/cJ and Sub13 male mice (n=5 per group) were euthanized at indicated time points after birth, and mRNA levels of Zhx2, Lpl, and Ear11 were analyzed by quantitative PCR as described in Methods. Results are expressed as the mean differences in expression levels for the indicated time points relative to expression in BALB/cJ at birth (set to 1) ±1 SD.

support this conclusion (A. Erbilgin, B.S., P.S. Gargalovic, Ph.D., R.C. LeBoeuf, Ph.D. and A.J. Lusis, Ph.D., unpublished data, 2009). It therefore seems likely that Zhx2 also mediates other pathways related to atherosclerosis. In particular, the effect on the eosinophil-associated ribonuclease A family, member 11 (Ear11), that plays a role in inflammation, is intriguing. Recent evidence suggests that members of the family are expressed in macrophages, an important cell type in atherogenesis.[32]

Clearly, future studies of Zhx2 and its role in lipoprotein metabolism and atherosclerosis are warranted. There are no reports of associations of Zhx2 polymorphisms with lipoprotein levels in human populations, but polymorphisms of the gene for Zhx3, which forms heterodimers with Zhx2,[19] have recently been significantly associated with triglyceride levels (S. Kathiresan, M.D., personal communication, 2009).

Acknowledgments

We thank Sarada Charugundla for assistance with lipoprotein measurements.

Sources of Funding

This work was supported by National Institutes of Health grants HL28481, HL094322 (AJL), HL079382 (RL), DK59866 (BTS, MLP) and Ruth L. Kirschstein National Research Service Award GM07185 (AE).

Disclosures

Peter Gargalovic is an employee of Bristol-Myers Squibb Co.

References

1. Aulchenko YS, Ripatti S, Lindqvist I, Boomsma D, Heid IM, Pramstaller PP, Penninx BW, Janssens AC, Wilson JF, Spector T, Martin NG, Pedersen NL, Kyvik KO, Kaprio J, Hofman A, Freimer NB, Jarvelin MR, Gyllensten U, Campbell H, Rudan I, Johansson A, Marroni F, Hayward C, Vitart V, Jonasson I, Pattaro C, Wright A, Hastie N, Pichler I, Hicks AA, Falchi M, Willemsen G, Hottenga JJ, de Geus EJ, Montgomery GW, Whitfield J, Magnusson P, Saharinen J, Perola M, Silander K, Isaacs A, Sijbrands EJ, Uitterlinden AG, Witteman JC, Oostra BA, Elliott P, Ruokonen A, Sabatti C, Gieger C, Meitinger T, Kronenberg F, Doring A, Wichmann HE, Smit JH, McCarthy MI, van Duijn CM, Peltonen L. Loci influencing lipid levels and coronary heart disease risk in 16 European population cohorts. *Nat Genet*. 2009;41:47–55.
2. Hegele RA. Plasma lipoproteins: genetic influences and clinical implications. *Nat Rev Genet*. 2009;10:109–121.
3. Kathiresan S, Willer CJ, Peloso GM, Demissie S, Musunuru K, Schadt EE, Kaplan L, Bennett D, Li Y, Tanaka T, Voight BF, Bonnycastle LL, Jackson AU, Crawford G, Surti A, Guiducci C, Burtt NP, Parish S, Clarke R, Zelenika D, Kubalanza KA, Morken MA, Scott LJ, Stringham HM, Galan P, Swift AJ, Kuusisto J, Bergman RN, Sundvall J, Laakso M, Ferrucci L, Scheet P, Sanna S, Uda M, Yang Q, Lunetta KL, Dupuis J, de Bakker PI, O'Donnell CJ, Chambers JC, Kooner JS, Hercberg S, Meneton P, Lakatta EG, Scuteri A, Schlessinger D, Tuomilehto J, Collins FS, Groop L, Altshuler D, Collins R, Lathrop GM, Melander O, Salomaa V, Peltonen L, Orho-Melander M, Ordovas JM, Boehnke M, Abecasis GR, Mohlke KL, Cupples LA. Common variants at 30 loci contribute to polygenic dyslipidemia. *Nat Genet*. 2009;41:56–65.
4. Ordovas JM, Corella D, Demissie S, Cupples LA, Couture P, Coltell O, Wilson PW, Schaefer EJ, Tucker KL. Dietary fat intake determines the effect of a common polymorphism in the hepatic lipase gene promoter on high-density lipoprotein metabolism: evidence of a strong dose effect in this gene-nutrient interaction in the Framingham Study. *Circulation*. 2002;106:2315–2321.

5. Sabatti C, Service SK, Hartikainen AL, Pouta A, Ripatti S, Brodsky J, Jones CG, Zaitlen NA, Varilo T, Kaakinen M, Sovio U, Ruokonen A, Laitinen J, Jakkula E, Coin L, Hoggart C, Collins A, Turunen H, Gabriel S, Elliot P, McCarthy MI, Daly MJ, Jarvelin MR, Freimer NB, Peltonen L. Genome-wide association analysis of metabolic traits in a birth cohort from a founder population. *Nat Genet*. 2009;41:35–46.
6. Manolio TA. Cohort studies and the genetics of complex disease. *Nat Genet*. 2009;41:5–6.
7. Ioannidis JP, Thomas G, Daly MJ. Validating, augmenting and refining genome-wide association signals. *Nat Rev Genet*. 2009;10:318–329.
8. Lusis AJ, Attie AD, Reue K. Metabolic syndrome: from epidemiology to systems biology. *Nat Rev Genet*. 2008;9:819–830.
9. Flint J, Valdar W, Shifman S, Mott R. Strategies for mapping and cloning quantitative trait genes in rodents. *Nat Rev Genet*. 2005;6:271–286.
10. Flint J, Mott R. Applying mouse complex-trait resources to behavioural genetics. *Nature*. 2008;456:724–727.
11. Gu L, Johnson MW, Lusis AJ. Quantitative trait locus analysis of plasma lipoprotein levels in an autoimmune mouse model: interactions between lipoprotein metabolism, autoimmune disease, and atherogenesis. *Arterioscler Thromb Vasc Biol*. 1999;19:442–453.
12. Wang X, Gargalovic P, Wong J, Gu JL, Wu X, Qi H, Wen P, Xi L, Tan B, Gogliotti R, Castellani LW, Chatterjee A, Lusis AJ. Hyplip2, a new gene for combined hyperlipidemia and increased atherosclerosis. *Arterioscler Thromb Vasc Biol*. 2004;24:1928–1934.
13. Moen CJ, Tholens AP, Voshol PJ, de Haan W, Havekes LM, Gargalovic P, Lusis AJ, van Dyk KW, Frants RR, Hofker MH, Rensen PC. The Hyplip2 locus causes hypertriglyceridemia by decreased clearance of triglycerides. *J Lipid Res*. 2007;48:2182–2192.
14. Perincheri S, Dingle RW, Peterson ML, Spear BT. Hereditary persistence of alpha-fetoprotein and H19 expression in liver of BALB/cJ mice is due to a retrovirus insertion in the Zhx2 gene. *Proc Natl Acad Sci U S A*. 2005;102:396–401.
15. Castellani LW, Weinreb A, Bodnar J, Goto AM, Doolittle M, Mehrabian M, Demant P, Lusis AJ. Mapping a gene for combined hyperlipidaemia in a mutant mouse strain. *Nat Genet*. 1998;18:374–377.
16. Gargalovic PS, Gharavi NM, Clark MJ, Pagnon J, Yang WP, He A, Truong A, Baruch-Oren T, Berliner JA, Kirchgessner TG, Lusis AJ. The unfolded protein response is an important regulator of inflammatory genes in endothelial cells. *Arterioscler Thromb Vasc Biol*. 2006;26:2490–2496.
17. Perincheri S, Peyton DK, Glenn M, Peterson ML, Spear BT. Characterization of the ETnII-alpha endogenous retroviral element in the BALB/cJ Zhx2 (Afr1) allele. *Mamm Genome*. 2008;19:26–31.
18. Kawata H, Yamada K, Shou Z, Mizutani T, Yazawa T, Yoshino M, Sekiguchi T, Kajitani T, Miyamoto K. Zinc-fingers and homeoboxes (ZHX) 2, a novel member of the ZHX family, functions as a transcriptional repressor. *Biochem J*. 2003;373:747–757.
19. Kawata H, Yamada K, Shou Z, Mizutani T, Miyamoto K. The mouse zinc-fingers and homeoboxes (ZHX) family; ZHX2 forms a heterodimer with ZHX3. *Gene*. 2003;323:133–140.
20. Morford LA, Davis C, Jin L, Dobierzewska A, Peterson ML, Spear BT. The oncofetal gene glypican 3 is regulated in the postnatal liver by zinc fingers and homeoboxes 2 and in the regenerating liver by alpha-fetoprotein regulator 2. *Hepatology*. 2007;46:1541–1547.
21. Yamada K, Ogata-Kawata H, Matsuura K, Kagawa N, Takagi K, Asano K, Haneishi A, Miyamoto K. ZHX2 and ZHX3 repress cancer markers in normal hepatocytes. *Front Biosci*. 2009;14:3724–3732.
22. Kirchgessner TG, LeBoeuf RC, Langner CA, Zollman S, Chang CH, Taylor BA, Schotz MC, Gordon JI, Lusis AJ. Genetic and developmental regulation of the lipoprotein lipase gene: loci both distal and proximal to the lipoprotein lipase structural gene control enzyme expression. *J Biol Chem*. 1989;264:1473–1482.
23. Peinado-Onsurbe J, Staels B, Deeb S, Ramirez I, Llobera M, Auwerx J. Neonatal extinction of liver lipoprotein lipase expression. *Biochim Biophys Acta*. 1992;1131:281–286.
24. Schoonjans K, Staels B, Devos P, Szpirer J, Szpirer C, Deeb S, Verhoeven G, Auwerx J. Developmental extinction of liver lipoprotein lipase mRNA expression might be regulated by an NF-1-like site. *FEBS Lett*. 1993;329:89–95.
25. Masuno H, Tsujita T, Nakanishi H, Yoshida A, Fukunishi R, Okuda H. Lipoprotein lipase-like activity in the liver of mice with Sarcoma 180. *J Lipid Res*. 1984;25:419–427.
26. Morin CL, Schlaepfer IR, Eckel RH. Tumor necrosis factor-alpha eliminates binding of NF-Y and an octamer-binding protein to the lipoprotein lipase promoter in 3T3-L1 adipocytes. *J Clin Invest*. 1995;95:1684–1689.
27. Currie RA, Eckel RH. Characterization of a high affinity octamer transcription factor binding site in the human lipoprotein lipase promoter. *Arch Biochem Biophys*. 1992;298:630–639.
28. Warden CH, Langner CA, Gordon JI, Taylor BA, McLean JW, Lusis AJ. Tissue-specific expression, developmental regulation, and chromosomal mapping of the lecithin: cholesterol acyltransferase gene: evidence for expression in brain and testes as well as liver. *J Biol Chem*. 1989;264:21573–21581.
29. Demmer LA, Levin MS, Elovson J, Reuben MA, Lusis AJ, Gordon JI. Tissue-specific expression and developmental regulation of the rat apolipoprotein B gene. *Proc Natl Acad Sci U S A*. 1986;83:8102–8106.
30. Semenkovich CF, Chen SH, Wims M, Luo CC, Li WH, Chan L. Lipoprotein lipase and hepatic lipase mRNA tissue specific expression, developmental regulation, and evolution. *J Lipid Res*. 1989;30:423–431.
31. Liu G, Clement LC, Kanwar YS, Avila-Casado C, Chugh SS. ZHX proteins regulate podocyte gene expression during the development of nephrotic syndrome. *J Biol Chem*. 2006;281:39681–39692.
32. Cormier SA, Yuan S, Crosby JR, Protheroe CA, Dimina DM, Hines EM, Lee NA, Lee JJ. T(H)2-mediated pulmonary inflammation leads to the differential expression of ribonuclease genes by alveolar macrophages. *Am J Respir Cell Mol Biol*. 2002;27:678–687.

Chapter 3

The role of Zhx2 in atherosclerosis

Introduction:

Coronary artery disease (CAD), an inflammatory disorder of the large blood vessels, is the number one cause of death in the western world. It is a highly complex disease, with many different environmental and genetic factors contributing to its etiology [1-3]. Mouse models of atherosclerosis serve as a useful tool to dissect the many genes that contribute to disease phenotypes [4]; identifying genes that contribute to atherosclerotic traits in mice can lead to valuable knowledge for potential treatments in humans. We previously identified a region on mouse chromosome 15 that controlled triglyceride and plasma cholesterol levels [5]. When congenic mice constructed to isolate the genetic region responsible for this trait were placed on an atherogenic diet containing cholic acid, we observed a significant difference in atherosclerotic lesion size [5]. Through the use of congenic strains, in which chromosomal regions from one strain are placed on the background of a second strain, we subsequently identified the gene responsible for the plasma lipid phenotype as Zhx2, with low transcription of the gene causing reduced levels of triglycerides and cholesterol [6]. It was validated for lipid levels using a liver-specific transgenic [6].

Zhx2 was initially identified in experiments studying the adult expression of alpha-fetal protein in the livers of BALB/cJ mice [7]. It was demonstrated that the Zhx2 allele found in the BALB/cJ substrain contained an endogenous retroviral insertion that rendered the transcript unstable and did not result in a functional protein. Other BALB strains, such as BALB/cBy, have a wild-type Zhx2 allele and have normal expression of

the gene. Zhx2 is hypothesized to repress AFP expression in adult mice, and the lack of a functional Zhx2 in BALB/cJ mice leads to the over-expression of AFP in this strain; this is consistent with the description of Zhx2 as a transcriptional repressor [8]. Chromatin immunoprecipitation studies have very recently demonstrated binding of Zhx2 to the promoters of the Cyclin A and Cyclin E genes in hepatocyte cell lines [9], although whether it binds directly to DNA or to other transcription factors is unclear.

In addition to its transcriptional role in hepatocytes, studies have shown an involvement of Zhx2 in lymphoma [10, 11] and myeloma [12, 13]; this supports both the characterization of Zhx2 as a transcriptional repressor, as it may act as a tumor suppressor in these instances, and its ubiquitous expression [8]. This is also of interest in the context of atherosclerosis, as both the liver [14] and leukocytes [15] play crucial roles in atherogenesis. Interestingly, Zhx2 has been absent from the list of candidate genes identified in genome-wide association studies for lipid levels [2], but was identified as the most significant gene in a GWAS for coronary intima medial thickness [16], a subclinical measure of atherosclerosis. Our studies aim to definitively demonstrate a role for Zhx2 in atherosclerosis, using a mouse model on an athero-susceptible background and genetically differing only in the Zhx2 allele. We will further identify the extent to which plasma lipid differences regulated by Zhx2 in the liver contribute to atherosclerosis, and whether or not this putative transcription factor affects additional systems, such as the cells of the immune systems, to promote CAD in mice. Finally, we use gene expression analysis to identify potential target pathways that Zhx2 may regulate.

Methods:

Animals: BALB/cJ mice containing the endogenous Zhx2 mutation were obtained from the Jackson Laboratory and mated with BALB/cBy Ldlr-/- mice with the wild-type Zhx2 allele. Pups heterozygous for Zhx2 and Ldlr were bred, and pups that were Ldlr -/- and heterozygous for Zhx2 were selected for breeding pairs. This mating of Ldlr -/- and Zhx2 het mice was continued for 5 generations in order to establish the BALB Ldlr -/- strains used for experiments. Experimental mice were pups of Ldlr -/- Zhx2 het breeding pairs, and were genotyped as either homozygous Zhx2 wt or Zhx2 null. Mice were maintained on a chow diet; mice for atherosclerosis data were placed on a western diet (Open Source D12079B) at 8 weeks of age for 18 weeks. Additional inbred mouse strains were obtained from Jackson labs or bred in our colony and maintained on a chow diet. All adult mice were euthanized using isofluorane in accordance with ARC policies; pups were euthanized using cervical dislocation.

Genotyping: DNA was isolated from mouse ear or tail tissue using the Qiagen DNeasy kit; genotyping was performed using PCR (TaKaRa reagents) followed by agarose gel separation of amplified products to determine size. DNA genotyping of blood isolated from bone marrow recipients was performed using Sigma Extract-n-amp kit. Zhx2 primers: Zhx2-F 5' ACTGTCTCAGCTCATTCCCTGCAA 3'; Zhx2-R 5' AATGCTTCACATGGCACACAGCAG 3'; MRZhx2-R 5' TCTGCCATTCTTCAGGTCCCTGTT; Ldlr primers: LDLR-F: 5' ACCCCAAGACGTGCTCCCAGGATGA 3', LDLR-Rwt: 5'

CGCAGTGCTCCTCATCTGACTTGT 3'; LDLR-Rko: 5' AGGTGAGATGACAGGAGATC 3'

Lesion analysis: After euthanization, chest cavity of mouse was opened and the vasculature was perfused with about 10 mL of PBS. Aortic root was then sectioned....

Plasma lipid analysis: Mice were fasted overnight and bled through the retro-orbital vein into microtainer tubes containing 0.5 M EDTA. After centrifugation, plasma was collected and subjected to quantitation of HDL and non-HDL lipids as previously described [6].

Gene expression: cDNA was synthesized with Applied Biosystems High-Capacity cDNA Reverse Transcription Kit. Roche and KAPA Biosystems SYBR green reagents were used for RT-qPCR, and reactions were processed on 384-well plates on the Roche LightCycler 480. RT-qPCR primer sequence for Zhx2-F:5'-ACACTGATAGGAAGCTGCCTGGT-3', Zhx2-R: 5'-TCAAATGCCTTTGGCTTCCCTTGG-3', 36B4-F: 5'-TGAAGCAAAGGAAGAGTCGGAGGA-3', 36B4-R: 5'-AAGCAGGCTGACTTGGTTGCTTTG-3'. Affymetrix HT Mouse Genome 430 array plates were used for microarray analysis.

Statistical analysis: Statistical analyses were executed in the R programming environment. T-tests were calculated for qPCR results using the t.test command.

Microarray results were normalized using RMA in the affy package, and differential expression p-values and venn diagrams were calculated using the limma package. Boxplots were constructed using boxplot command. Microarray p-values were corrected using benjamini hochberg.

Liver tissue collection and RNA isolation: Livers were collected from mouse at time of sacrifice, snap-frozen in liquid nitrogen, and stored at -80 C. RNA was isolated using Qiagen RNeasy kit according to manufacturer's protocol and stored at -80 C.

Macrophage collection, treatment, and RNA isolation: Mice at 16 weeks of age fed a chow diet were injected in the intraperitoneal cavity with 4% Thioglycolate (Brewer Thioglycollate Medium, BD#211716). On the fourth day after injection, macrophages were collected through lavage of the peritoneal cavity using PBS buffer. Collected cells were treated with ACK lysis buffer to remove red blood cells and were then cultured overnight in DMEM media with 20% FBS. The next morning the cell culture dishes were rinsed with PBS, and RNA from the cell cultures was collected using buffer RLT from the Qiagen RNeasy kit. RNA was isolated with the Qiagen RNeasy kit following the manufacturer's protocol. LPS treatment: after rinse with PBS the morning after cell harvest, media containing 1% FBS was added to cell cultures; LPS at a final concentration of 2 ng/mL was used for the subset of samples to be treated. After 4 hours, RNA from the cell cultures was collected and isolated as above.

Macrophage eQTL analysis: Briefly, primary macrophages were obtained from 92 mouse inbred strains of the HMDP [17], and the cells were treated with control media or media containing bacterial lipopolysaccharide (LPS) for four hours [18]. Genome-wide expression was measured using the Affymetrix MOE430A microarray platform, followed by association mapping of transcript expression using single nucleotide polymorphisms (SNPs) across the mouse genome. Efficient Mixed Model Association (EMMA) was used for the association calculation. Since Zhx2 expression was not measured on the array, it was not possible to identify a cis-eQTL for this gene. The genome was divided into 2-Mb size bins and the number of trans eQTL that mapped to each bin was counted in order to identify gene expression hotspots.

Bone marrow transplants: Bone marrow donors were euthanized at approximately 6 weeks of age on the day of the transplant, and bone marrow was collected from the tibias and femurs. Briefly, the bones were flushed with DMEM media into a falcon tube using a syringe. Media containing the flushed bone marrow was kept on ice. After all bone marrow was harvested, the collected media was passed through a 70 um filter (BD falcon 352350), treated with ACK lysis buffer, and rinsed with fresh DMEM. Hematopoetic stem cells (HSCs) were counted and kept on ice; a minimum of 10 million cells were given to each recipient. Bone marrow recipients were between 6 and 8 weeks of age. On the day of the transplant, recipients were given a dose of 8 Gy radiation using a cesium source, and HSCs were transplanted using tail-vein injection. Mice were maintained in sterile cages with antibiotics in the water and autoclaved food

for a four-week recovery period, after which they were placed on a western diet for 18 weeks.

Results:

Absence of Zhx2 in mice is atheroprotective: In male mice, the presence of a functional Zhx2 gene led to an average atherosclerotic lesion size nine-fold higher than in mice homozygous for the Zhx2 null allele (Fig 1). In female mice, the average lesion size was more than two-fold larger in mice with the functional Zhx2 allele (Fig 2). Similar differences were seen in aortic aneurysm and aortic calcification measures in both sexes. Zhx2 null male mice had minimal evidence of aortic aneurysm and medial calcification, whereas these events were present in males with wild-type Zhx2 (Fig 3a). Although aneurysm and calcification were observed in the aortas of female Zhx2 null mice, aneurysms were four-fold higher and calcification was more than 10-fold higher in Zhx2 wild-type female mice (Fig 3b).

Zhx2 has minimal impact on plasma lipid levels: Blood samples taken from the same mice as the atherosclerosis studies were analyzed for plasma lipid levels. Male mice with wild-type Zhx2 genotype have an approximate two-fold increase in both triglyceride and total cholesterol levels, and close to 40% increase in HDL levels compared to Zhx2-null mice (Fig 4). Plasma lipids taken from female mice showed no difference in total cholesterol or HDL levels and a 60% increase in triglycerides (Fig 5).

Expression data on Zhx2 wild-type and Zhx2 null livers show differential expression of inflammatory genes, lack of perturbation of published/traditional lipid metabolism genes: RNA isolated from the livers of mice used for atherosclerosis and lipid data were subjected to microarray analysis. The 22 genes that exhibited significant differential expression between Zhx2 wt and Zhx2 null samples in both male and female samples are listed in Table 1. Several genes have little or no published literature regarding their function (B930041F14RIK, SLC44A3, BHLHB9, D330045A20RIK, EG381438, and HIST1H2AO). Many of these genes are involved with hematopoiesis (IRF2[19], MEIS1[20]), leukemias (MEIS1, SULT1C2[21]), or with other aspects of inflammation and the immune system (APRT[22], HCP-1[23], MMD2[24], MPP1[25], ZAP70[26]). Four genes have been described as being involved with the nervous system (AMER2[27], CALN1[28], DACT2[29], SLC1A2[30]), two of these with neural embryogenesis (AMER2, DACT2). None of these genes have been directly linked to atherosclerosis or lipid metabolism.

Zhx2 mRNA transcript levels in macrophages is induced by treatment with lipopolysaccharide: As the differential expression data from liver suggested immune system involvement, we wanted to study the expression of Zhx2 in macrophages. Macrophages isolated from our BALB/cBy/BALB/cJ Ldlr -/- mouse strains were isolated, cultured, and a subset treated with the pro-inflammatory factor lipopolysaccharide (LPS). Macrophages isolated from Zhx2 wt mice showed an increase of approximately 8-fold in Zhx2 transcript levels after LPS treatment in both male and female mice; Zhx2

transcript levels in Zhx-null mice were unaffected (Fig 6a). These results were replicated with studies in macrophages isolated from BL6 and C3H mice. The levels of Zhx2 in BL6 mice and C3H mice did not vary significantly at baseline levels (Fig 6b). However, after treatment with LPS Zhx2 transcript level was induced by almost ten-fold in BL6 mice with no induction in the LPS non-responsive C3H mice.

Zhx2 mRNA levels in macrophages isolated from inbred mouse strains vary in responses to LPS: As the gene expression of Zhx2 transcript appears to respond strongly to treatment with LPS in the inbred mouse strains BL6 and BALB/cBy, we wanted to survey its responsiveness among a wider set of inbred mouse strains with varying susceptibilities to atherosclerosis. By surveying Zhx2 levels in many strains, we can map regulatory elements and relate to clinical traits [17]. In the 70 inbred strains tested, we observed Zhx2 levels in untreated macrophages, those treated with LPS, and we also calculated the fold-induction of Zhx2 after LPS treatment for each strain. While most strains had minimal macrophage Zhx2-levels at baseline, there were a few strains with high Zhx2 levels (Fig 7a). After LPS treatment, Zhx2 transcript levels increased in nearly all strains tested, although to varying degrees (Fig 7b). The variance in fold-induction can be visualized in Figure 7c, where we see up to a 25-fold induction of Zhx2. The strains exhibiting minimal induction are BALB/cJ, containing the Zhx2-null mutation, and a subset of BXH strains which presumably contain the C3H TLR4-null allele and do not respond to LPS treatment. Macrophage microarray data gathered from this panel of inbred mice were analyzed to identify eQTL that maps near the Zhx2 gene

on chromosome 15 [17]. We found 60 genes whose expression maps to the interval in this region (Table 2), suggesting that their expression may be controlled by Zhx2.

Macrophage microarray expression data indicates central role of the immune system in Zhx2 action: Nearly 1400 probes were differentially expressed between macrophages isolated from chow-fed Zhx2 wild-type and null mice, in both males and females. The presence of Zhx2 in macrophages appears to drastically affect the gene expression profile: of the genes differentially expressed among both sexes, approximately 600 are regulated more than two-fold, with some genes expressed over 100-fold (Table 3). The top differentially expressed genes are all up-regulated in the absence of Zhx2, as the largest fold-change for a down-regulated gene is 6-fold compared to the maximum of over 300-fold in up-regulated genes; these findings are consistent with the role of Zhx2 as a transcriptional repressor. Gene ontology analysis performed on these genes identifies the immune response category as the most enriched in the dataset, with a corrected p-value of 2.0 x 10-25 (Supplemental table 1). Other notable significantly enriched GO categories include nucleotide and ribonucleotide binding, a finding consistent with the role of Zhx2 as a transcriptional regulator, and apoptosis.

The most differentially expressed gene, with a 322-fold upregulation in Zhx2 null female macrophages and a 354-fold upregulation in Zhx2 null male macrophages, is immunoresponsive gene 1 (Irg1). This gene was initially identified as an LPS-inducible cDNA in RAW macrophages [31]; no studies have been published describing a role in atherosclerosis. Other genes with over 100-fold upregulation in Zhx2-null macrophages

are Fpr2, a lipoxin receptor that may have an anti-inflammatory role [32]; Cfb, a complement factor expressed in macrophages and induced by LPS [33]; Clec4e, which is expressed predominantly on macrophages [34]; the chemokine Cxcl2; and Il1b, a cytokine produced by activated macrophages [35]. Other notable highly differentially expressed genes include the interferon-induced protein with tetratricopeptide repeats genes 1,2, and 3, which may be involved in the LPS response as well [36] and Zbp1, a DNA-dependent activator of innate immune responses [37]. Among these differentially-expressed genes are six that are also regulated by the hotspot near Zhx2: Abcg2, Acss2, Amdhd1, Ifitm3, Ms4a7, and Mxd4. The top differentially expressed genes found in livers of Ldlr -/- mice fed a western diet described earlier were not perturbed in chow-fed macrophages.

Contrary to the extensive differential expression observed when comparing the baseline expression of Zhx2 wild-type and null macrophages, the overall response of these genotypes to LPS are similar. A comparison of microarray expression data of macrophages isolated from the two Zhx2 genotypes treated with LPS yielded no statistically significant differentially expressed genes. Differentially expressed genes from untreated to LPS-treated macrophages were calculated for each genotype and compared, identifying an overlap of 3039 LPS-induced genes (Fig 8). A few notable genes with differences in LPS induction are Cxcl13, a chemokine which is induced over 2-fold in Zhx2 null macrophages but not in wild-type macrophages, and Thrombospondin 1 (Thbs1), an extracellular matrix protein which affects cell migration [38] and has over 2-fold induction in wild-type macrophages but is not perturbed in

Zhx2-null cells (Table 4). When the threshold of differential expression was raised to 5-fold or greater, we did not identify any differentially regulated genes, as all genes have a similar magnitude of expression (Supplemental Table 2).

Transplantation of bone-marrow from Zhx2-null mice to wild-type mice significantly reduces size of atherosclerotic lesions: As described earlier, male BALB/cBy Ldlr -/- mice with the wild-type allele of Zhx2 develop lesions about nine times larger than mice with the null Zhx2 allele (Fig 1). In order to determine the contribution of cells arising from hematopoietic stem cells (HSCs), such as macrophages, towards this phenotype we performed a bone-marrow transplant on Zhx2 wild-type mice, replacing their bone marrow with Zhx2-null bone marrow (Fig 9). Preliminary data showed a marked decrease in atherosclerosis in the wild-type mice transplanted with Zhx2-null HSCs, with more than a four-fold decrease in size of lesions compared to control mice that were transplanted with wild-type HSCs (Fig 10). Lipid data analyzed from the blood plasma of the bone-marrow recipient mice showed no difference in triglycerides or HDL and a 30% decrease in total cholesterol in the mice with Zhx2-null HSCs (Fig 11).

Discussion:

Our studies provide definitive evidence that an absence of Zhx2 is athero-protective (Figures 1, 2). The dramatic pro-atherogenic effect of Zhx2 that results in up to a nine-fold increase of lesion size is not completely explained by its relatively minor effect on plasma lipid levels (Figures 4, 5), a comparison that is particularly noticeable in

females, who do not exhibit cholesterol differences between the two Zhx2 genotypes but have a 2.5-fold difference in lesion size. The expression data acquired from the livers of these mice provides support to the hypothesis that lipids are not primarily responsible for the atherosclerosis phenotype, as none of the differentially expressed genes between the Zhx2 wild-type and null livers are previously described as lipid metabolism genes. An analysis of the function of the 22 differentially expressed genes in both male and female mice point in the direction of the inflammatory response and cells of the hematopoietic system.

Following the leads provided from the liver gene expression data, we questioned if Zhx2 is involved with the inflammatory response of macrophages, a leukocyte whose activation has a central role in atherogenesis. We observed a striking induction of Zhx2 in response to the pro-inflammatory stimulus LPS. We further studied this response in a panel of inbred mice with varying susceptibilities to atherosclerosis that was designed for the fine-mapping of phenotypic traits [17]. LPS induces the inflammatory response in macrophages through the activation of the TLR4 receptor; the lack of Zhx2 induction in C3H mice, which have a mutation in the TLR4 receptor that attenuates their transcriptional response to LPS [39], suggests that the Zhx2 transcript induction by LPS is modulated through this pathway. Recent studies describe downstream TLR4 activation of XBP1s, a potent transcriptional activator [40]. Separate studies on a Hodgkin Lymphoma cell line identified a chromosomal rearrangement that represses Zhx2 expression [11] and further study identified that these mutations prevented the binding of XBP1 to the Zhx2 regulatory region [10]. These findings are consistent with a

hypothesis of LPS regulation of Zhx2 through the Tlr4-Xbp1 pathway but further studies are needed to confirm this assessment. The set of differentially expressed genes in Zhx2-null macrophages and the 60 transcripts with eQTL that map near Zhx2, some of which are also perturbed in Zhx2-null macrophages, provide potential targets of Zhx2 regulation. Additional studies on the binding of Zhx2 to specific DNA targets using ChIP-seq methods might help determine the direct regulatory targets of Zhx2.

The macrophage expression data support the role of Zhx2 as a transcriptional regulator of immune response genes. In addition to the strong up-regulation of Zhx2 after LPS treatment, we see differential expression in hundreds of genes in macrophages taken from Zhx2 null mice. This set of perturbed transcripts is enriched for immune response genes and has over 100-fold induction of the immune-related genes Irg1, Cfb, Clec4e, Cxcl2, and Il1b. Bone marrow transplant experiments further emphasize a role of the immune system in mediating the impact of Zhx2 impact on atherosclerosis. The preliminary BMT results shown here demonstrate a four-fold decrease of lesion size in wild-type mice which have Zhx2-null bone marrow. These mice express Zhx2-null macrophages and other immune cells but the rest of their tissues, including the vessel wall and liver, express functional Zhx2, demonstrating the effect that Zhx2 null leukocytes play in preventing atherogenesis. The slight decrease in plasma cholesterol in Zhx2 wild-type mice with Zhx2-null HSCs may be a result of the decreased atherosclerosis in these mice; it could also be interpreted as a result of the difference in inflammatory response. Atherosclerosis studies on liver-specific transgenic

Zhx2 mouse on Ldlr -/- background will allow us to determine the contribution of the immune system versus the liver to cholesterol levels.

Based on our findings, we hypothesize that a main function of Zhx2 is as a transcriptional repressor of anti-inflammatory factors. The absence of Zhx2 results in a reduced inflammatory response, which subsequently reduces atherogenesis by affecting cells of the immune system, notably the macrophages that are a significant contributor to atheromas. As seen in the transcriptional data from macrophages, Zhx2 may also control apoptosis. A pro-apoptotic role of Zhx2 would be consistent with its role as a tumor suppressor in lymphomas, where a lack of Zhx2 is pro-cancerous, as well as in atherosclerosis, where apoptosis of leukocytes contributes to the growing atherosclerotic lesions. ChIP-seq may provide some definitive answers by identifying direct DNA targets of this gene and allow for the parsing of individual transcriptional and activation cascades. We believe that further work on Zhx2 may identify novel inflammatory pathways in the cells of immune system, and provide new drug targets for the treatment of atherosclerosis.

Figure 1: Zhx2 absence is atheroprotective in male mice. Boxplot showing lesion data for male Zhx2 wild-type and Zhx2-null mice on a BALB/cJ background. Mice were placed on a western diet at 8 weeks of age and euthanized after 18 weeks of diet. Zhx2 wild-type n=19, Zhx2 null n=17; outliers removed.

Figure 2: Zhx2 absence is atheroprotective in female mice. Boxplot showing lesion data for female Zhx2 wild-type and Zhx2-null mice on a BALB/cJ background. Mice were placed on a western diet at 8 weeks of age and euthanized after 18 weeks of diet. Zhx2 wild-type n=24, Zhx2 null n=17.

Figure 3: Absence of Zhx2 reduces aneurysm and aortic calcification. Bar graphs showing aneurysm and aortic calcification data for male and female Zhx2 wild-type and Zhx2-null mice on a BALB/cJ background. No aneurysms were observed for male Zhx2 null mice. Mice were placed on a western diet at 8 weeks of age and euthanized after 18 weeks of diet. Female Zhx2 wild-type n=24, Zhx2 null n=18; male Zhx2 wild-type n=19, Zhx2 null n=17

Figure 4: Blood plasma levels in males are affected by Zhx2 expression. Bar graph showing blood plasma lipid data for male Zhx2 wild-type and Zhx2-null mice on a BALB/cJ background. Mice were placed on a western diet at 8 weeks of age and euthanized after 18 weeks of diet. Zhx2 wild-type n=17, Zhx2 null n=10. Error bars indicate standard error.

Figure 5: Cholesterol levels in female mice are not affected by Zhx2 expression. Bar graph showing blood plasma lipid data for female Zhx2 wild-type and Zhx2-null mice on a BALB/cJ background. Mice were placed on a western diet at 8 weeks of age and euthanized after 18 weeks of diet. Zhx2 wild-type n=24, Zhx2 null n=17. Error bars indicate standard error.

Figure 6: Zhx2 transcript levels in macrophages are induced after LPS treatment. A. Zhx2 transcript levels in macrophages isolated from Zhx2 wild-type and null LDLR -/- mice on a chow diet before and after LPS treatment; levels as determined by RT-qPCR and normalized to the housekeeping gene 36B4, n=3 B. Zhx2 transcript levels in macrophages isolated from BL6 and C3H mice, before and after LPS treatment; expression data from Illumina arrays, pooled samples of 3 mice each.

Figure 7: Zhx2 expression in macrophages varies across 64 strains of inbred mice A: Baseline levels of Zhx2 in macrophages isolated from 64 strains of inbred strains of mice ordered according to expression levels; expression values are measured by RT-qPCR and normalized to Rpl4. B. Zhx2 levels after treatment with LPS expression ordered according to expression of Zhx2; values are measured by RT-qPCR and normalized to Rpl4 C. Fold-induction of Zhx2 after LPS treatment for each strain ordered according to induction; normalized Zhx2 value of LPS induced value divided by baseline Zhx2 value.

Figure 8: Venn diagram of LPS induced genes in Zhx2 wild-type vs null macrophages

Figure 9: Bone marrow transplants change the genotype of HSC in recipient mice. DNA genotyping of blood isolated from bone marrow transplant recipients. Recipients are Zhx2 wild-type; after bone marrow repopulation the HSCs are Zhx2 null. Genotyping performed using PCR genotyping, bands separated using gel electrophoresis on 2% agarose gel.

Figure 10: Zhx2-null bone marrow reduces size of atherosclerotic lesions in Zhx2 wild-type mice. Boxplot showing lesion data for bone marrow transplant recipients. Zhx2 wild-type male mice were transplanted with bone marrow isolated from Zhx2-null or Zhx2 wild-type as a control at 6 to 8 weeks of age. After a recovery period, they were fed a western diet for 18 weeks. Data shows 7 mice transplanted with wild-type bone marrow and 9 mice transplanted with Zhx2-null bone-marrow.

Figure 11: Bar graph showing blood plasma lipid data for BMT recipients. Error bars indicate standard error.

Table1: Differentially expressed genes in LDLR -/- livers on western diet are enriched for inflammatory and hematopoetic genes. Microarray expression data on RNA isolated from the liver of both male and female mice analyzed for atherosclerosis. Statistically significant differentially expressed genes were identified from Zhx2 wild-type and null livers; the overlap of those genes are shown in this table. The fold-change of the genes

in the direction of Zhx2 wild-type to null mice. Statistical significance is defined as an adjusted p-value of less than 0.05

Table 2: eQTL hotspot near Zhx2 shows regulation for 60 unique genes. Gene expression of 60 transcripts maps to the genomic region on chromosome 15 between 58-60 Mb; Zhx2 is located from 57.5-57.66 Mb.

Table 3: Zhx2 absence in macrophages results in a de-regulation of a large number of genes. Differentially expressed genes in macrophages isolated from Zhx2 wild-type and null mice organized by fold-change. Statistically significant differential expression determined by an adjusted p-value of less than 0.05.

Table 4: LPS-induced genes that differ between Zhx2 genotypes Direction in fold-change is from untreated to LPS treated.

Supplemental Table 1: Gene ontology results for Zhx2 wild-type and null macrophage gene expression data. Differentially expressed genes in macrophages collected from Zhx2 wild-type vs null were analyzed for gene ontology enrichment using DAVID gene ontology tools. Ontology categories with Bonferroni adjusted p-values over 0.05 are shown.

Supplemental Table 2: Gene expression fold-changes in response to LPS treatment in Zhx2 wild-type and null macrophages are similar. Differentially expressed genes in

macrophages collected from Zhx2 wild-type vs null were analyzed for differential expression after LPS treatment; genes up-regulated 5+ in Zhx2 wild-type macrophages are shown.

Figure 1:

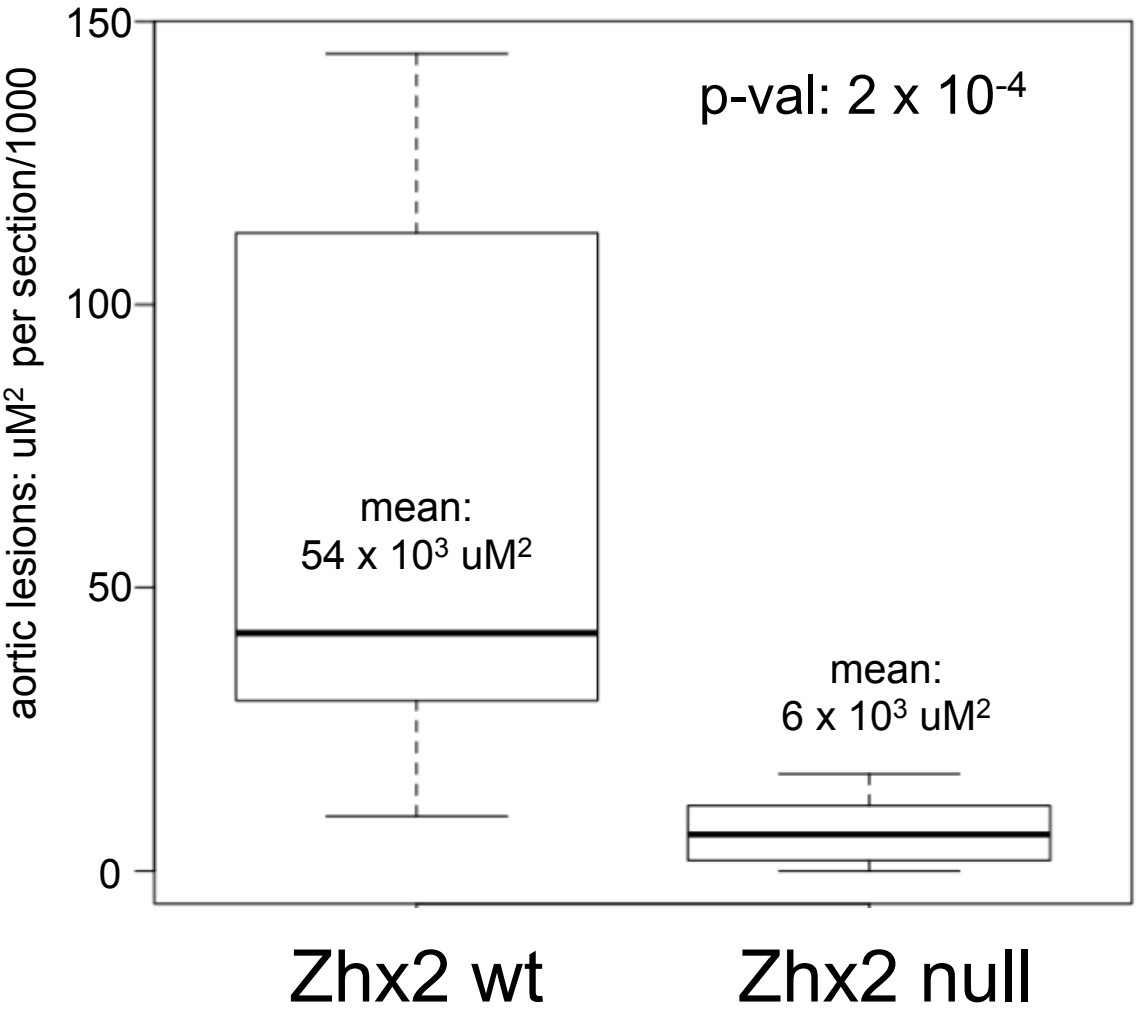
150
100
50
0
aortic lesions: uM² per section/1000
p-val: 2 x 10-4
mean:
54 x 10³ uM²
mean:
6 x 10³ uM²
Zhx2 wt
Zhx2 null

Figure 2:

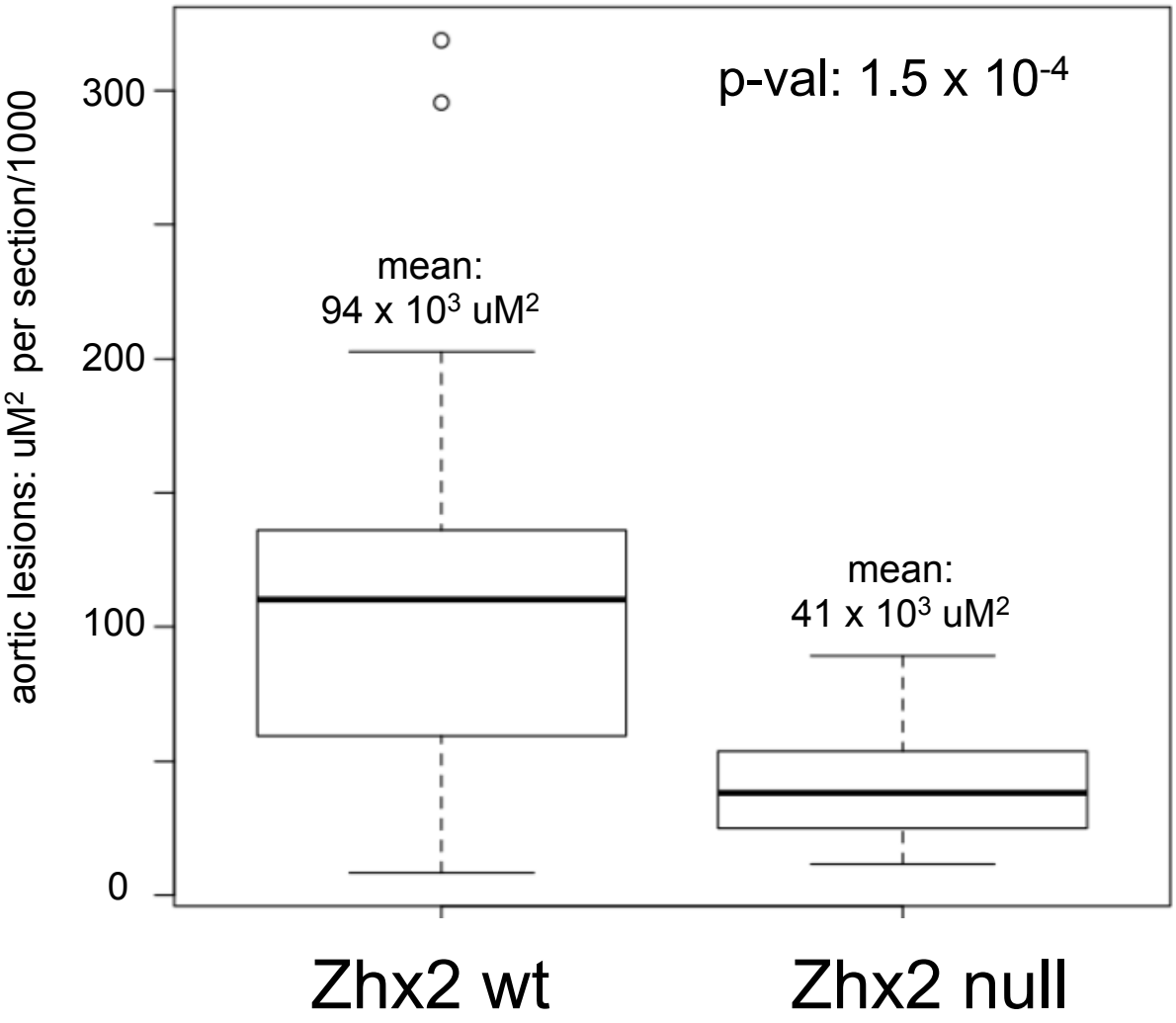
p-val: 1.5 x 10-4
aortic lesions: uM2 per section/1000
300
200
100
0
mean:
94 x 10³ uM²
mean:
41 x 10³ uM²
Zhx2 wt
Zhx2 null

Figure 3

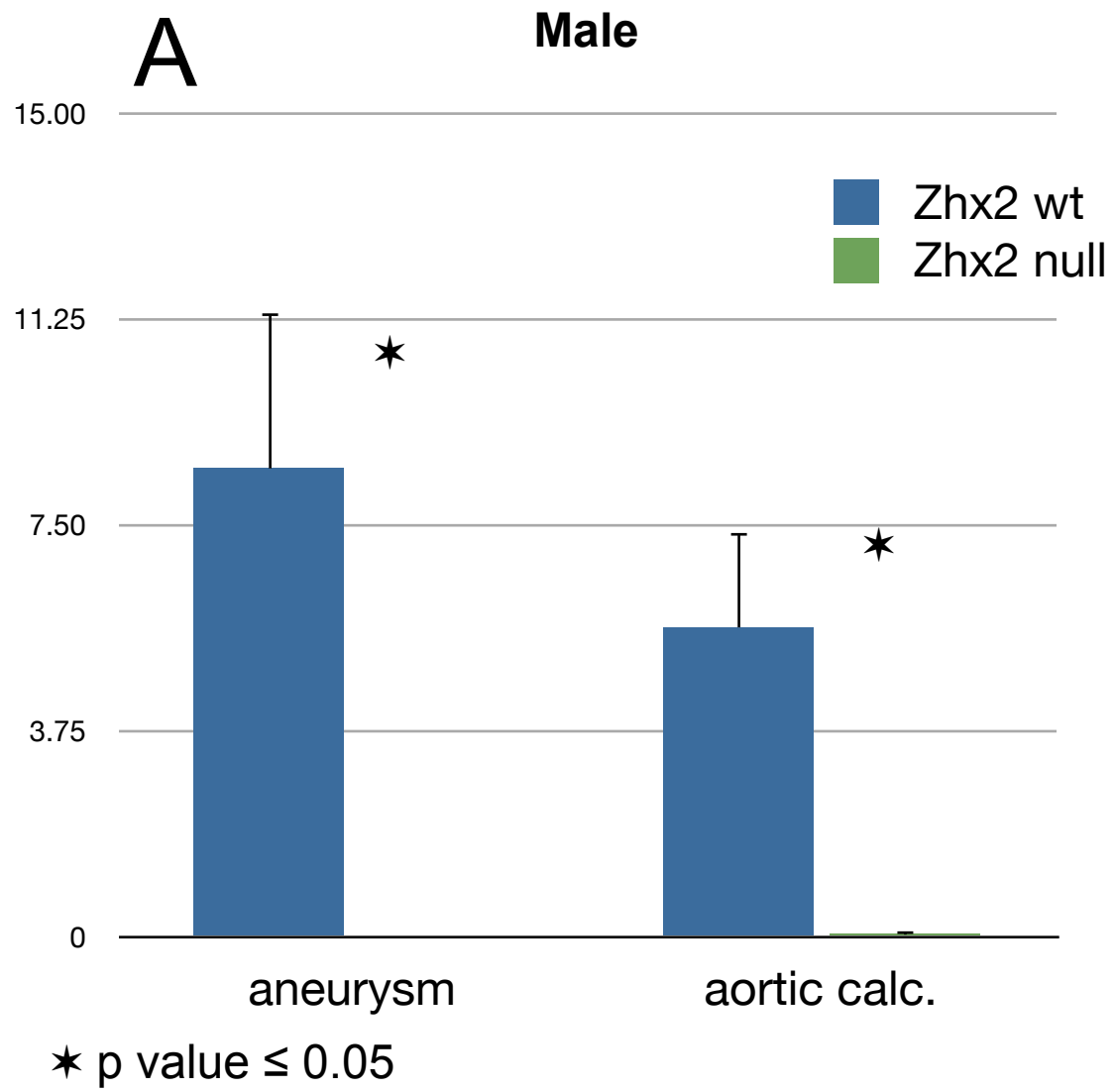
A
Male
15.00
11.25
7.50
3.75
0
Zhx2 wt
Zhx2 null
aneurysm
aortic calc.
✶ p value ≤ 0.05

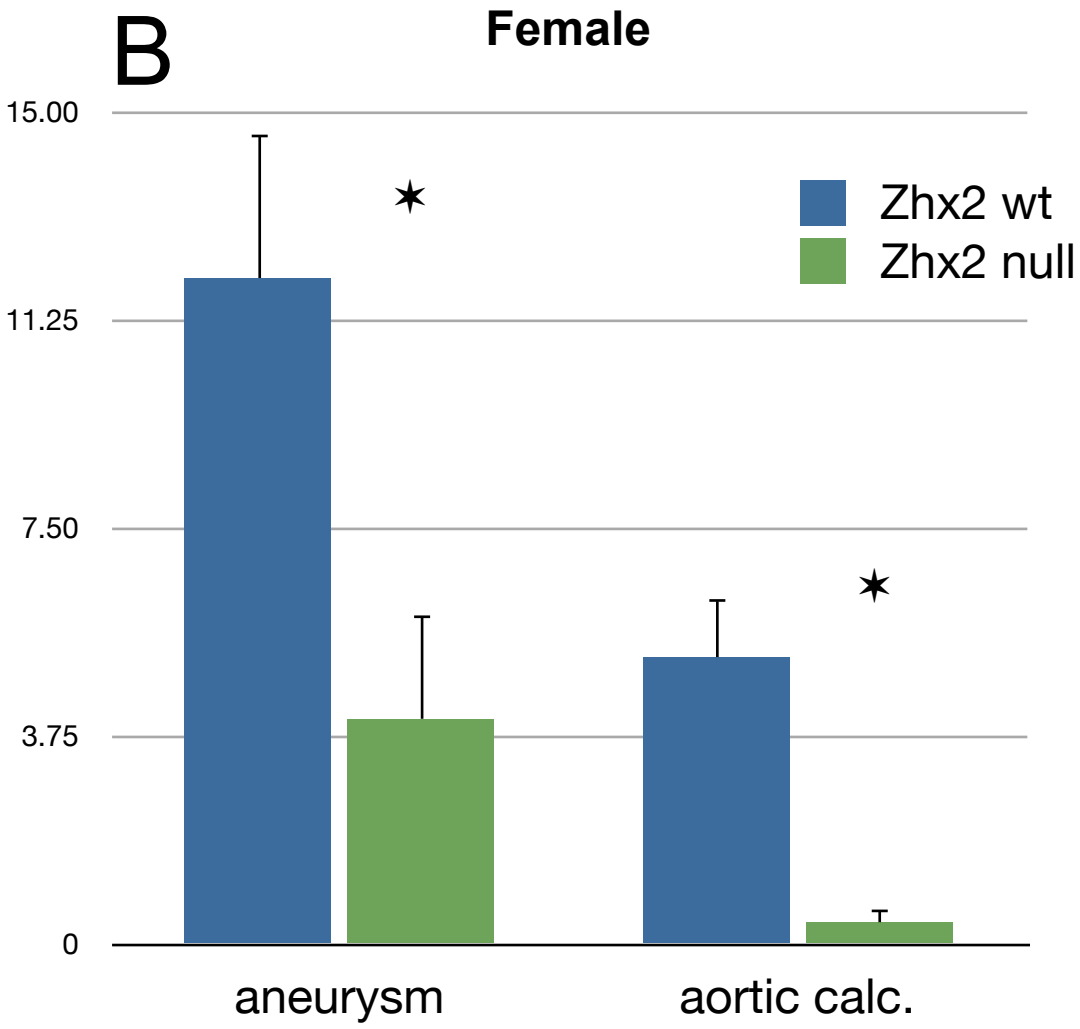
B
Female
15.00
11.25
7.50
3.75
0
Zhx2 wt
Zhx2 null
aneurysm
aortic calc.

Figure 4:

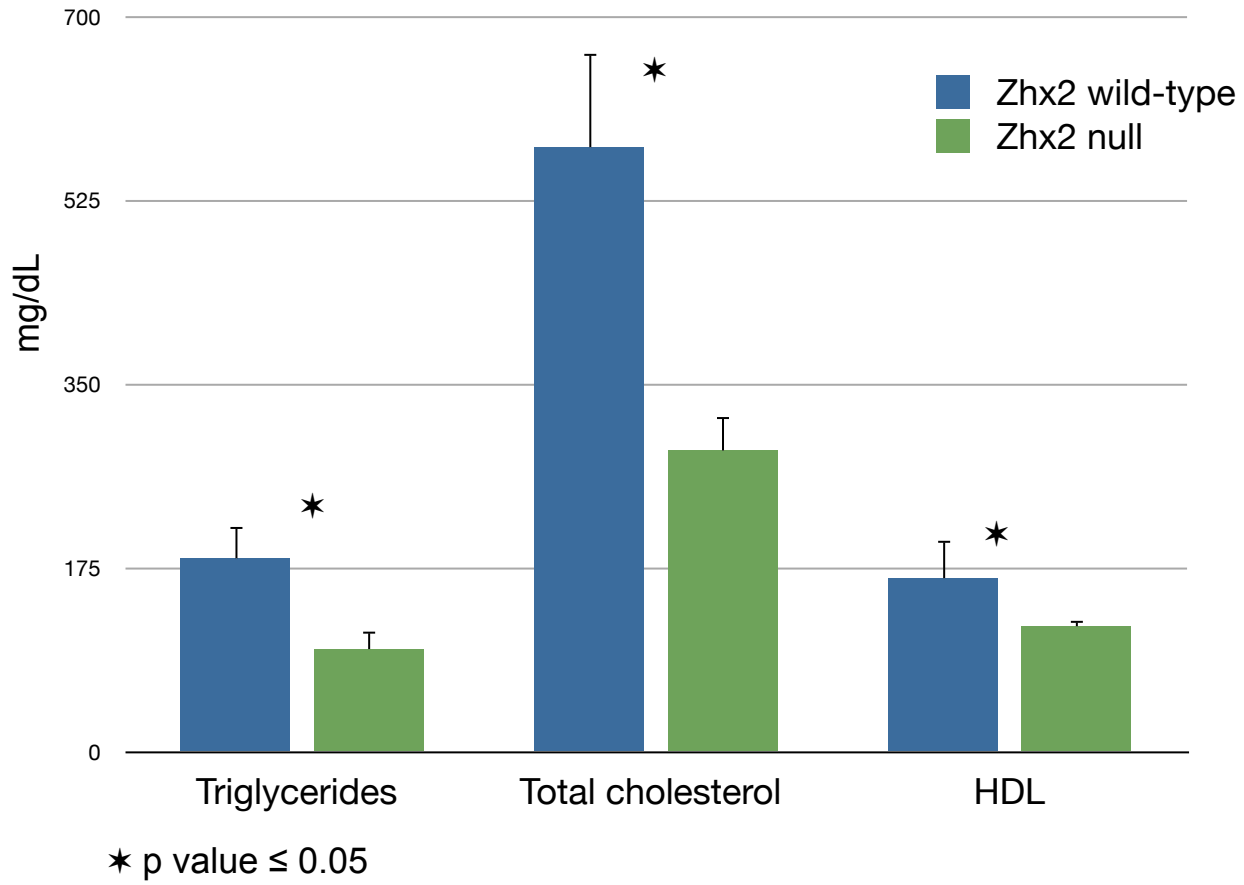
700
525
350
175
0
mg/dL
Zhx2 wild-type
Zhx2 null
Triglycerides
Total cholesterol
HDL
✶ p value ≤ 0.05

Figure 5:

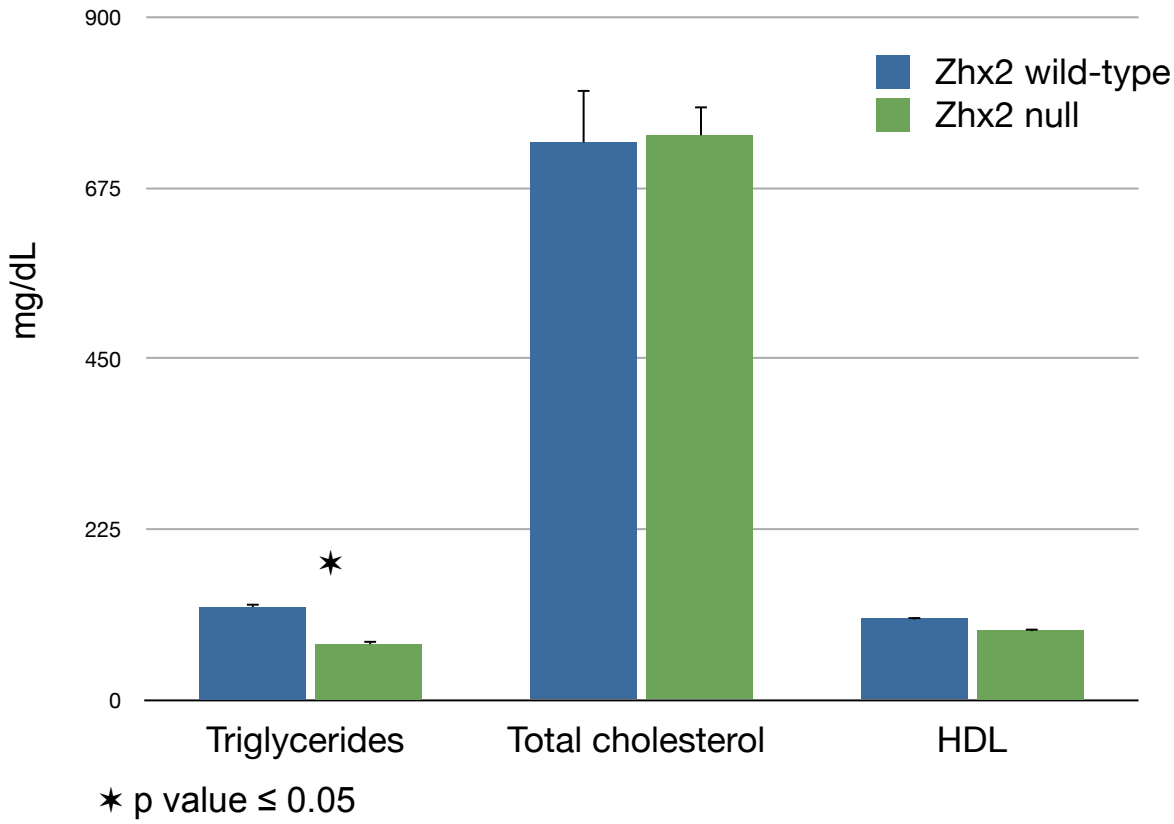
900
675
450
225
0
mg/dL
Zhx2 wild-type
Zhx2 null
✶
Triglycerides
Total cholesterol
HDL
✶ p value ≤ 0.05

Figure 6:

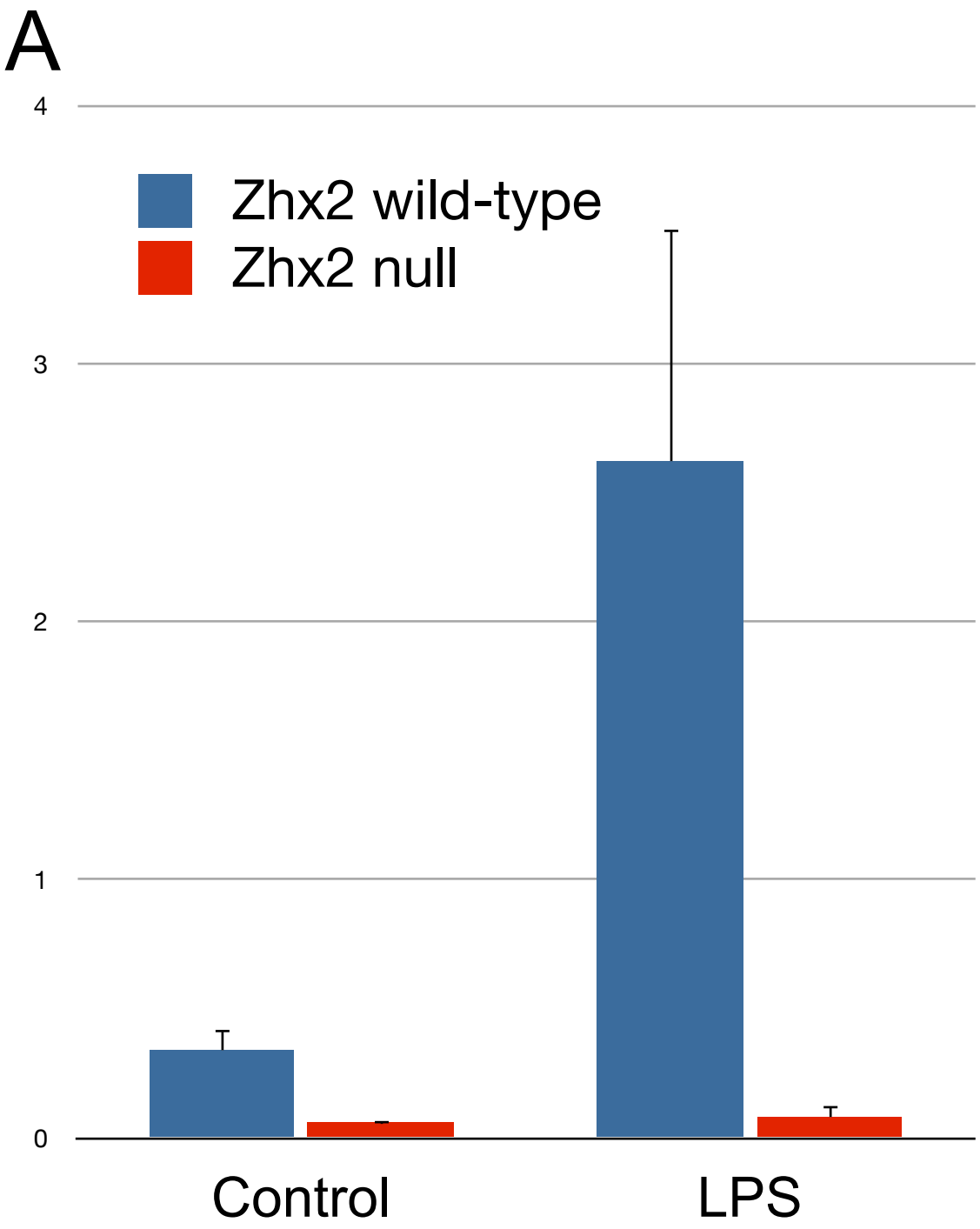

B

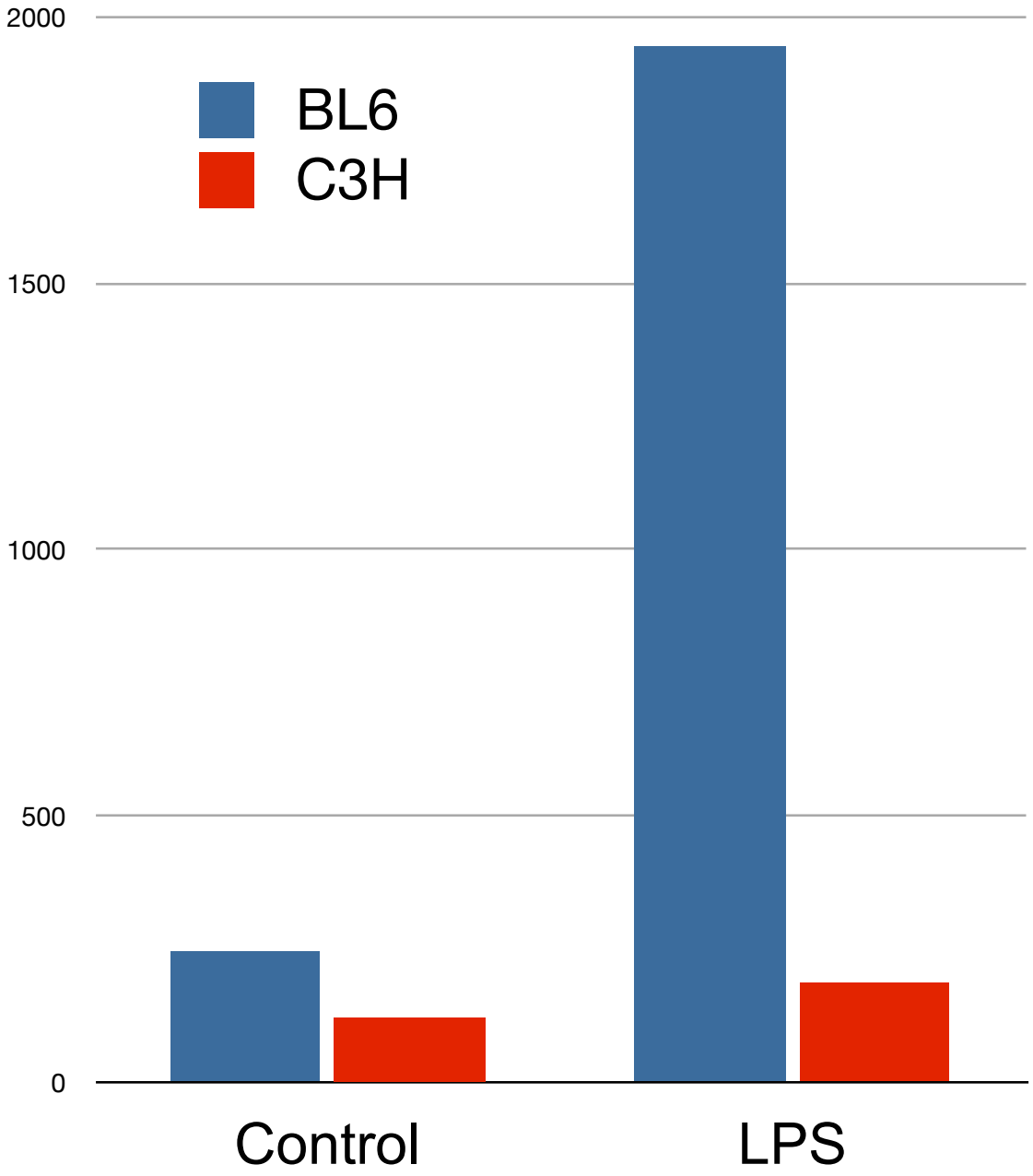

Figure 7:

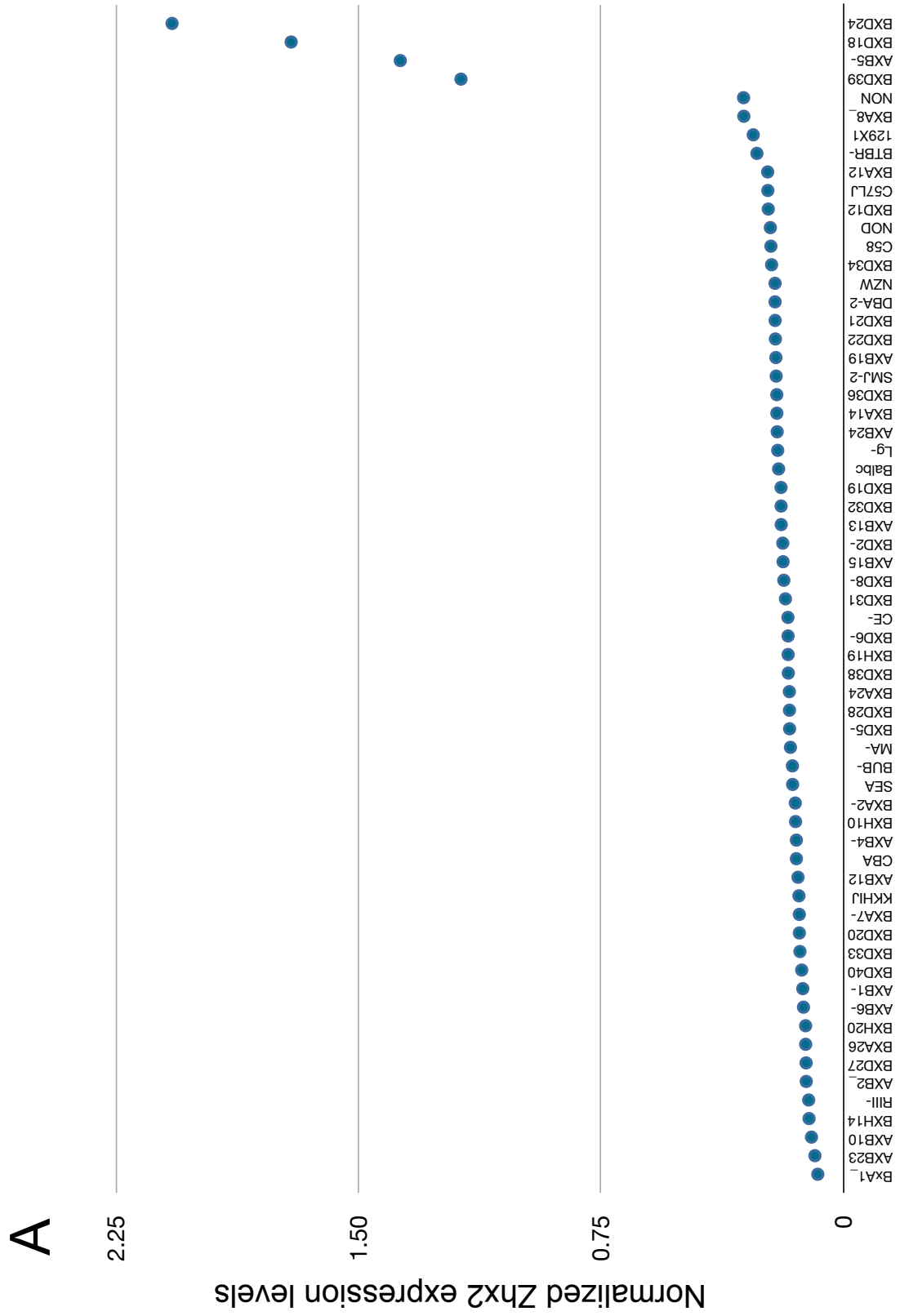
A
Normalized Zhx2 expression levels
2.25
1.50
0.75
0
BXD24
BXD18
AXB5-
BXD39
NON
BXA8_
129X1
BTBR-
BXA12
C57LJ
BXD12
NOD
C58
BXD34
NZW
DBA-2
BXD21
BXD22
AXB19
SMJ-2
BXD36
BXA14
AXB24
Lg-
Balbc
BXD19
BXD32
AXB13
BXD2-
AXB15
BXD8-
BXD31
CE-
BXD6-
BXH19
BXD38
BXA24
BXD28
BXD5-
MA-
BUB-
SEA
BXA2-
BXH10
AXB4-
CBA
AXB12
KKHIJ
BXA7-
BXD20
BXD33
BXD40
AXB1-
AXB6-
BXH20
BXA26
BXD27
AXB2_
RIII-
BXH14
AXB10
AXB23
BxA1_

B
Normalized Zhx2 expression levels
0
1.75
3.50
Balbc
BUB-
BXH10
BXH20
RIII-
BXH14
CE-
MA-
BXA8_
Lg-
AXB23
CBA
SEA
AXB6-
NZW
AXB2_
C58
BXA12
DBA-2
BXD24
BTBR-
129X1
AXB15
BXD20
BxA1_
BXA14
BXD22
BXD8-
BXH19
KKHIJ
BXD31
BXD27
AXB4-
NON
AXB12
AXB24
SMJ-2
NOD
BXD19
BXA7-
BXD40
AXB13
BXD28
BXA26
BXA2-
BXD2-
BXD32
AXB10
C57LJ
BXD33
AXB5-
BXD18
BXD5-
BXD39
BXD36
AXB1-
BXD12
BXD6-
BXD34
BXD21
BXD38
AXB19
BXA24

C
25.00
18.75
12.50
6.25
0
Fold-induction of Zhx2
Balbc
BXD24
BUB-
BXD18
BXH10
AXB5-
BXD39
BXA8_
CE-
BXH20
Lg-
RIII-
BXH14
MA-
129X1
BTBR-
C58
NZW
BXA12
NON
DBA-2
SEA
CBA
BXD22
BXA14
NOD
AXB15
SMJ-2
AXB24
C57LJ
BXD8-
BXD31
AXB6-
BXD12
BXD19
BXH19
AXB13
BXD34
BXD36
BXD32
AXB2_
AXB23
BXD2-
BXD20
BXD21
BXD28
AXB4-
KKHIJ
AXB19
AXB12
BXD5-
BXD6-
BXA2-
BXA7-
BXD40
BXD27
BXD38
BXD33
BXA24
BXA26
AXB1-
BxA1_
AXB10

Figure 8:

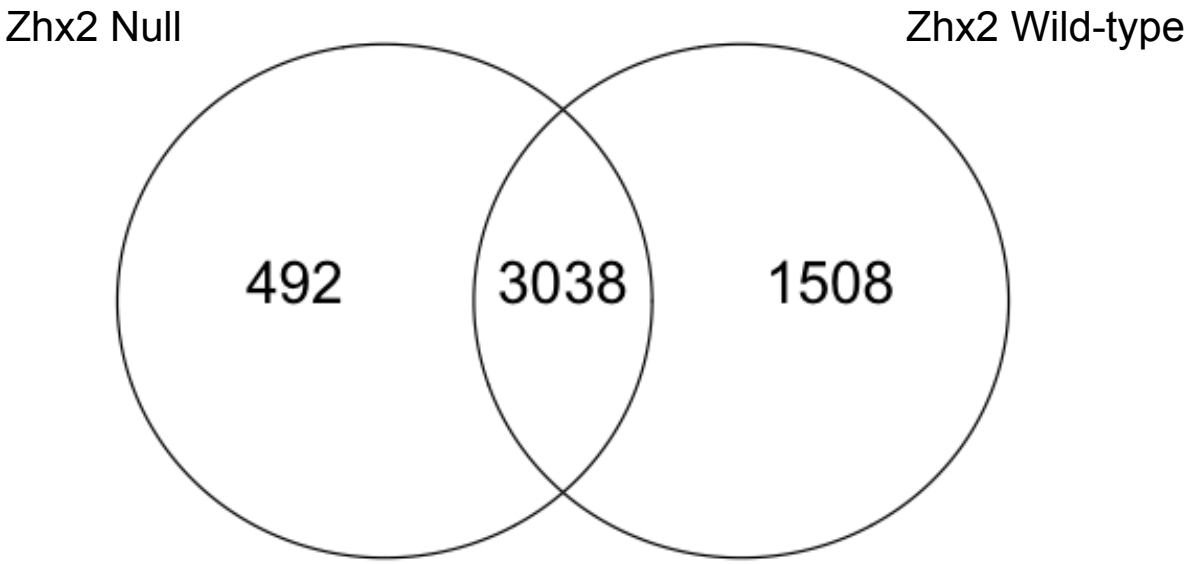

Figure 9:

Figure 9: Bone marrow transplants change the genotype of HSC in recipient mice. DNA genotyping of blood isolated from bone marrow transplant recipients. Recipients are Zhx2 wild-type; after bone marrow repopulation the HSCs are Zhx2 null. Genotyping performed using PCR genotyping, bands separated using gel electrophoresis on 2% agarose gel.

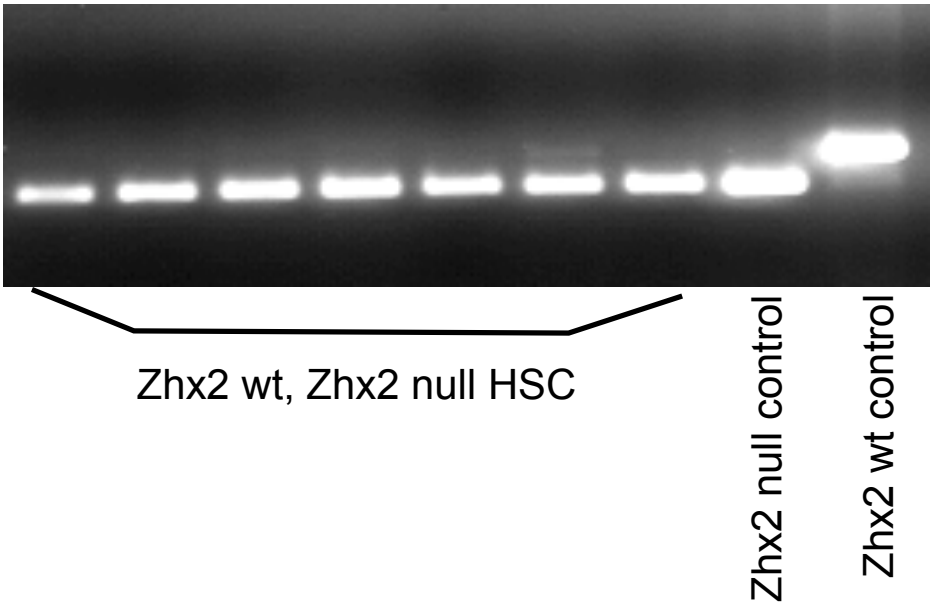

Figure 10:

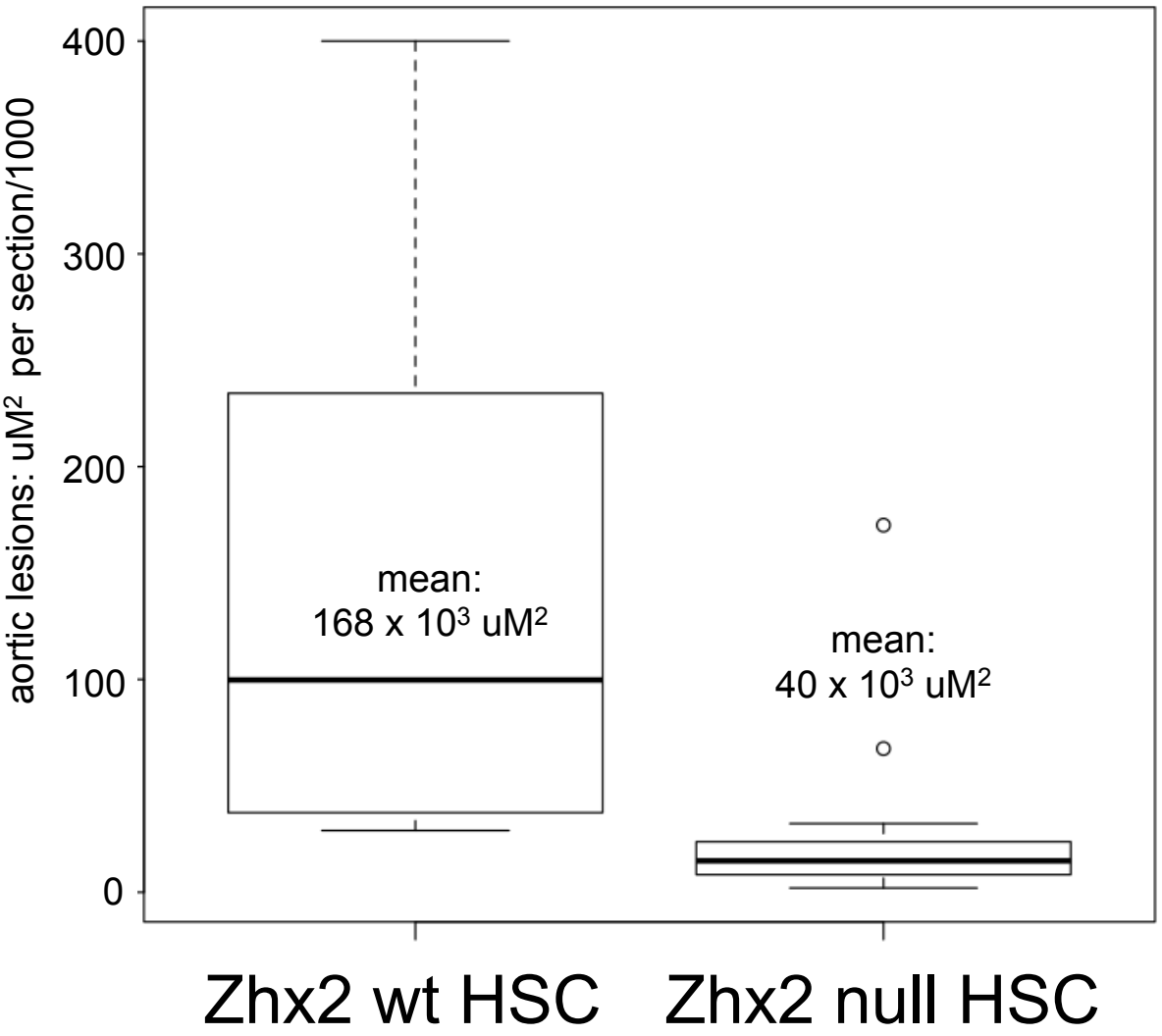
400
300
200
100
0
aortic lesions: uM2 per section/1000
mean:
168 x 10^3 uM^2
mean:
40 x 10^3 uM^2
Zhx2 wt HSC
Zhx2 null HSC

Figure 11:

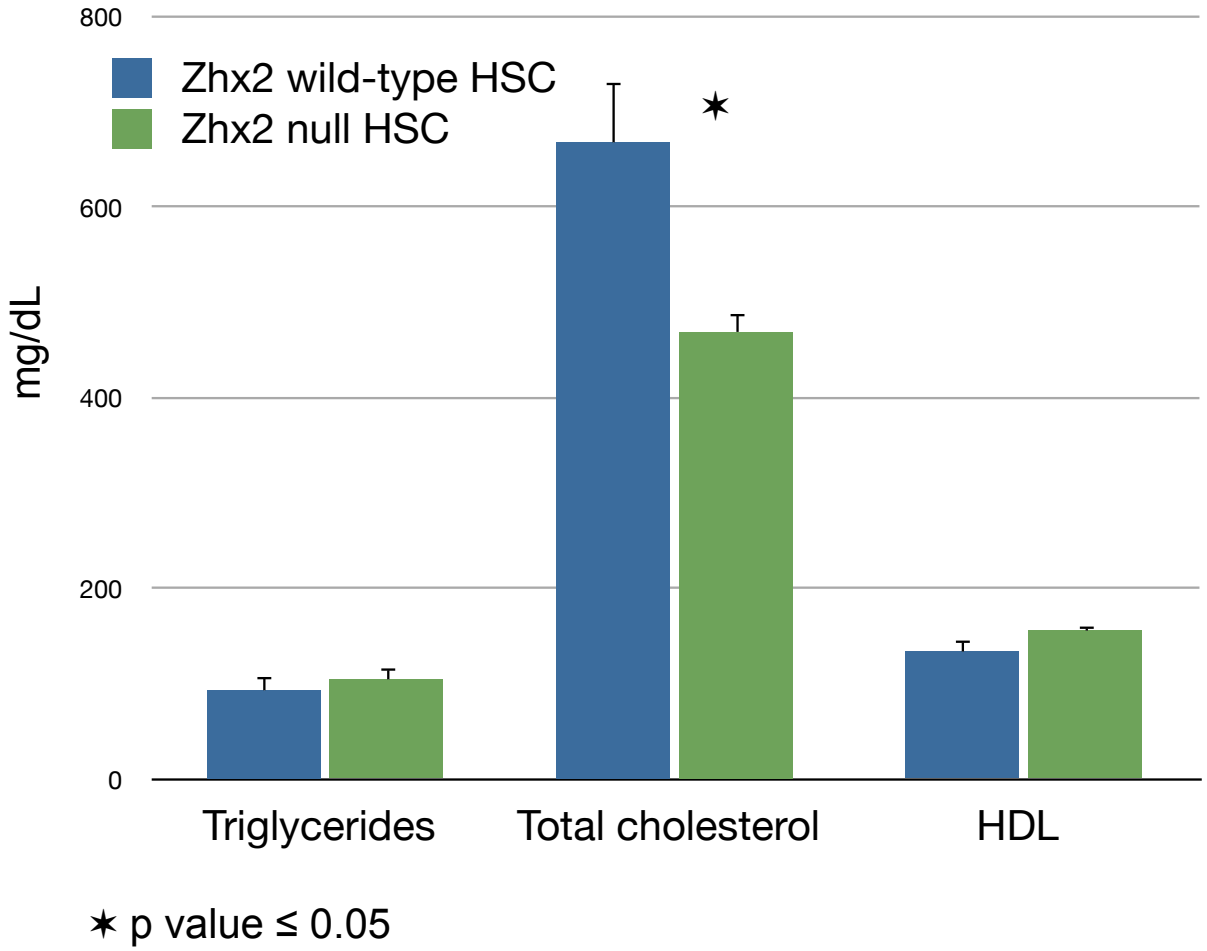

✶ p value ≤ 0.05

Table1:

gene	fold-change male	fold-change female
Amer2	2.26**	3.20***
Aprt	-1.86**	-1.79***
B930041F14RIK	2.27*	3.34***
Slc44a3	2.85**	2.05**
Bhlhb9	3.66***	3.11***
Caln1	1.84**	1.41*
Hcp-1	1.82**	1.59***
D330045A20RIK	5.10**	6.57***
DAct2	-2.87**	-2.52***
EG381438	1.93*	1.73**
Heatr1	-1.66*	-1.50**
Hist1h2ao	1.91*	1.80**
Irf2	-1.70*	-1.47**
Meis1	2.24*	2.30***
Mmd2	-4.22*	-2.35*
Mpp1	2.36*	2.51***
Oat	-2.56*	-1.74*
Pdir	-1.99	-1.77***
Slc1a2	-2.14**	-2.37***
Spc25	3.07**	2.81***
Sult1c2	3.01**	3.97***
Zap70	-5.16**	-4.76***

Table 2:

Abcg2	D17892	Mgea5	Tmc4
Abhd1	Efcab7	Mllt11	Top1mt
Acss2	Elac2	Mpst	Tsc22d1
Alg12	Eny2	Ms4a7	Tsg101
Als2	Epb4.1l1	Mxd4	Ttc30a1
Amdhd1	Gdpd3	Ndrg1	Ugp2
Angel1	Gna11	Pank3	Vgll4
Apbb3	Hyi	Pitpnc1	Wbscr27
Basp1	Ifitm3	Pja1	Yipf2
BC023814	Ift80	Psmc3	Zbtb25
Bcl2	Itpr3	Ptpmt1	Zfp91
Ccdc137	Kat2a	Ptpn21	Zfp94
Ccdc84	Kdm5d	Rcbtb2	
Cdc37l1	Leng1	Rpl14	
Chmp6	Limk2	Rusc1	
Cotl1	Lnx2	Sfrs12	

Table 3:

Female

Fold-change	no. genes
100+	4
20+	26
10+	64
5+	137
2+	625

Male

Fold-change	no. genes
100+	5
20+	29
10+	69
5+	151
2+	597

Table 4:

	Zhx2 wild-type Fold-change	Zhx2 null Fold-change
Thbs1	2.48	
Edr1l/1427820_at	2.29	
Speg	-2.34	
Mgp	-2.79	
Cxcl13		2.65
Bcl6		-1.88
Cacna1a		-2.13

Supplemental Table 1

Category	Term	Count	Adj. p-value
GOTERM_BP_FAT	GO:0006955~immune response	99	2.00E-25
SP_PIR_KEYWORDS	proteasome	23	1.52E-11
GOTERM_CC_FAT	GO:0000502~proteasome complex	23	5.78E-11
SP_PIR_KEYWORDS	immune response	37	1.74E-08
KEGG_PATHWAY	mmu03050:Proteasome	20	4.11E-08
GOTERM_CC_FAT	GO:0009986~cell surface	47	1.99E-07
SP_PIR_KEYWORDS	phosphoprotein	446	2.77E-07
GOTERM_MF_FAT	GO:0032553~ribonucleotide binding	164	1.89E-06
GOTERM_MF_FAT	GO:0032555~purine ribonucleotide binding	164	1.89E-06
GOTERM_MF_FAT	GO:0017076~purine nucleotide binding	169	2.19E-06
GOTERM_BP_FAT	GO:0019882~antigen processing and presentation	24	2.49E-06
GOTERM_CC_FAT	GO:0005773~vacuole	35	2.91E-06
GOTERM_BP_FAT	GO:0042127~regulation of cell proliferation	70	3.06E-06
GOTERM_CC_FAT	GO:0005764~lysosome	32	4.61E-06
GOTERM_CC_FAT	GO:0000323~lytic vacuole	32	5.29E-06
SP_PIR_KEYWORDS	acetylation	192	7.34E-06
GOTERM_CC_FAT	GO:0005829~cytosol	64	1.08E-05
GOTERM_CC_FAT	GO:0005839~proteasome core complex	11	1.12E-05
GOTERM_CC_FAT	GO:0009897~external side of plasma membrane	34	1.31E-05
KEGG_PATHWAY	mmu04620:Toll-like receptor signaling pathway	25	2.38E-05
SP_PIR_KEYWORDS	nucleotide-binding	143	2.51E-05
SP_PIR_KEYWORDS	Apoptosis	46	2.56E-05
SP_PIR_KEYWORDS	threonine protease	11	2.69E-05
GOTERM_BP_FAT	GO:0001817~regulation of cytokine production	29	3.03E-05
KEGG_PATHWAY	mmu04623:Cytosolic DNA-sensing pathway	18	3.92E-05
INTERPRO	IPR001353:Proteasome, subunit alpha/beta	11	4.31E-05
SP_PIR_KEYWORDS	lysosome	27	4.95E-05
SP_PIR_KEYWORDS	cytoplasm	233	6.00E-05
GOTERM_MF_FAT	GO:0004298~threonine-type endopeptidase activity	11	7.81E-05
GOTERM_MF_FAT	GO:0070003~threonine-type peptidase activity	11	7.81E-05
GOTERM_MF_FAT	GO:0000166~nucleotide binding	183	1.12E-04
GOTERM_BP_FAT	GO:0008285~negative regulation of cell proliferation	37	1.36E-04
GOTERM_BP_FAT	GO:0012501~programmed cell death	59	3.48E-04
GOTERM_BP_FAT	GO:0006915~apoptosis	58	4.50E-04
KEGG_PATHWAY	mmu04060:Cytokine-cytokine receptor interaction	40	5.19E-04
SMART	SM00252:SH2	22	5.94E-04
GOTERM_BP_FAT	GO:0042981~regulation of apoptosis	65	6.46E-04
SP_PIR_KEYWORDS	disulfide bond	191	8.81E-04
INTERPRO	IPR000980:SH2 motif	22	9.95E-04
GOTERM_BP_FAT	GO:0043067~regulation of programmed cell death	65	0.001019101
INTERPRO	IPR001353:Proteasome, alpha and beta subunits	9	0.001105222
GOTERM_BP_FAT	GO:0010941~regulation of cell death	65	0.00123475
KEGG_PATHWAY	mmu04621:NOD-like receptor signaling pathway	17	0.001257516

Category	Term	Count	Bonferroni
GOTERM_BP_FAT	GO:0048002~antigen processing and presentation of pe	13	0.001285259
SP_PIR_KEYWORDS	atp-binding	112	0.0013044
GOTERM_BP_FAT	GO:0001819~positive regulation of cytokine production	17	0.001336873
GOTERM_BP_FAT	GO:0008219~cell death	60	0.001625373
SP_PIR_KEYWORDS	hydrolase	126	0.001640055
GOTERM_MF_FAT	GO:0005524~ATP binding	126	0.002669841
INTERPRO	IPR016050:Proteasome, beta-type subunit, conserved s	8	0.002964788
GOTERM_MF_FAT	GO:0001883~purine nucleoside binding	133	0.003031889
GOTERM_BP_FAT	GO:0016265~death	60	0.003553496
GOTERM_BP_FAT	GO:0006952~defense response	54	0.003789945
GOTERM_MF_FAT	GO:0001882~nucleoside binding	133	0.004173604
GOTERM_MF_FAT	GO:0032559~adenyl ribonucleotide binding	126	0.004717151
GOTERM_MF_FAT	GO:0030554~adenyl nucleotide binding	131	0.005103762
SP_PIR_KEYWORDS	P-loop	15	0.005267561
SP_PIR_KEYWORDS	SH2 domain	19	0.006976603
KEGG_PATHWAY	mmu04142:Lysosome	23	0.008612313
KEGG_PATHWAY	mmu05332:Graft-versus-host disease	15	0.010464115
GOTERM_BP_FAT	GO:0002822~regulation of adaptive immune response b	15	0.010487294
GOTERM_BP_FAT	GO:0019221~cytokine-mediated signaling pathway	15	0.010487294
GOTERM_BP_FAT	GO:0002819~regulation of adaptive immune response	15	0.010487294
KEGG_PATHWAY	mmu04062:Chemokine signaling pathway	30	0.010536127
GOTERM_BP_FAT	GO:0051174~regulation of phosphorus metabolic proce	40	0.011218342
GOTERM_BP_FAT	GO:0019220~regulation of phosphate metabolic proces	40	0.011218342
SP_PIR_KEYWORDS	transmembrane protein	42	0.011241728
GOTERM_BP_FAT	GO:0002237~response to molecule of bacterial origin	14	0.011397544
GOTERM_BP_FAT	GO:0042325~regulation of phosphorylation	39	0.011421566
GOTERM_BP_FAT	GO:0009611~response to wounding	44	0.011678257
GOTERM_BP_FAT	GO:0002694~regulation of leukocyte activation	26	0.012663019
GOTERM_BP_FAT	GO:0048584~positive regulation of response to stimulus	29	0.01557816
GOTERM_BP_FAT	GO:0050865~regulation of cell activation	26	0.016018749
KEGG_PATHWAY	mmu04612:Antigen processing and presentation	19	0.016690243
SMART	SM00338:BRLZ	13	0.017927723
SP_PIR_KEYWORDS	glycoprotein	253	0.019443921
SP_PIR_KEYWORDS	nucleotide binding	14	0.020621492
SMART	SM00429:IPT	10	0.021067178
KEGG_PATHWAY	mmu04210:Apoptosis	18	0.030132313
GOTERM_MF_FAT	GO:0032561~guanyl ribonucleotide binding	42	0.033622597
GOTERM_MF_FAT	GO:0019001~guanyl nucleotide binding	42	0.033622597
INTERPRO	IPR000243:Peptidase T1A, proteasome beta-subunit	6	0.036427115
GOTERM_BP_FAT	GO:0051249~regulation of lymphocyte activation	24	0.039403007
GOTERM_BP_FAT	GO:0002684~positive regulation of immune system proc	30	0.039799819
GOTERM_MF_FAT	GO:0005525~GTP binding	41	0.041173189
GOTERM_BP_FAT	GO:0002697~regulation of immune effector process	18	0.041777618
INTERPRO	IPR004827:Basic-leucine zipper (bZIP) transcription fact	13	0.044967336
GOTERM_BP_FAT	GO:0001914~regulation of T cell mediated cytotoxicity	7	0.045590847

Supplemental Table 2

	fold-change	
Gene	Zhx2 wild-type	Zhx2 null
Il1b	387	367
Tnfsf9	139	151
Cxcl2	126	147
Tnf	107	95
Ifit1	101	115
Irg1	91	73
Cxcl1	86	143
Ccl5	81	66
Il6	78	87
C78513	75	59
Ccl4	62	50
Cd40	51	53
Rsad2	48	54
Isg15	47	54
Ptgs2	46	59
Rsad2	45	54
Oasl1	41	45
Nfkbiz	40	48
Cd40	38	43
Cxcl10	36	45
Marcksl1	36	24
Mx1	34	49
Pde4b	34	25
Niacr1	34	30
Cmpk2	33	42
Pde4b	31	30
Gbp3	28	31
Nfkbiz	28	29
Fpr2	27	22
Il12a	26	39
Gbp1	26	22
Ifit2	26	42
Clec4e	25	24
Socs3	25	22
Rsad2	25	29
Gpr84	23	16
Rtp4	22	34
Nlrp3	22	19
Il12b	21	45
Ccl3	21	23
Il1a	21	23

	fold-change	
Gene	Zhx2 wild-type	Zhx2 null
Trex1	20	20
Marcksl1	20	15
Mpa2l	20	24
Mir155	19	17
Mefv	19	20
Ifit3	19	31
Traf1	19	19
Socs3	19	20
Icam1	18	18
Maff	17	14
Socs3	17	19
Nfkbie	16	14
Gbp6	15	20
Vcam1	15	14
Irf1	15	12
Olr1	15	12
Ifih1	14	14
F10	14	11
Tgtp1/Tgtp2	14	24
Mx2	14	18
F10	14	9.9
Gbp2	14	15
Parp14	14	13
Inhba	14	11
Casp4	14	11
Gpr85	14	19
Gem	14	13
Ptgs2	13	16
Ccl2	13	12
AW112010	13	13
Gbp6	12	19
Gbp2	12	13
Ehd1	11	10
Edn1	11	16
Marcksl1	11	8.6
Cflar	11	12
Zc3h12c	11	11
Il12b	10	18
Ehd1	10	9.5
Ifi44	10	15
H28	10	14

	fold-change	
Gene	Zhx2 wild-type	Zhx2 null
Cd38	10	9.1
Nfkbia	9.9	8.7
Rel	9.8	7.8
Clec4e	9.8	12
Tnfaip3	9.7	7.8
Ets2	9.6	7.9
Tlr2	9.5	7.4
Ccl7	9.4	6.9
BC006779	9.3	9.4
A630072M18Rik	9.1	13
Marcksl1	9.1	8.3
Ralgds	9.0	7.7
Cflar	8.9	8.7
Ehd1	8.9	8.9
Ccrn4l	8.8	10
Spata13	8.6	5.9
Ifi47	8.6	14
Nfkb2	8.5	7.3
H28	8.5	12
Prdm1	8.5	7.5
Adora2a	8.4	9.5
Irgm2	8.2	13
Slc7a2	8.1	8.1
Slfn8	8.0	8.6
Nfkbia	7.9	7.5
Ehd1	7.6	6.2
Slc7a2	7.5	6.6
Sdc4	7.3	8.3
Adora2a	7.2	5.7
Zbp1	7.2	12
Slc7a11	7.1	7.6
Peli1	7.1	6.1
Mmp13	7.1	8.4
Src	7.0	8.2
Oasl2	6.9	9.1
Peli1	6.9	6.5
Sdc4	6.8	7.4
Cflar	6.8	6.1
1600029D21Rik	6.8	5.5
Zc3h12a	6.7	5.3
Slfn2	6.7	6.9

	fold-change	
Gene	Zhx2 wild-type	Zhx2 null
Pstpip2	6.7	6.2
Slc25a37	6.6	6.5
Nfkb2	6.6	5.9
F10	6.5	5.0
Nfkbia	6.5	5.5
Phldb1	6.5	4.8
Arrdc4	6.4	6.2
Ripk2	6.4	5.7
Il23a	6.4	7.0
Cdkn1a	6.3	5.3
Tcfec	6.3	7.6
Lcn2	6.3	7.1
Ch25h	6.0	4.5
Cflar	6.0	6.2
Calcrl	6.0	4.8
Oas2	6.0	9.5
Cdkn1a	5.9	5.1
Igtp	5.9	8.6
Bcl3	5.9	6.0
Pstpip2	5.8	5.0
Jak2	5.8	5.5
Ripk2	5.6	5.2
Akna	5.6	4.9
Nfkb1	5.6	4.6
Sh3bp5	5.5	4.8
Ccl9	5.5	7.4
Trim13	5.4	4.3
Lcp2	5.4	5.0
Gdf15	5.4	5.4
Junb	5.4	5.0
Relb	5.3	4.2
Pim1	5.3	4.8
Ptprj	5.3	4.1
Akna	5.2	4.9
Phldb1	5.2	5.0
Pim1	5.2	4.6
Ifi204	5.1	6.3
Slc7a2	5.1	4.9
Ptges	5.1	6
Agrn	5.1	6.1
Gpr85	5.1	6.7

Bibliography

1. Maclellan, W.R., Y. Wang, and A.J. Lusis, *Systems-based approaches to cardiovascular disease.* Nature reviews. Cardiology, 2012.
2. Holmes, M.V., et al., *Utility of genetic determinants of lipids and cardiovascular events in assessing risk.* Nature reviews. Cardiology, 2011. **8**(4): p. 207-21.
3. Weber, C. and H. Noels, *Atherosclerosis: current pathogenesis and therapeutic options.* Nature medicine, 2011. **17**(11): p. 1410-22.
4. Daugherty, A., *Mouse models of atherosclerosis.* The American journal of the medical sciences, 2002. **323**(1): p. 3-10.
5. Wang, X., et al., *Hyplip2, a new gene for combined hyperlipidemia and increased atherosclerosis.* Arteriosclerosis, Thrombosis, and Vascular Biology, 2004. **24**(10): p. 1928-34.
6. Gargalovic, P.S., et al., *Quantitative trait locus mapping and identification of Zhx2 as a novel regulator of plasma lipid metabolism.* Circulation. Cardiovascular genetics, 2010. **3**(1): p. 60-7.
7. Perincheri, S., et al., *Hereditary persistence of alpha-fetoprotein and H19 expression in liver of BALB/cJ mice is due to a retrovirus insertion in the Zhx2 gene.* Proceedings of the National Academy of Sciences of the United States of America, 2005. **102**(2): p. 396-401.
8. Kawata, H., et al., *Zinc-fingers and homeoboxes (ZHX) 2, a novel member of the ZHX family, functions as a transcriptional repressor.* The Biochemical journal, 2003. **373**(Pt 3): p. 747-57.

9. Yue, X., et al., *Zinc Fingers and Homeoboxes 2 Inhibits Hepatocellular Carcinoma Cell Proliferation and Represses Expression of Cyclins A and E.* Gastroenterology, 2012.

10. Nagel, S., et al., *Transcriptional deregulation of homeobox gene ZHX2 in Hodgkin lymphoma.* Leukemia research, 2011.

11. Nagel, S., et al., *t(4;8)(q27;q24) in Hodgkin lymphoma cells targets phosphodiesterase PDE5A and homeobox gene ZHX2.* Genes, chromosomes & cancer, 2011. **50**(12): p. 996-1009.

12. Legartova, S., et al., *Expression of RAN, ZHX-2, and CHC1L genes in multiple myeloma patients and in myeloma cell lines treated with HDAC and Dnmts inhibitors.* Neoplasma, 2010. **57**(5): p. 482-7.

13. Armellini, A., et al., *Low expression of ZHX2, but not RCBTB2 or RAN, is associated with poor outcome in multiple myeloma.* British journal of haematology, 2008. **141**(2): p. 212-5.

14. Hegele, R.A., *Plasma lipoproteins: genetic influences and clinical implications.* Nature reviews. Genetics, 2009. **10**(2): p. 109-21.

15. Hansson, G.K. and A. Hermansson, *The immune system in atherosclerosis.* Nature immunology, 2011. **12**(3): p. 204-12.

16. Bis, J.C., et al., *Meta-analysis of genome-wide association studies from the CHARGE consortium identifies common variants associated with carotid intima media thickness and plaque.* Nature genetics, 2011.

17. Bennett, B.J., et al., *A high-resolution association mapping panel for the dissection of complex traits in mice.* Genome research, 2010. **20**(2): p. 281-90.

18. Luz D. Orozco, B.J.B., Charles R. Farber, Anatole Ghazalpour, Calvin Pan, Nam Che, Pingzi Wen, Hong Xiu Qi, Bo Guan, Peter Gargalovic, Matteo Pellegrini, Todd Kirchgessner, Aldons J. Lusis, *Unraveling inflammatory responses through systems genetics and gene-environment interactions in mammalian macrophages. manuscript submitted*, 2012.

19. Sato, T., et al., *Interferon regulatory factor-2 protects quiescent hematopoietic stem cells from type I interferon-dependent exhaustion.* Nature medicine, 2009. **15**(6): p. 696-700.

20. Cvejic, A., et al., *The role of meis1 in primitive and definitive hematopoiesis during zebrafish development.* Haematologica, 2011. **96**(2): p. 190-8.

21. Monzo, M., et al., *Genomic polymorphisms provide prognostic information in intermediate-risk acute myeloblastic leukemia.* Blood, 2006. **107**(12): p. 4871-9.

22. Engle, S.J., et al., *Adenine phosphoribosyltransferase-deficient mice develop 2,8-dihydroxyadenine nephrolithiasis.* Proceedings of the National Academy of Sciences of the United States of America, 1996. **93**(11): p. 5307-12.

23. Schaer, C.A., et al., *Heme carrier protein (HCP-1) spatially interacts with the CD163 hemoglobin uptake pathway and is a target of inflammatory macrophage activation.* Journal of leukocyte biology, 2008. **83**(2): p. 325-33.

24. Tang, Y.T., et al., *PAQR proteins: a novel membrane receptor family defined by an ancient 7-transmembrane pass motif.* Journal of molecular evolution, 2005. **61**(3): p. 372-80.

25. Quinn, B.J., et al., *Erythrocyte scaffolding protein p55/MPP1 functions as an essential regulator of neutrophil polarity.* Proceedings of the National Academy of Sciences of the United States of America, 2009. **106**(47): p. 19842-7.

26. Fischer, A., et al., *ZAP70: a master regulator of adaptive immunity.* Seminars in immunopathology, 2010. **32**(2): p. 107-16.

27. Pfister, A.S., et al., *Amer2 protein is a novel negative regulator of Wnt/beta-catenin signaling involved in neuroectodermal patterning.* The Journal of biological chemistry, 2012. **287**(3): p. 1734-41.

28. Wu, Y.Q., et al., *Identification of a human brain-specific gene, calneuron 1, a new member of the calmodulin superfamily.* Molecular genetics and metabolism, 2001. **72**(4): p. 343-50.

29. Fisher, D.A., et al., *Three Dact gene family members are expressed during embryonic development and in the adult brains of mice.* Developmental dynamics : an official publication of the American Association of Anatomists, 2006. **235**(9): p. 2620-30.

30. Kim, K., et al., *Role of excitatory amino acid transporter-2 (EAAT2) and glutamate in neurodegeneration: opportunities for developing novel therapeutics.* Journal of cellular physiology, 2011. **226**(10): p. 2484-93.

31. Lee, C.G., et al., *Molecular cloning and characterization of a murine LPS-inducible cDNA.* Journal of immunology, 1994. **152**(12): p. 5758-67.

32. Waechter, V., et al., *Characterization of the promoter and the transcriptional regulation of the lipoxin A4 receptor (FPR2/ALX) gene in human monocytes and macrophages.* Journal of immunology, 2012. **188**(4): p. 1856-67.

33. Luo, C., et al., *Expression of Complement Components and Regulators by Different Subtypes of Bone Marrow-Derived Macrophages.* Inflammation, 2012.

34. Wells, C.A., et al., *The macrophage-inducible C-type lectin, mincle, is an essential component of the innate immune response to Candida albicans.* Journal of immunology, 2008. **180**(11): p. 7404-13.

35. Kominato, Y., et al., *Monocyte expression of the human prointerleukin 1 beta gene (IL1B) is dependent on promoter sequences which bind the hematopoietic transcription factor Spi-1/PU.1.* Molecular and cellular biology, 1995. **15**(1): p. 58-68.

36. Berchtold, S., et al., *Forced IFIT-2 expression represses LPS induced TNF-alpha expression at posttranscriptional levels.* BMC immunology, 2008. **9**: p. 75.

37. Takaoka, A., et al., *DAI (DLM-1/ZBP1) is a cytosolic DNA sensor and an activator of innate immune response.* Nature, 2007. **448**(7152): p. 501-5.

38. Chen, H., M.E. Herndon, and J. Lawler, *The cell biology of thrombospondin-1.* Matrix biology : journal of the International Society for Matrix Biology, 2000. **19**(7): p. 597-614.

39. Poltorak, A., et al., *Defective LPS signaling in C3H/HeJ and C57BL/10ScCr mice: mutations in Tlr4 gene.* Science, 1998. **282**(5396): p. 2085-8.

40. Martinon, F., et al., *TLR activation of the transcription factor XBP1 regulates innate immune responses in macrophages.* Nature immunology, 2010. **11**(5): p. 411-8.

Chapter 4

Genomic analysis of atherosclerosis initiation in the major vascular cell types in mice

Genomic analysis of atherosclerosis initiation in the major vascular cell types in mice

Erbilgin, A Gene expression of atherosclerotic cell types

Ayca Erbilgin[1], Nathan Siemers[2], Paul Kayne[2], Wen-pin Yang[2], Judith Berliner[3,6], Aldons J. Lusis[1,4,5,6]

[1]Department of Microbiology, Immunology, and Molecular Genetics, University of California, Los Angeles, [2]Bristol-Myers Squibb, Applied Genomics, Princeton, NJ, Departments of [3]Pathology and Laboratory Medicine, [4]Medicine, and [5]Human Genetics, University of California, Los Angeles. [6]These authors contributed equally to this work

Correspondence to Aldons J. Lusis, PhD, 675 Charles E. Young Dr, MRL #3730, Los Angeles, CA 90095 (E-mail jlusis@mednet.ucla.edu); or Ayca Erbilgin, 675 Charles E. Young Dr, MRL #3220, Los Angeles, CA 90095 (E-mail aych@ucla.edu)

Total word count: 8,008

Subject codes:[130] Animal models of human disease, [142] Atherosclerosis gene expression, [89] Genetics of cardiovascular disease, [96] Mechanism of atherosclerosis/ growth factors

Abstract:

Background: Our goal is to study the contribution of endothelial, smooth muscle, and macrophage gene expression to early atherosclerosis using vessels from healthy, pre-lesioned, and lesioned mice. To accomplish this, we developed a method to isolate endothelial cells directly from the aorta and quantitate transcripts in RNA isolated from these cells.

Methods and Results: We performed expression array analysis on RNA isolated directly from the vascular cells of individual control, pre-lesioned, and atherosclerotic mouse aortas; our methods allowed for the separation of discrete cell types. We identified 797 genes differentially expressed in the pre-lesioned endothelium in hyperlipidemic as compared to normal-lipidemic mice. Most of the highly expressed genes in the endothelial cells of early lesions have not been previously described in atherosclerosis. We also examined the effect of inflammatory stimuli on vessel wall gene expression ex vivo and observed significant overlap of pre-lesioned changes with the effects of oxidized phospholipids. Of 56 coronary artery disease genes at loci identified in genome-wide association studies, 31 were differentially expressed in one or more cell types in control versus pre-lesion or lesion states.

Conclusions: We demonstrate that RNA can be isolated directly from the major vascular cell types of the aorta after in vivo and in vitro treatments in mice and used in expression array analysis. This enabled us to identify pre-lesional changes in response

to hyperlipidemia and to examine the regulation of genes identified using genetic approaches in specific vascular cell types.

Keywords: atherosclerosis, genetics, endothelium, smooth muscle cells, macrophages

Non-standard Abbreviations and Acronyms: CAD (coronary artery disease), GWAS (genome-wide association study), EC (endothelial cell), SMC (smooth muscle cell), MAEC (mouse aortic endothelial cells), HAEC (human aortic endothelial cells), LPS (lipopolysaccharide), oxPAPC (1-palmitoyl-2-arachidonoyl-sn-glycero-3-phosphocholine), oxLDL (oxidized low-density lipoprotein).

Introduction:

The cells that comprise a healthy artery, namely the vascular endothelial cells that line the lumen and the smooth muscle cells of the media, are critical to the development of the plaques that define atherosclerosis [1, 2]. The activation of endothelial cells (ECs) leads to the recruitment of leukocytes, such as monocytes, and the increased permeability of the endothelial layer permits the entry of low-density lipoprotein (LDL) to the intima, where they are taken up by macrophages to form foam cells [3]. As atherosclerosis progresses, smooth muscle cells (SMCs) that reside in the media of the artery migrate to the developing lesion, where they proliferate and join the accumulating foam cells and cellular debris in the growing atheroma. Although the general events that occur in the vessel wall during the transition of a healthy artery to an

atherogenic vessel have been established, many of the specific molecular changes that take place during disease progression remain unclear. Identifying the transcriptional changes that occur in the main cell types involved in the development of an atheroma could provide leads towards elucidating disease mechanisms and determining potential therapeutic pathways.

Mouse strains that are susceptible to atherosclerosis have served as the primary disease model for CAD [4, 5]. Unfortunately, obtaining pure, differentiated cell cultures of mouse aortic endothelial cells (MAECs) has remained a challenge, possibly due to cell culture conditions that require growing cells away from their native environment and leading to rapid de-differentiation of ECs [6]. The study of cells isolated directly from the aorta offers significant advantages. The data gathered would closely represent the in vivo physical state of these cells, as the cell-cell interactions remain intact up until the moment of cell isolation, and it would be possible to assess the transcriptional response of the cells to in vivo conditions, such as hyperlipidemia. Although previous studies have explored the effect of hyperlipidemia on the expression of individual genes in MAECs [7, 8], a whole-genome transcriptional study has not been reported. While studies on whole vessel ApoE -/- mouse aortas [9] and microarrays on LCM-dissected aortas [10] have been published, the cell types in these studies were not clearly separated.

We now characterize cells obtained by a method to isolate the intimal layer from disease-free mouse aortas [11] as endothelial cells, and adapt this method to allow for treatment of these cells with pro-inflammatory agents in vitro. We then apply these

methods to determine the gene expression of MAECs isolated from aortas pre-disposed to atherosclerosis and compare these profiles to those from healthy vessels in order to determine the major transcriptionally perturbed genes. The gene expression profiles of MAECs exposed to oxidized phospholipids and oxLDL and the more general pro-inflammatory molecule LPS are determined and compared to the profiles of the pre-lesion MAECs.

Large scale genome-wide association studies (GWAS) have recently provided some insight into the many different genetic factors that contribute the disease [12-21]. Collectively, these studies have identified 35 genetic loci associated with CAD [22] and represent tens of thousands of patient samples and years of work. As GWAS data provides no functional information on the loci identified, additional studies on the individual candidate genes are needed in order to determine their role in disease. Although a few genes represented by these loci are well-characterized, the majority of GWAS candidates have no additional studies directly linking them to CAD. A thorough survey of the cells in which these genes are expressed and increased in atherosclerosis would define a context in interpreting these invaluable data. This type of complete expression dataset from atherosclerosis-susceptible mice has not previously been feasible, due to the aforementioned difficulty in isolating pure MAECs.

We now examine the expression of CAD GWAS genes in the three major cell types: EC, SMC, and macrophage foam cells from both healthy and pre-lesioned intima. The intimal layer isolation method is further applied to obtain preps of the

heterogeneous cells present in more advanced atherosclerotic lesions and to compare GWAS gene expression in all RNA preparations. We present our findings of novel genes perturbed in vascular ECs during the early stages of atherogenesis, and describe the gene expression patterns of human CAD candidate genes in atherosclerotic cells using a mouse model.

Methods:

Animals: Unless otherwise indicated, C57BL/6J (BL6) male mice fed a chow diet were used for experiments. BL6 mice were obtained from the Jackson Laboratory or bred in our colony; BL6 ApoEtm1Unc null mice (ApoE -/-) were maintained in a colony in the UCLA vivarium. Wild-type BL6 mice were used in samples representing healthy vascular cells, and ApoE -/- BL6 mice were used for pre-lesioned vascular cells. The aortas from BL6 ApoE -/- mice fed a chow diet at four weeks of age were considered pre-lesioned, and BL6 ApoE -/- mice at 24-weeks of age exhibited clear atherosclerosis. LDLR null mice on a BALB/cJ background were either maintained on a chow diet or placed on a western diet (Open Source D12079B) at 8 weeks of age. These mice were used for studies comparing macrophages and foam cells. Mice were euthanized using isofluorane in accordance with ARC policies. A minimum of three mice for each condition was used, unless otherwise noted.

Microscopy/oilredO staining: Sections of aortic arch were fixed onto Superfrost slides and stained with Oil red O dye. Microscopy photos were taken at a magnification of 20x.

MAEC and intimal cell isolation procedure: The cell isolation protocol was adapted from a previously published method for intimal cell isolation [11] (Supplemental Figure 1). After euthanization of the mouse, the chest cavity was opened, lungs, trachea, and esophagus removed, and the aortic arch excised under a dissecting microscope. Care was taken to maintain consistency in dissection of the arch region. No perfusion of vasculature was performed. After rinsing in cold PBS, the vessel was placed on a glass slide, the surrounding connective tissue was removed, and the aorta was opened en face. In order to visualize the endothelial layer, the opened aorta was stained with 30 uL hematoxylin for 3 minutes. The stain was rinsed off with cold PBS. The collagenase liberase blendzyme 2 (Roche) was diluted 1:100 with PBS, and 25 uL was added to the top of the aorta on the slide and incubated at 37 C for 8 minutes. The slide with collagenase-treated aorta was then placed under a dissecting microscope, and the endothelial cells were gently pried off using a 26-gauge needle. This process continued until all endothelial cells were removed, determined by the lack of hematoxylin-dyed nuclei on the surface of the sample. The liquid containing the endothelial cells was then pipetted with a thin pipet tip into RNA extraction buffer.

Aorta treatment procedure (Supplemental Figure 1): DMEM with 1% FBS was used as the cell culture medium; vessels were incubated for 4 hours in a cell culture incubator at 37 C, 5% CO2. 1-palmitoyl-2-arachidonoyl-sn-glycero-3-phosphocholine (OxPAPC) and oxLDL were prepared as previously described [23, 24] Lipopolysaccharide (LPS) was purchased from List Biological Laboratories. OxPAPC and oxLDL were added to DMEM

for a final concentration of 50 ug/mL, LPS was formulated for a final concentration of 4 ng/mL. After aortas were opened en face, each was placed in one well of a 12-well cell culture plate along with 1 mL of the appropriate DMEM formulation pre-warmed to 37C. After the 4 hour treatment, aortas were removed from media and placed lumen side up on a glass slide; isolation continued as described above, beginning with hematoxylin treatment.

Intimal/MAEC RNA extraction: RNA was extracted using the RNAqueous®-Micro Kit by Ambion. The buffer and collagenase solution containing scraped endothelial cells was pipetted directly into 100 uL of Lysis buffer in a 200 uL PCR tube, vortexed, then incubated at 42 C for 30 minutes on a PCR thermalcycler. RNA isolation continued following the manufacturer's protocol, including suggestions to pre-wet the filter assembly with 30 uL Lysis buffer prior to isolation and to preheat elution solution to 95 C. RNA was stored at -80 C after isolation.

RNA amplification: The NuGEN WT-Ovation One-Direct RNA amplification system was used to amplify RNA isolated from MAECs. The procedure followed manufacturer's protocol; pre-amplification work was conducted in a sterile hood treated with RNase ZAP and DNA-OFF and using pipetmen and other lab materials exclusive to pre-amplification in order to eliminate contamination.

Smooth muscle cell RNA isolation procedure: BL6 wt and ApoE -/- mice were used for SMCs from healthy and diseased vessels, respectively. Aortas with the intimal layer

removed using procedure described above were homogenized in Qiazol for 30 seconds, and RNA was isolated with the Qiagen RNeasy kit standard protocol. The complete removal of cells present in the intimal layer was observed by lack of cells stained with hematoxylin.

Macrophage and foam cell induction and RNA isolation procedure: LDLR -/- mice at 16 weeks of age either on chow or western diet were injected intraperitoneally with 4% Thioglycolate (Brewer Thioglycollate Medium, BD#211716). On the fourth day after injection, macrophages were collected through lavage of the peritoneal cavity using PBS buffer. Collected cells were treated with ACK lysis buffer to remove red blood cells and were then cultured overnight in DMEM media with 20% FBS. The next morning the cell culture dishes were rinsed with PBS and RNA from adherent cells was collected using buffer RLT from the Qiagen RNeasy kit. RNA was isolated with the Qiagen RNeasy kit following the manufacturer's protocol.

cDNA synthesis and RT-qPCR: As the output of the NuGEN WT-Ovation One-Direct RNA amplification system is cDNA, no separate cDNA synthesis was required for amplified RNA. Macrophage and SMC cDNA was synthesized with Applied Biosystems High-Capacity cDNA Reverse Transcription Kit. Roche and KAPA Biosystems SYBR green reagents were used for RT-qPCR, and reactions were processed on 384-well plates on the Roche LightCycler 480. Of the 59 genes represented by published GWAS loci [22], mouse gene homologs were identified for 56 genes and primers were designed for the mouse genes. Sequences for RT-qPCR primers are presented in

Supplemental Table 1. Mouse gene 9530008L14Rik is the homolog of human gene C6orf105, mouse gene ZFP259 is the homolog of human gene ZNF259. All other mouse genes share the names of their human homologs.

Expression microarrays: The products of RNA amplification were treated with the NuGEN Encore Biotin Module prior to hybridization according to manufacturer's protocol. Affymetrix HT Mouse Genome 430 array plates were used for microarray analysis.

Statistical analyses: Statistical analyses were executed in the R programming environment. T-tests were calculated for qPCR results using the t.test command. Microarray results were normalized using RMA in the "affy" package, and differential expression p-values and venn diagrams were calculated using the "limma" package. Heatmaps were constructed using the "heatmap.2" package. Microarray p-values were corrected using Benjamini-Hochberg.

Results:

Cells isolated from the intimal layer of healthy mouse aortas are endothelial cells: Transcript levels of the endothelial cell specific markers vWF and CD31 were significantly enriched in healthy aortic intimal cell preps from wt BL6 mice compared to RNA extracted from whole mouse aortas (Fig 1a), indicating the intimal preps are predominantly endothelial cells. Expression levels of macrophage, leukocyte, and

adipose markers were below detection thresholds (Supplemental Table 2), indicating the lack of these cell types in our preps. RNA expression levels of the SMC protein marker Acta2 was significantly lower in the intimal preps compared to whole aortas (Fig 1a). To further explore the possibility of SMC contamination of our intimal preps, we compared the mRNA expression levels of eight different SMC protein markers in our MAEC preps to those present in human aortic endothelial cell (HAEC) cell cultures (Fig 1b). These HAEC cultures have previously been characterized as at least 95% pure as judged by EC protein marker, and smooth muscle proteins were not expressed in these cells [25]. We found that all SMC protein markers tested are expressed as mRNA transcripts in HAEC cultures tested. Thus HAEC express several mRNA characteristic of SMC but do not express these proteins. This was reported in previous studies on endothelial cells [26]. These data indicate that cells isolated from the intimal layer of healthy mouse aortas are comprised of endothelial cells and can be used as such with the same level of confidence as HAEC cultures.

MAECs isolated from treated whole aortas respond to activation with pro-inflammatory agents: In order to determine whether endothelial cells collected using this method could be treated with pro-inflammatory agents prior to collection, we applied a protocol used for treating HAEC cultures to whole mouse aortas [27] (Supplemental Figure 1). Incubation of the aortas in media prior to endothelial cell isolation did not significantly impact the expression levels of EC markers (Fig 2a), nor did treatment of the oxidized phospholipid oxPAPC (Fig 2b). We next determined if endothelium isolated from treated vessels displayed gene regulation previously observed with HAEC. We found that

expression of HMOX-1, a gene induced during oxidative stress and the inflammatory response in HAECs, is up-regulated nearly 10-fold in response to oxPAPC (Fig 2b), a response also seen in HAEC cultures [28]. A similar response was seen after treatment with oxLDL (Fig 2c). LPS treatment (Fig 2d), showed increased expression of pro-inflammatory marker VCAM1 but no induction of HMOX-1, consistent with our prior observations in HAECs. Since gene regulation was consistent with past studies, we proceeded with expression array analysis.

Amplification of RNA isolated from MAECs does not affect relative abundance of transcripts: As the MAEC isolation process yielded approximately 3 ng of RNA per mouse, we wanted to identify a RNA amplification procedure that would not alter the relative expression levels of transcript in the samples. We tested four samples: two that had been treated with oxPAPC prior to isolation, and two control samples incubated in media only. After isolation, half the RNA was converted to cDNA and the other half was amplified using the NuGEN RNA amplification kit. Both the cDNA and amplified RNA product (aRNA) were assayed for transcript levels of vWF, HMOX1, and VCAM1. Both the raw and normalized RT-qPCR values of the native cDNA and aRNA products correspond very closely, indicating that expression data acquired from amplified RNA will provide relative expression levels consistent with the native RNA sample (Supplemental Fig 2).

Pre-lesion MAECs show a differential expression pattern compared to healthy MAECs: BL6 mice on an ApoE -/- background develop atherosclerotic lesions on a chow diet and

acquire aortic lipid deposits by 12 weeks of age, while BL6 wt mice do not show evidence of fatty streaks even at 24 weeks (Supplemental Figure 3). However, at 4 weeks of age BL6 ApoE -/- mice have not yet acquired observable lipid deposits in the intimal layer of the aortic arch (Supplemental Figure 3), the region from which we isolate cells, and are thus termed “pre-lesioned” endothelial cells. Therefore, MAECs isolated from 4 week old wt BL6 mice and BL6 ApoE -/- mice represent healthy (normal-lipidemic) and pre-lesioned (hyperlipidemic) endothelial cells, respectively. MAEC RNA was isolated, amplified, and subjected to gene expression microarray analysis. Nearly 800 genes were differentially expressed at a false-discovery rate of 10% (Figure 3), and 32 genes were differentially expressed at the stringent standards of 2-fold change at 5% FDR (Table 1).

The differential expression pattern elicited by oxPAPC shows the most overlap/similarity with pre-lesioned cells: Since many of the early endothelial cell changes in atherogenesis are thought to be affected by activation of the inflammatory response, we compared the endothelial gene expression profile after treatment with pro-inflammatory agents to the gene expression of MAECs in the early stages of atherosclerosis as determined in the previous section. An additional set of MAEC expression data was generated by treating aortas with media containing the pro-inflammatory substances oxPAPC, oxLDL, and LPS prior to cell isolation, then amplifying the RNA and performing microarray analysis. Differentially expressed genes were determined using MAECs collected from aortas incubated in control media as the baseline. Of the 797 differentially expressed genes from healthy to pre-lesioned endothelial cells, nearly half

are regulated in the same direction after treatment with oxPAPC, followed closely with treatment of LPS and the oxLDL (Figure 3). Although there is overlap among the three different pro-inflammatory treatments, there are also distinct sets of genes that differ among treatments. There are also smaller sets of genes that are differentially expressed in opposite direction in the pre-lesioned samples compared to the treated samples, and a subset of genes in the pre-lesioned ECs whose regulation is not replicated by the treatments tested, represented by the black areas on the heatmap presented in Figure 3.

Differential expression analysis identifies new candidates for role in atherosclerosis: In order to identify genes that may play a critical role in endothelial cell-mediated atherogenesis, we identified the top differentially expressed gene transcripts from healthy to pre-lesioned MAECs as determined by fold-change in the microarray data. The expression levels of the genes represented by these microarray probe sets were tested by RT-qCR, and genes that were determined to have significant differential expression in both microarray and RT-qPCR data are shown in Table 2. Among these genes are several that have not been previously linked with a role in atherogenesis, including four histocompatibility II genes (H2-AA, H2-AB1, H2-D1, and H2-EA), two sarcomere protein genes (ACTC1[29] and TNNT2 [30]), the semaphorin gene family member SEMA5A [31], and the previously unstudied gene 2610019E17RIK. Among the differentially expressed genes previously described in atherosclerosis are the platelet-related genes PPBP and PF4 [32], both down-regulated at nearly 10-fold in pre-lesioned endothelial cells, ABCA1 [33] and SERPINA1 [34], two genes involved in HDL

regulation, and PTN, which has previously reported to be expressed by endothelial cells and present in atherosclerotic lesions [35]. PVRL2, a gene expressed by endothelial cells and involved with the immune response [36], also shows significant differential expression; however it is also located close to the ApoE gene and therefore this may be a result of its proximity to the ApoE mutation [37]. Expression of some of these highly-responsive genes are also perturbed after treatment with pro-inflammatory factors; three of the four histocompatibility II genes are differentially expressed after treatments, and expression of 2610019E17RIK, PTN, and TNNT2 are perturbed after treatment with oxLDL.

Expression of GWAS candidate genes in the cell types present in atherosclerotic lesions: We applied the aortic intimal isolation protocol that we used for MAEC isolation at 4 weeks of age to obtain samples of intimal cells at 24 weeks of age (Figure 4). Intimal samples were collected from BL6 wt and BL6 ApoE -/- mouse aortas at 24 weeks; we consider the samples collected from the atherosclerosis-susceptible ApoE -/- strain to represent the heterogenous cell composition present in advanced atherosclerotic lesions. By comparison to intimal cells taken from BL6 wt mice at the corresponding age, which do not have discernible lipid deposits in the intima, we are able to identify the transcriptional profile of the cells that compose atherosclerotic lesions. The intimal isolation procedure leaves the aorta without an intimal layer and consisting primarily of the medial layer, which contains predominantly SMCs. Comparison of the SMCs of the medial layer in healthy vs diseased arteries at the time-points of 4 and 24 weeks can identify differentially expressed transcripts in the SMCs

that will eventually migrate to the intimal layer to join the growing lesion. We were also able to assay transcriptional differences in macrophages compared to lipid-loaded foam cells resembling those found in lesions [38]. Including the 4-week MAEC cells previously described, we were able to assay transcriptional profiles of three predominant cell types present in atherosclerotic lesions and compare them to their healthy cell states, in addition to the transcriptional status of the entire lesion (Figure 4).

The 35 published GWAS loci for CAD represent 59 candidate genes. We utilized RT-qPCR to asses the presence of the mouse homologs for 56 of these transcripts among the four sets of mouse cell types we collected. Although most of the GWAS candidate genes were expressed in at least one of the cell preps, there were six transcripts whose expression was below the detection threshold in all samples: ABCG8, ABO, APOA4, APOA5, HNF1A, and KCNE (Table 3). We did not identify any transcripts that were undetectable under the healthy condition of a cell type and detectable in the diseased condition, or vice-versa.

Similar to the calculations used for MAEC experiments described above, differential expression for SMCs, macrophages, and 24-week intimal cells was determined using cells isolated from the healthy condition as the baseline condition. Of the 50 GWAS candidate genes that are expressed in one of the four cell categories tested, slightly more than half showed differential expression from healthy to disease state in at least one of the cell types (Table 4).

The pattern of GWAS differential expression among the three cell types present in atherosclerotic lesions varies (Table 4, Figure 5). Some genes are differentially expressed only in foam cells (ADAMTS7, ATP5G1, CDKN2A, CELSR2, and SORT1), some only in pre-lesioned MAECs (CYP17A1, COL4A1, GIP, ZFP259, 9530008L14Rik), and PEMT and SNF8 are only differentially expressed in 24-week medial SMCs. Four genes are only differentially expressed in lesions (MORF4L1, MRPS6, PDGFD, and SH2B3). None of the GWAS candidate genes are differentially expressed in medial smooth muscle cells at the 4-week time point. Several genes show dysregulation in the diseased condition in three of the four cell preps tested (COL4A2, CXCL12, FBN1, MIA3, PSRC1, and TRIB1).

Discussion:

We adapted the method of Cybulsky and colleagues [11] to isolate ECs from aortas such that we could profile gene expression in specific cell types during the early stages of atherosclerosis in mice. This method provides a quick, efficient way to collect MAEC RNA, generally yielding RNA from a mouse in less than an hour after harvesting, and has several advantages over cell culture methods. Not only do we avoid the passage and de-differentiation issues that occur during cell culture procedures, but we are able to directly assay the transcriptional state of the cells that closely represents their in vivo status. In these experiments, we were able to obtain the transcriptional state of ECs in pre-lesioned aortas, and through the use of RNA amplification we were

able to perform microarray analysis on MAECs taken from a single mouse. Moreover, we demonstrate that the whole aorta, with its endothelium intact, can be treated in cell culture medium similar to conventional cell culture with the added advantage of not disrupting the natural environment and cell-to-cell connections. We envision that this method and its adaptations will be useful in many vascular and CAD studies and can complement and enhance data obtained using cell culture methods.

This method was applied to assay the transcriptional profile of pre-lesioned mouse aortic endothelial cells for the first time. In addition, we adapted this method to assess the role of biologically relevant pro-inflammatory substances in atherogenic transcriptional regulation. We found that the top differentially expressed genes from healthy to pre-lesioned MAECs include some that have not previously been described in the endothelial cell contribution to atherosclerosis. The four histocompatibility genes identified as differentially expressed do not come as a surprise, given that endothelial cells are antigen presenting cells. In addition, a very recent GWAS study reports a MHC region as a novel locus for coronary artery disease [39], and previous studies on HAECs grown in 3D matrix cultures note differential expression of MHC II genes under various culture conditions [40]. Three of these genes are down-regulated in pre-lesioned MAECs, two of which are correspondingly regulated by treatment of healthy cells with oxidized phospholipids, increasing the likelihood that these are truly expressed by ECs and not due to the infiltration of other cell types in the arteries predisposed to lesions. Furthermore, the corresponding regulation of two of these four MHC II genes by either oxPAPC or oxLDL suggest that the oxidative stress in the intimal region contributes to

MHC II regulation during the early stages of atherogenesis. ABCA1 promotes the efflux of cholesterol from cells, and its endothelial-specific expression has been shown to reduce diet-induced atherosclerosis [41]; the up-regulation in hyperlipidemic endothelial cells that we observe is also described in porcine aortic ECs [42]. This may be a response of the endothelium to reduce the accumulation of lipid during the early stages of atherogenesis. SERPINA1, a protein present in HDL [34], may be similarly involved. SERPINA1 is also characterized as an antitrypsin molecule [43], and its down-regulation in pre-lesioned ECs could be reflective of the change in morphology of ECs during atherogenesis. The increase of SEMA5A expression, a gene that promotes proliferation and migration of endothelial cells [31], is consistent with its role in the angiogenesis that accompanies atherosclerosis. The strong down-regulation of the previously unstudied gene 2610019E17RIK in both pre-lesioned and oxLDL-treated MAECs suggest the involvement of this gene in oxidative stress-mediated endothelial cell activation. We also observe differential expression of two genes implicated in cardiomyopathy, ACTC1 [29] and TNNT2 [30]. Cardiomyopathy is one of the complications that can occur as a result of atherosclerosis [44]; our findings suggest that some of the genes involved with heart failure may begin their role in disease early. Additional genes that have been previously described with atherosclerosis-related roles are the platelet factors PF4 and PPBP [32], and PTN [35]. ACTC1, TNNT2, and PF4 have been previously described as expressed exclusively in one cell-type; our findings that they are also expressed in endothelial cells may be due to the aforementioned difficulty of directly assessing endothelial-specific expression in mice.

The characterization of the cells gathered during the intimal isolation procedure allowed us to assemble a comprehensive data set consisting of three major cell types that contribute to atherosclerosis: ECs, SMCs, and macrophages. In addition, we were able to collect intimal cells from aortas with atherosclerotic lesions using this method. This data set allowed for the thorough assessment of GWAS candidate gene expression, many of which lack additional studies linking them to atherosclerosis (Figure 5). We identified the genes that are expressed in lesions and in the contributing cells, and those that are differentially expressed in healthy compared to disease state. The resulting data provide new information for most of the 56 candidate genes tested. Using this data set, we can make some preliminary conclusions for GWAS loci that represent more than one gene. For example, four genes are represented by the human locus 17q21.32: UBE2Z, GIP, ATP5G1, and SNF8 [12]. The gene ATP5G is only differentially expressed in foam cells, the genes UBE2Z and GIP are differentially expressed exclusively in the intimal layer, and SNF8 is up-regulated specifically in the medial SMCs. Since the genes marked by this locus are expressed in different cell types, this suggests that this locus may be a marker for more than one gene contributing to CAD. The human locus 10q24.32 corresponds to the genes CYP17A1, CNNM2, and NT5C2 [12], only one of which (CYP17A1) is differentially expressed in our data set, suggesting that this may be the gene marked by this locus.

There are many GWAS CAD genes for which additional information linking them to the disease is not available. Among the differentially expressed genes shown in Table 4, 9530008L14Rik, ADAMTS7, ATP5G1, CYP17A1, KIAA1462, MIA3, MORF4L1,

PHACTR1, PPAP2B, SH2B3, SMG6, SRR, TCF21, UBE2Z, and ZFP259 have no studies other than genomic association studies linking them to CAD. Of the differentially expressed genes that have additional data describing their involvement in atherosclerosis, the genes CELSR2, PCSK9, PIK3CG, PSRC1, and SRR have no prior data of their contribution to atherosclerosis in the context of the cell type(s) in which we have observed differential expression. Our GWAS gene expression data set provides new information for nearly all CAD candidate genes. For example, while a recent study describes the protein transcribed by KIAA1462 as present in endothelial cell-cell junctions [45], no data directly linking this gene to atherosclerosis has been published. From our data, we see that this transcript is expressed by endothelial cells early in atherogenesis, and is further up-regulated during progression of the atherogenic lesion. Prior studies on MIA3 report that this gene product promotes migration of premonocytic cells in human microvascular endothelial cell cultures (HMECs) [46], a function that corresponds to the more than 2-fold up-regulation observed in our pre-lesioned endothelial cells. This study also reports a lack of MIA3 expression in cells of the hematopoetic system, whereas we see a significant induction of transcript in foam cells compared to macrophages. The relatively well-studied gene PCSK9 promotes LDLR degradation and has a direct pro-atherogenic effect [47, 48] and has emerged as a new pharmacological target for hypercholesterolemia with various PCSK9 inhibitors now being evaluated in clinical trials [49, 50]. Although this gene has been reported as present in human atherosclerotic plaques [51], no previous studies describe expression in pre-atherosclerotic endothelial cells. Our study provides information suggesting an additional role for this potential therapeutic target. In addition to clarifying the role of

human CAD candidate genes, our results may help focus studies on genes within quantitative trait loci for atherosclerosis in mice [4, 52]. Studies over the last two decades have robustly identified over 30 such loci, but it has been difficult to identify the underlying genes because of the poor mapping resolution of such studies.

In summary, we believe our study provides several valuable leads for the study of the genes mediating atherosclerosis in the vessel wall. Our characterization of a vascular endothelium isolation method and demonstration that it is applicable to cell-culture methods may serve as a guide to researchers performing individual gene follow-up studies. Furthermore, our dataset on GWAS gene expression provides a fundamental guide in interpreting these results of vital human studies that require interpretation on the road to applying these results to diagnosis and therapeutic goals of CAD study.

Acknowledgements

We would like to acknowledge Jan Danciger for her advice on endothelial cells, Ladan Vakili for the oxLDL, and Xuping Wang and Judy Wu for sectioning and staining the aortic arch samples. We also thank Myron Cybulsky for providing direction on the intimal cell isolation method.

Funding Sources

This research was funded by NIH grant PO1-HL030568 (A.J.L., J.A.B.), NIH grant HL-064731 (J.A.B.), American Heart Association predoctoral fellowship (AE), Ruth L. Kirschstein National Research Service Award GM007185 (AE).

Disclosures

Nathan Siemers, Paul Kayne, and Wen-pin Yang are employees of Bristol-Myers Squibb. The authors have no conflicts.

Figure Legends

Figure 1: Cells isolated from the intima of healthy mouse aortas are endothelial cells. Figure 1a: Graph represents relative expression of RNA normalized to the housekeeping gene B2M. RNA was isolated from MAEC preps and whole aortas, from three animals each. Normalized gene expression for the two EC markers vWF and CD31 show significant enrichment in the intimal preps and are nearly undetectable in the whole aorta samples, while the smooth muscle cell protein marker SMCa is expressed much higher in the whole aorta samples. Error bars show standard deviation for two technical replicates. Figure 1b: Relative transcription levels of eight different smooth muscle cell protein markers and the EC marker CD31 in MAECs and HAEC cultures as determined by RT-qPCR, normalized to the housekeeping gene B2M. mRNA transcript levels for all SMC protein markers are present in the HAEC cell cultures, which have been confirmed as SMC-free using protein markers and serve as a positive control for our purposes. SMC protein transcript levels for the mouse homologs of these genes show similar expression levels in our intimal preps, indicating a confidence level of EC purity equal to that for HAEC cultures. Error bars show standard error for six biological replicates for each sample set.

Figure 2: Treatment of whole aortas with pro-inflammatory factors prior to MAEC isolation effectively perturbs gene expression of inflammatory markers without altering EC cell marker levels. Relative transcription levels of EC marker genes and select stress-response genes in MAECs isolated after treatment with DMEM cell culture

medium containing various treatments, as determined by RT-qPCR and normalized to B2M A: expression levels of the EC markers vWF and CD31 in native MAEC preps compared with MAECs isolated from aortas incubated in DMEM for 4 hours. No significant expression differences in EC cell marker expression after incubation in cell culture media. Error bars show standard error from 4 biological replicates for each condition. B: EC markers and HMOX1 in MAECs isolated from aortas incubated in DMEM compared to DMEM containing oxPAPC for 4 hours. While the transcription levels of EC cell markers remain the same, there is a strong induction of HMOX-1 in response to treatment with oxidized phospholipid. Error bars show standard error from 2 biological replicates. C: expression levels of EC markers HMOX1 in MAECs isolated from aortas incubated in DMEM vs DMEM containing oxLDL for 4 hours. We see an induction of HMOX-1 but not EC markers in response to treatment. Error bars show standard errors from 2 biological replicates. D:Transcription levels of EC markers, HMOX1, and VCAM in MAECs isolated from aortas incubated in DMEM vs DMEM containing LPS for 4 hours. No response is observed in HMOX-1 expression, but VCAM1 transcript levels are induced as expected. Error bars show standard errors from 2 biological replicates.

Figure 3: Differential gene expression of pre-lesioned MAECs compared to healthy MAECs and the overlap with treated MAECs. Heatmap displaying differential expression of genes in MAECs. The top bar displays differential expression from healthy to pre-lesioned MAECs with 10% FDR. The red bars indicate up-regulation of expression from healthy to pre-diseased, while green bars indicate down-regulation. The next three rows show differential expression data of the the same 797 differentially

expressed pre-lesioned genes in MAECs treated with oxPAPC, oxLDL, or LPS, respectively. Gene expression cut-off for treatment is 1.2-fold, and is maximized at an absolute value of 4 for purposes of graph visualization. Numbers below treatments indicate the number of genes that are regulated in the same direction as pre-lesioned samples.

Figure 4: Experimental outline of cell collection for GWAS gene expression studies. MAECs isolated from 4-week BL6 wt aortas represent healthy MAECs, while MAECs isolated from ApoE -/- aortas are from pre-lesioned vessels and are considered diseased. Aortas isolated from 24-week old ApoE -/- mice have developed atherosclerotic lesions and their intimal cells are diseased, while the intima from wt mice at 24 weeks remain free of lipid deposits and are thus termed healthy. After the 4- and 24- week vessels have been stripped of their intimal cells, the remainder is composed primarily of SMCs and are used for the appropriate SMC preps. Macrophages isolated from LDLR -/- mice have the same characteristics of the foam cells found in lesions and are considered diseased, while those collected from chow-fed LDLR -/- mice do not have lipids present and serve as the healthy control. Differential expression is determined as the fold-change from the expression level of a gene at the baseline condition of healthy to the expression level of the gene in the diseased condition.

Figure 5: Overview of GWAS differential gene expression in the cells of the vessel wall and novel differentially expressed genes identified in pre-lesion MAECs. Results seen in Tables 2 and 4 are summarized. The left side of the figure shows

differentially expressed novel and GWAS genes in healthy to pre-lesioned MAECs taken from the aortas of 4-week old BL6 wild-type and ApoE -/- mice, respectively. The right side diagrams differentially expressed CAD GWAS genes in intimal and medial SMCs taken from healthy and lesioned 24-week old BL6 wild-type and ApoE-/- mice, and macrophages taken from chow fed LDLR -/- mice compared to those on a western diet.

Supplemental Figure 1: Overview of MAEC isolation and treatment procedure. Aorta is removed from mouse and the arch region is isolated and opened en face. If MAECs are to be treated, aorta is submerged in media containing treatment and kept in cell culture conditions for 4 hours. Afterwards, endothelial cells are stained with hematoxylin, treated with collagenase, and intimal cells are pried off using a needle. Cells are immediately pipetted into RNA extraction buffer.

Supplemental Figure 2: Amplification of MAEC RNA does not impact relative gene expression levels. Relative gene expression values as determined by RT-qPCR and normalized to vWF. Expression values are shown for both native and amplified RNA samples collected from the same mouse. Samples 1-3, VCAM1 mRNA levels in samples treated in DMEM; samples 4-6, VCAM1 mRNA levels in samples treated with oxPAPC; samples 7-9, HMOX-1 levels in samples treated in DMEM; samples 10-12, HMOX-1 levels in samples treated with oxPAPC.

Supplemental Figure 3: ApoR -/- BL6 mice at 4 weeks of age do not have the visible lipid deposits that are present in 24 week ApoE -/- BL6 mice, while 24 week

wild-type BL6 mice do not develop atherosclerosis. Histology slides of sectioned aortic arch stained with oil red o, magnification 20x. A: 4 week, BL6 ApoE -/-; no lipid deposits observed B: 24 week BL6 ApoE -/-; intimal lesions visible C: 24 week BL6 wild-type; no lipid deposits observed

T**able 1: Number of genes differentially expressed from healthy MAECs to pre-lesioned MAECs.** Fold-changes of 1.2, 1.5, and 2+ and FDR cut-offs of 5 and 10% are shown.

Table 2: Top differentially expressed genes as determined in microarray analysis identify 14 highly regulated transcripts. Fold-changes from healthy to diseased MAECs as measured by qPCR are shown; p-values are determined by t-test.

Table 3: Gene transcript presence of 56 GWAS genes in atherosclerotic cell types identifies differential expression patterns among the four cell types tested. Gene transcript presence established by RT-qPCR.

Table 4: Fold-change of GWAS candidate genes from healthy to diseased cell types. Gene transcript levels established by RT-qPCR, fold change is defined by expression change from healthy to diseased cells; t-test p-values shown.

Supplemental Table 1: RT-qPCR primer sequences. Sequences are shown from 5’ to 3’ direction; primers are designed for mouse except for those with an “h” preceding the gene name, which are designed for human cells.

Supplemental Table 2: Low levels of adipose, leukocyte, and macrophage cell markers in MAEC preps indicate prep purity. RT-qPCR values for adipose, leukocyte, and macrophage markers from intimal preps and whole mouse aortas. Expression values normalized to housekeeping gene B2M

Figure 1

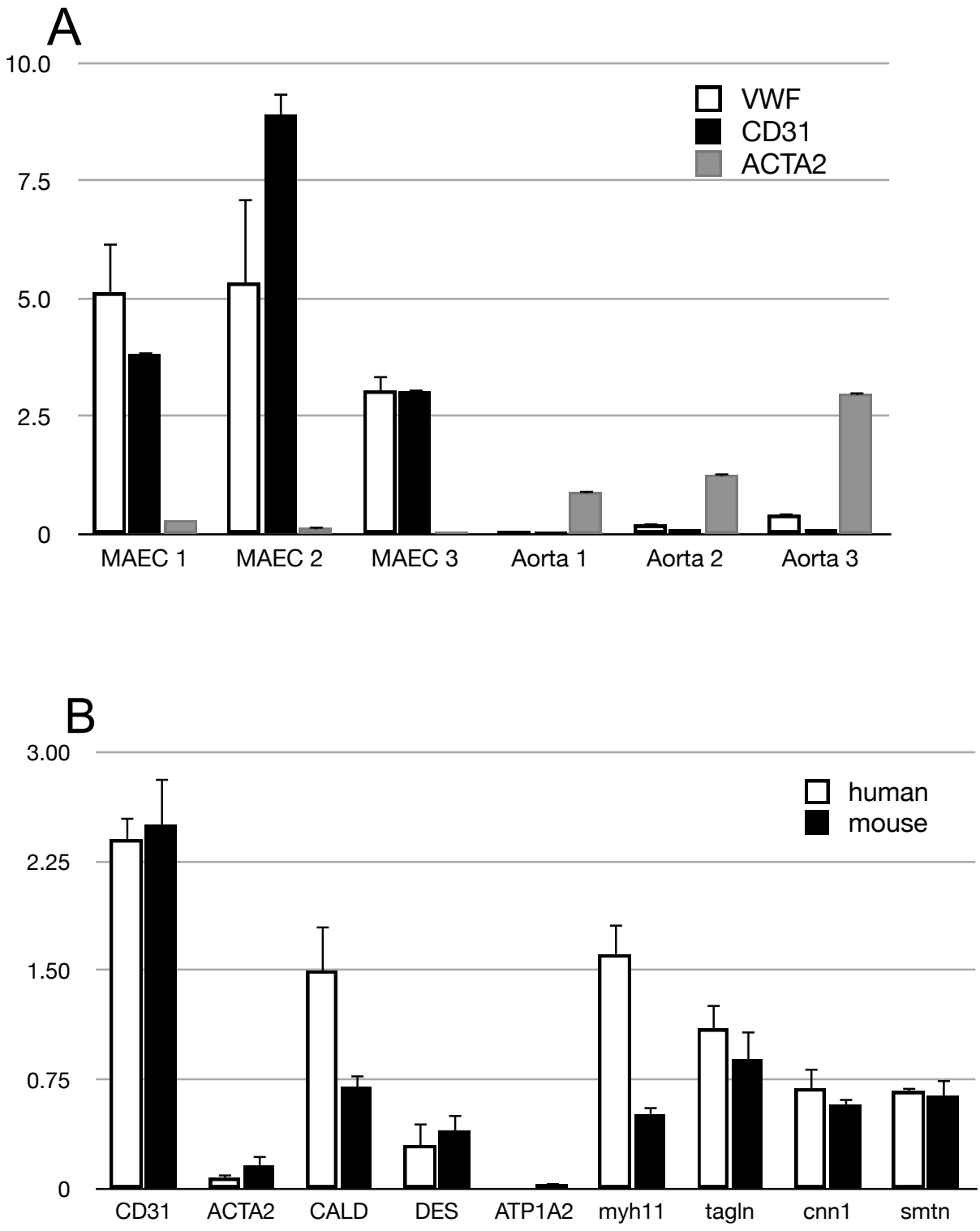
A
10.0
7.5
5.0
2.5
0
VWF
CD31
ACTA2
MAEC 1
MAEC 2
MAEC 3
Aorta 1
Aorta 2
Aorta 3
B
3.00
2.25
1.50
0.75
0
human
mouse
CD31
ACTA2
CALD
DES
ATP1A2
myh11
tagln
cnn1
smtn

Figure 2

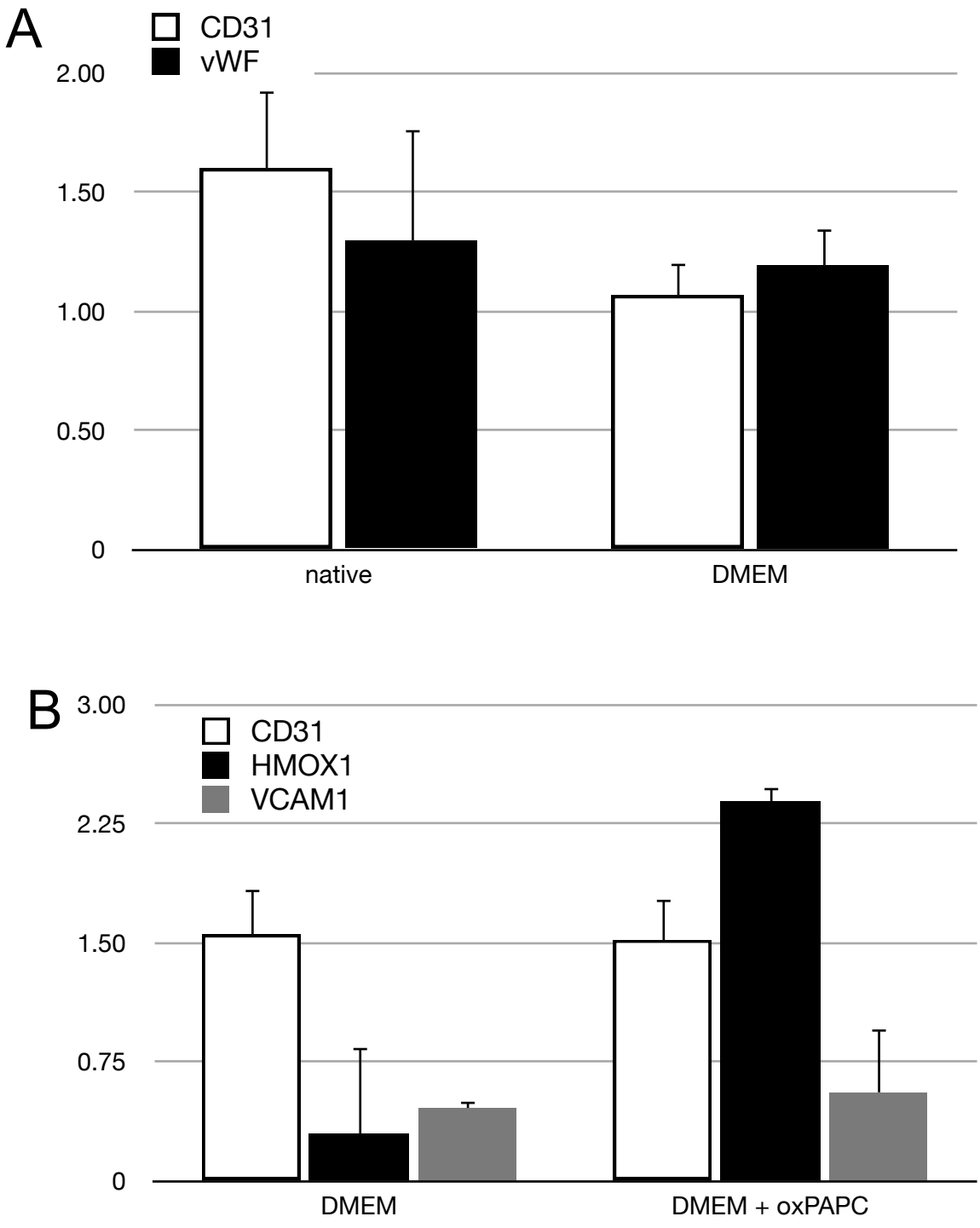
A
CD31
vWF
2.00
1.50
1.00
0.50
0
native
DMEM
B
3.00
CD31
HMOX1
VCAM1
2.25
1.50
0.75
0
DMEM
DMEM + oxPAPC

C

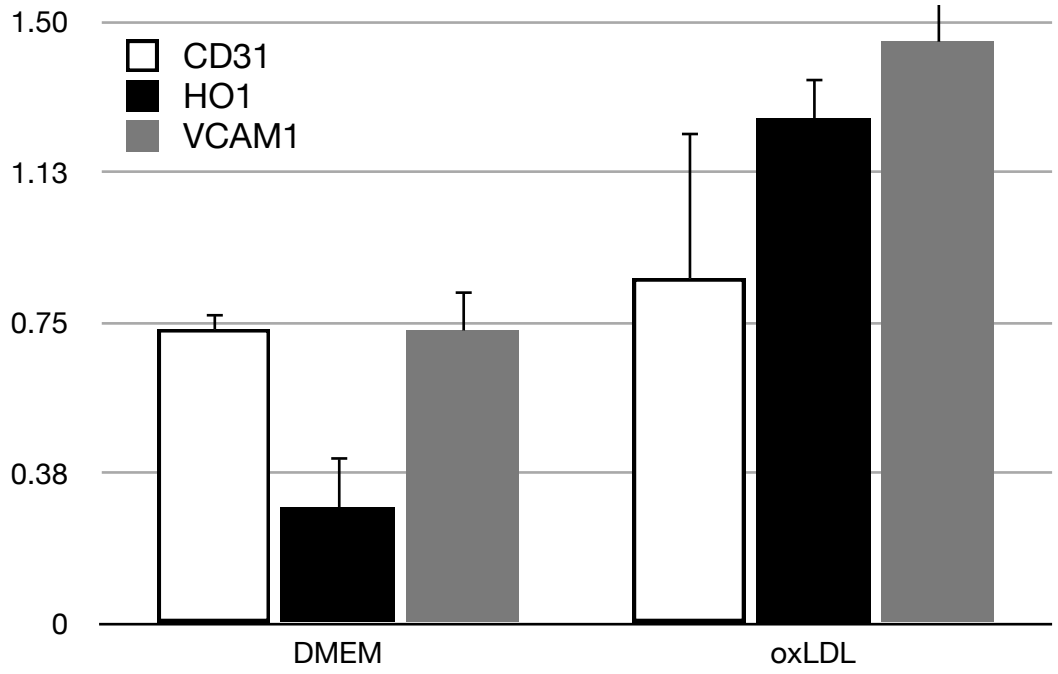
1.50
1.13
0.75
0.38
0
CD31
HO1
VCAM1
DMEM
oxLDL

D

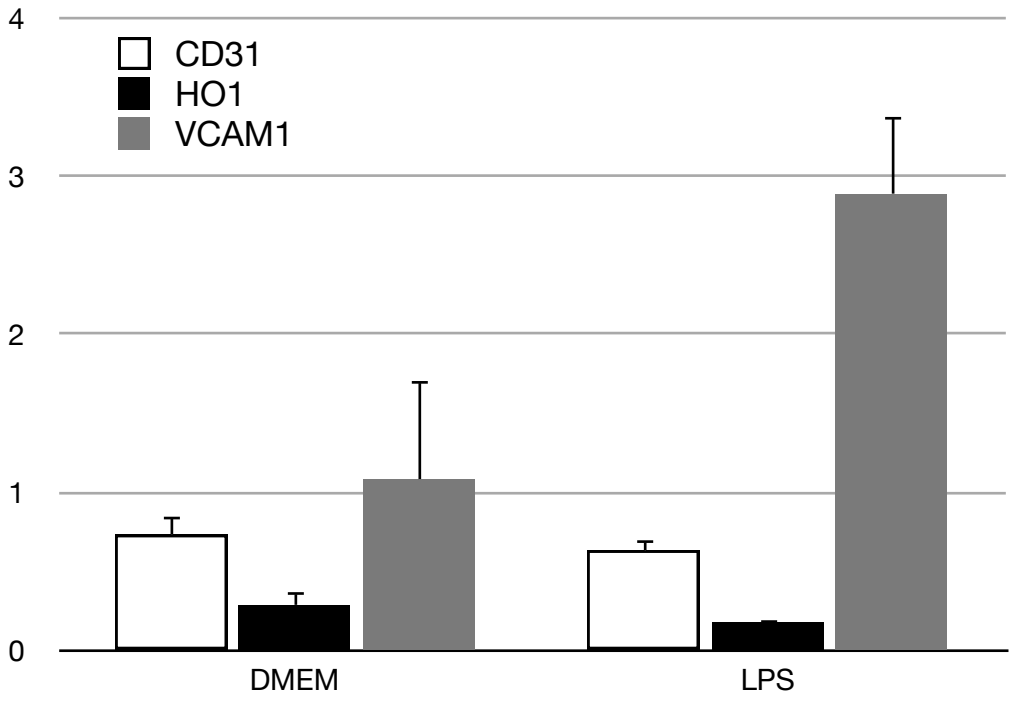
4
3
2
1
0
CD31
HO1
VCAM1
DMEM
LPS

Figure 3

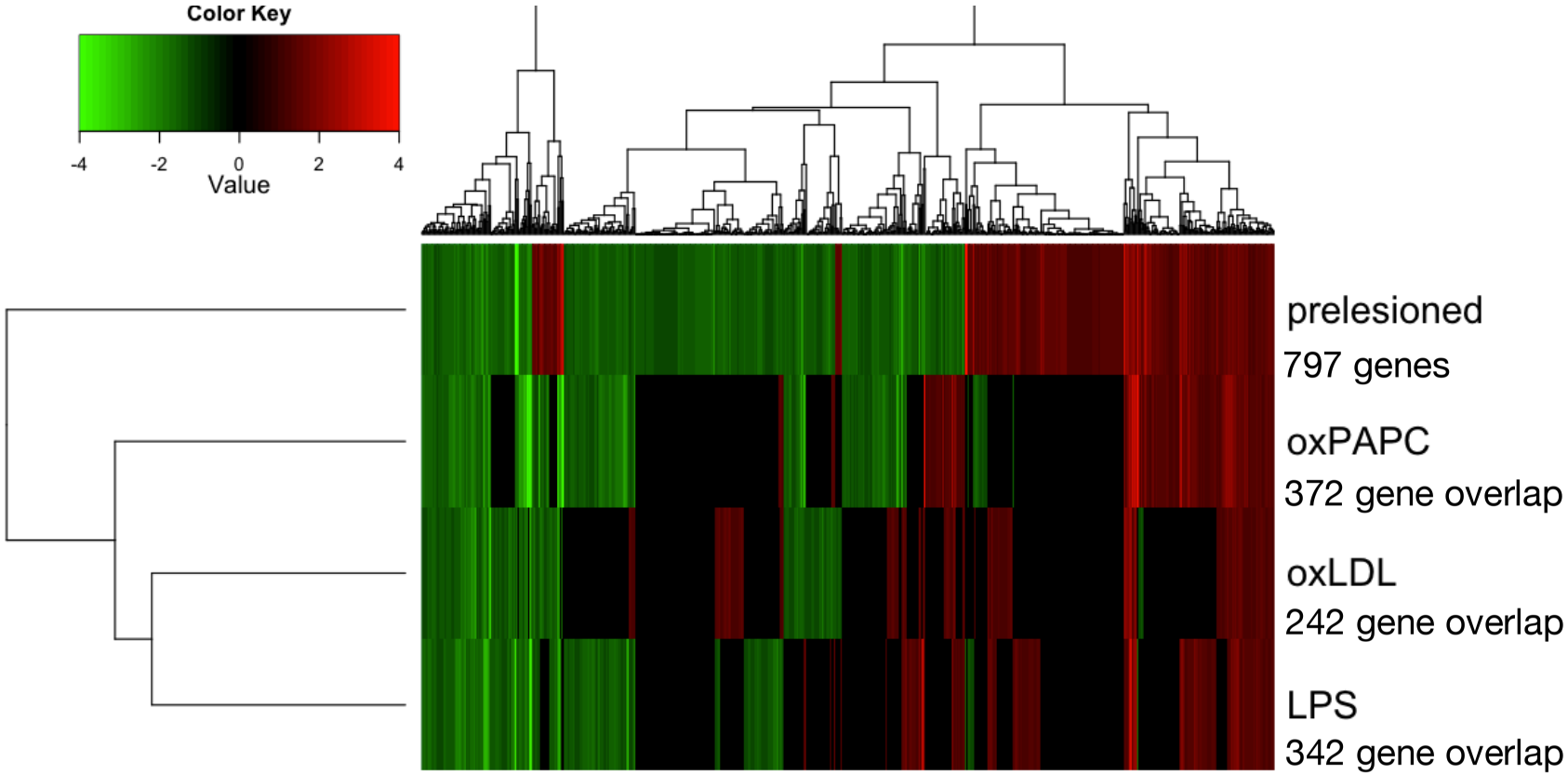
Color Key
-4
-2
0
2
4
Value
prelesioned
797 genes
oxPAPC
372 gene overlap
oxLDL
242 gene overlap
LPS
342 gene overlap

Figure 4

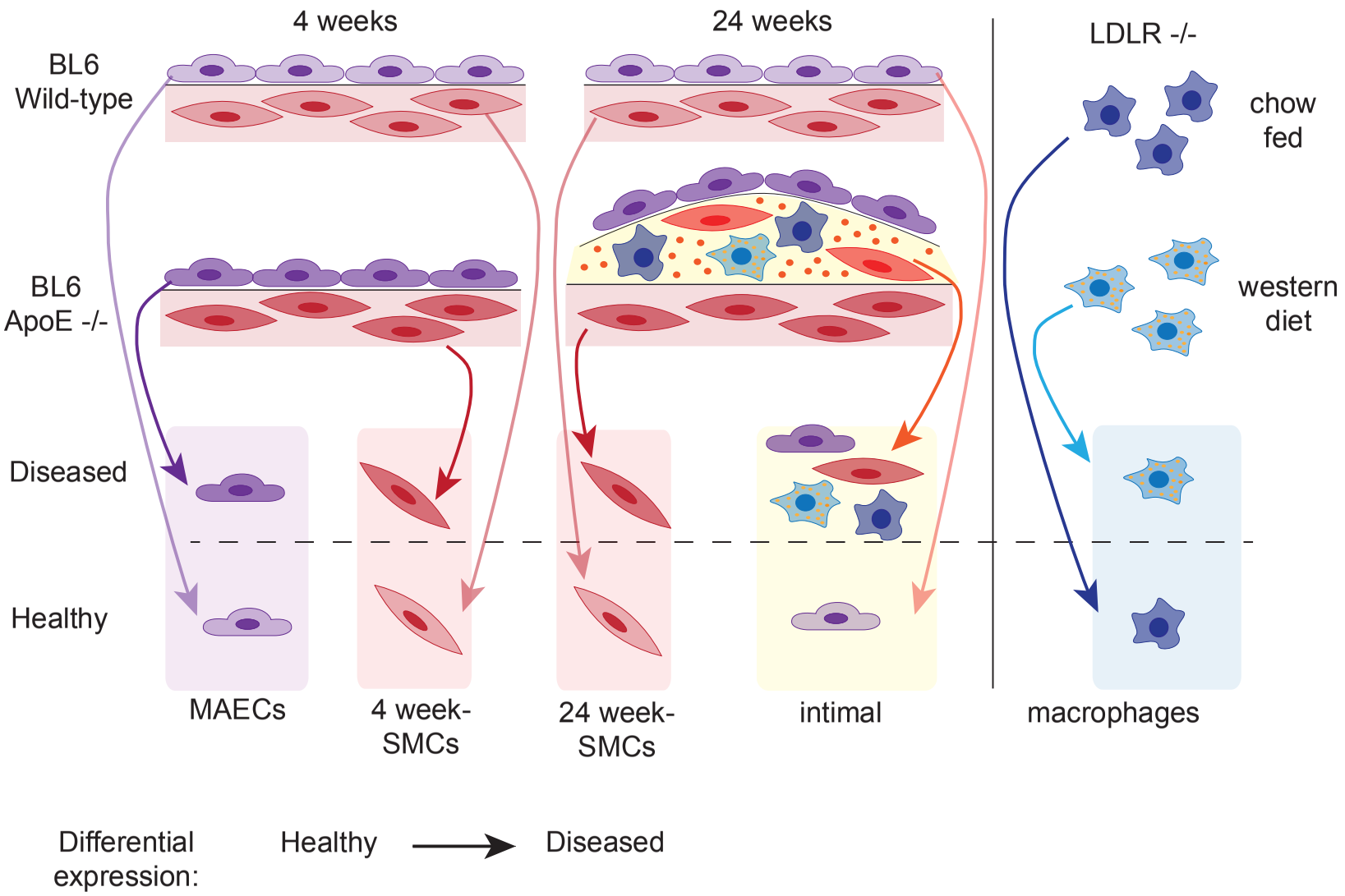
4 weeks
24 weeks
LDLR -/-
BL6
Wild-type
BL6
ApoE -/-
chow
fed
western
diet
Diseased
Healthy
MAECs
4 week-
SMCs
24 week-
SMCs
intimal
macrophages
Differential
expression:
Healthy
Diseased

Figure 5

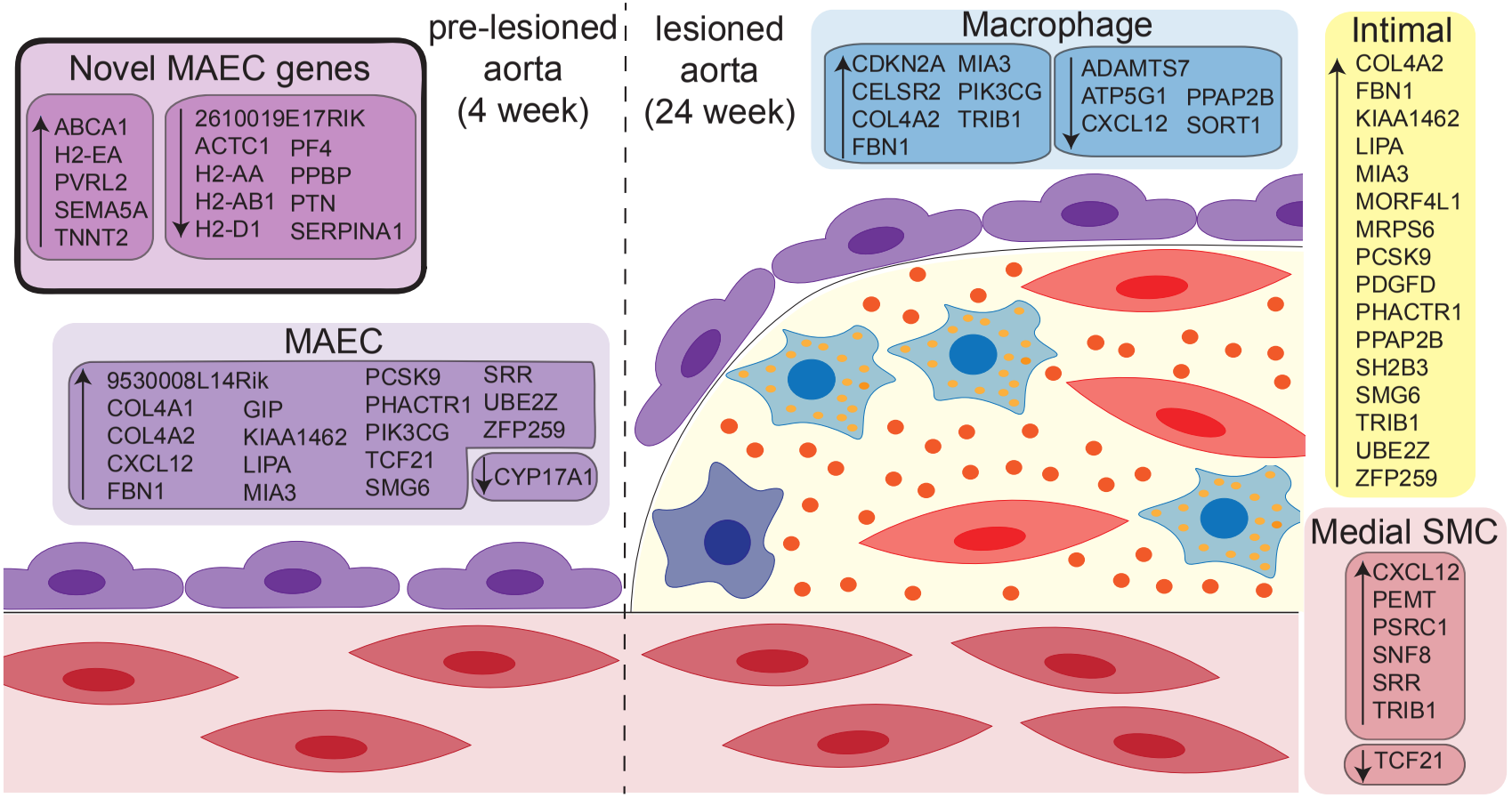
Novel MAEC genes
ABCA1
H2-EA
PVRL2
SEMA5A
TNNT2
2610019E17RIK
ACTC1
H2-AA
H2-AB1
H2-D1
PF4
PPBP
PTN
SERPINA1
pre-lesioned aorta (4 week)
lesioned aorta (24 week)
Macrophage
CDKN2A
CELSR2
COL4A2
FBN1
MIA3
PIK3CG
TRIB1
ADAMTS7
ATP5G1
CXCL12
PPAP2B
SORT1
Intimal
COL4A2
FBN1
KIAA1462
LIPA
MIA3
MORF4L1
MRPS6
PCSK9
PDGFD
PHACTR1
PPAP2B
SH2B3
SMG6
TRIB1
UBE2Z
ZFP259
MAEC
9530008L14Rik
COL4A1
COL4A2
CXCL12
FBN1
GIP
KIAA1462
LIPA
MIA3
PCSK9
PHACTR1
PIK3CG
TCF21
SMG6
SRR
UBE2Z
ZFP259
CYP17A1
Medial SMC
CXCL12
PEMT
PSRC1
SNF8
SRR
TRIB1
TCF21

Supplemental Figure 1

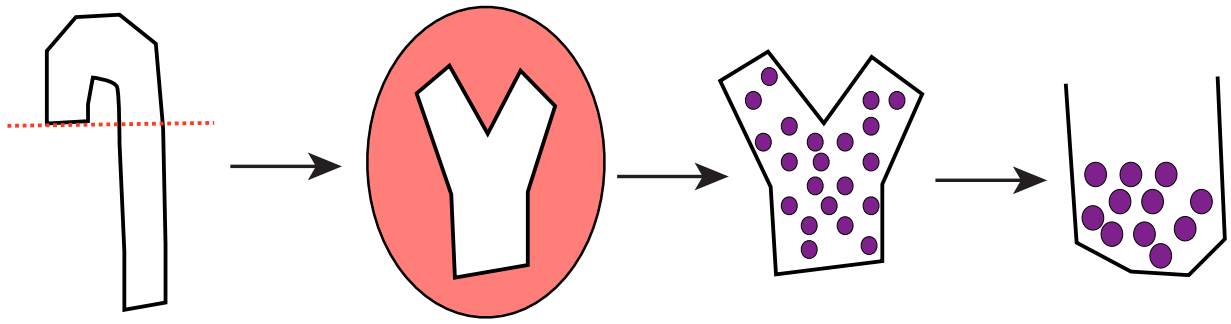

Supplemental Figure 2

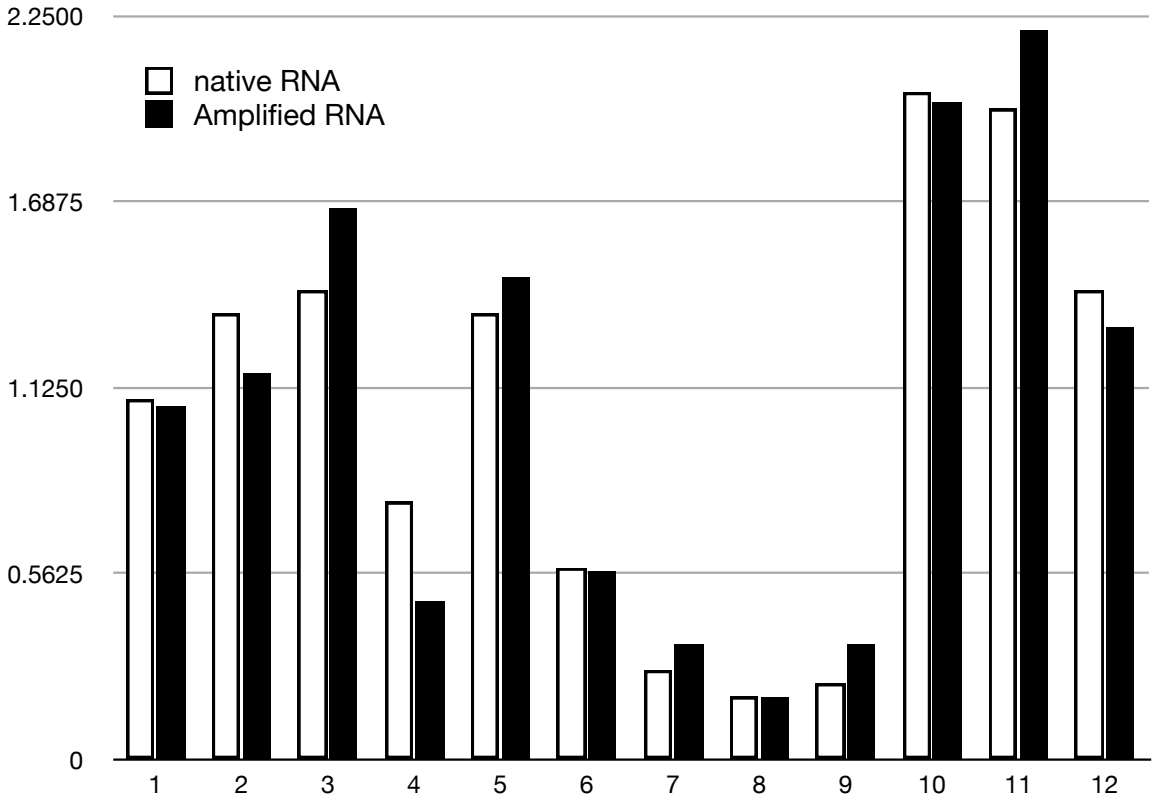

Supplemental Figure 3

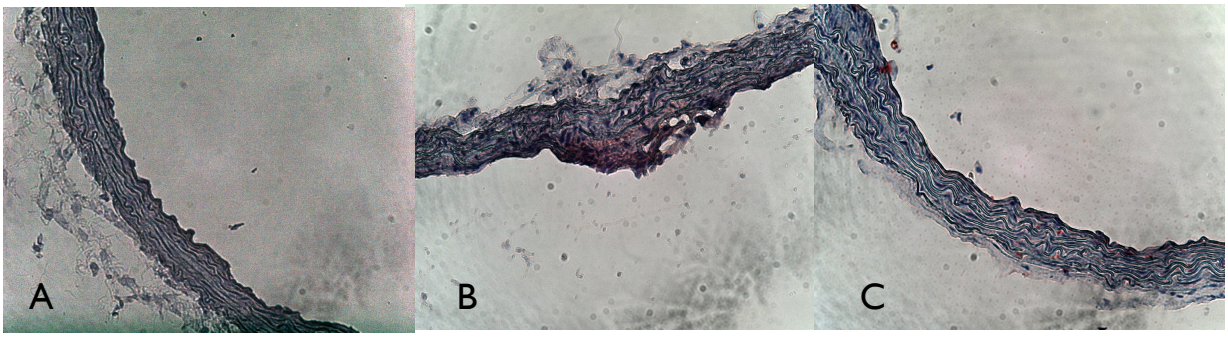

Table 1

	FDR 5%	FDR 10%
1.2 + fold change	316	748
1.5 + fold change	175	341
2+ fold change	32	51

Table 2

gene	pre-lesioned MAECs
2610019E17RIK	-2.97*
ABCA1	3.13**
ACTC1	-4.68
H2-AA	-5.60**
H2-AB1	-10.20*
H2-D1	-2.29**
H2-EA	442^
PF4	-9.59*
PPBP	-9.63**
PTN	-3.37*
PVRL2	5.88*
SEMA5A	1.76*
SERPINA1	-14.25*
TNNT2	2.87*

* P-value ≤ 0.05

** P-value ≤ 0.01

^ *extreme differential expression from very low expression at base level; p-value of 0.112*

Table 3

	9530008L14Rik	ABCG8	ABO	ADAMTS7	ANKS1A	APOA1	APOA4	APOA5	APOC3	ATP5G1
MAECs	yes	no	no	yes	yes	no	no	no	no	yes
medial cells	yes	no	no	yes	yes	yes	no	no	yes	yes
intimal lesions	yes	no	no	yes	yes	no	no	no	no	yes
macrophages	yes	no	no	yes	yes	yes	no	no	no	yes

	CDKN2A	CDKN2B	CELSR2	CNNM2	COL4A1	COL4A2	CXCL12	CYP17A1	FBN1	GIP
MAECs	no	yes	yes	yes	yes	yes	yes	yes	yes	yes
medial cells	no	yes	yes	yes	yes	yes	yes	no	yes	no
intimal lesions	no	yes	yes	yes	yes	yes	yes	yes	yes	yes
macrophages	yes	yes	yes	yes	yes	yes	yes	no	yes	no

	HHIPL1	HNF1A	IL5	KCNE	KIAA1462	LDLR	LIPA	MIA3	MORF4L1	MRAS
MAECs	yes	no	yes	no	yes	yes	yes	yes	yes	yes
medial cells	yes	no	no	no	yes	yes	yes	yes	no	yes
intimal lesions	yes	no	yes	no	yes	yes	yes	yes	yes	yes
macrophages	yes	no	no	no	yes	yes	yes	yes	no	yes

	MRPS6	MTHFD1L	NT5C2	PCSK9	PDGFD	PEMT	PHACTR1	PIK3CG	PPAP2B	PSRC1
MAECs	yes	yes	yes	yes	yes	yes	yes	yes	yes	yes
medial cells	yes	yes	yes	yes	yes	yes	yes	yes	yes	yes
intimal lesions	yes	yes	yes	yes	yes	yes	yes	yes	yes	yes
macrophages	yes	yes	yes	yes	no	yes	no	yes	yes	yes

	RASD1	SH2B3	SLC17A4	SLC22A3	SLC5A3	SMAD3	SMG6	SNF8	SORT1	SRR
MAECs	yes	yes	yes	yes	yes	yes	yes	yes	yes	yes
medial cells	yes	yes	no	yes	yes	yes	yes	yes	yes	yes
intimal lesions	yes	yes	yes	yes	yes	yes	yes	yes	yes	yes
macrophages	yes	yes	no	no	yes	yes	yes	yes	yes	yes

	TRIB1	TCF21	UBE2Z	WDR12	ZC3HC1	ZFP259
MAECs	yes	yes	yes	yes	yes	yes
medial cells	yes	yes	yes	yes	yes	yes
intimal lesions	yes	yes	yes	yes	yes	yes
macrophages	yes	yes	yes	yes	yes	yes

Table 4

	9530008L14Rik	ADAMTS7	ATP5G1	CDKN2A	CELSR2	COL4A1	COL4A2	CXCL12	CYP17A1
4 week MAECs	1.89*					3.61*	11.2***	3.05*	-14*
4 week medial SMCs									
24 week medial SMCs								1.28*	
24 week intimal cells							3.10*		
macrophages		-3.36**	-1.5*	1.74*	17.10**		1.82*	-2.81*	

	FBN1	GIP	KIAA1462	LIPA	MIA3	MORF4L1	MRPS6	PCSK9	PDGFD
4 week MAECs	2.52***	9.33**	1.46*	1.82*	2.23*			3.72*	
4 week medial SMCs									
24 week medial SMCs									
24 week intimal cells	3.36**		2.46***	17.62	2.23*	2.92*	2.18*	9.44***	2.08**
macrophages	1.79*				1.41**				

	PEMT	PHACTR1	PIK3CG	PPAP2B	PSRC1	SH2B3	SMG6	SNF8	SORT1
4 week MAECs		2.09*	3.14*				2.50*		
4 week medial SMCs									
24 week medial SMCs	2.11*				1.83*			1.53	
24 week intimal cells		1.55*		8.58**		6.41*	2.96***		
macrophages			1.65*	-2.63**	-8.87*				-2.32*

	SRR	TCF21	TRIB1	UBE2Z	ZFP259
4 week MAECs	2.89**	1.82**		3.61**	2.47**
4 week medial SMCs					
24 week medial SMCs	1.45*	-1.78*	1.66*		
24 week intimal cells			15.4*	2.43**	3.71**
macrophages			8.64*		

* P-value ≤ 0.05
** P-value ≤ 0.01
*** P-value ≤ 0.001

Supplemental Table 1

2610019E17RIK-F; TAGTGCTCGCCGAATGGAACTCAA
2610019E17RIK-R; TCAGATACACGGATGCCCAGCTTA
36B4-F; TGAAGCAAAGGAAGAGTCGGAGGA
36B4-R; AAGCAGGCTGACTTGGTTGCTTTG
9530008L14Rik-F: TGGATACTGGTTTGAAGGGAGGCA
9530008L14Rik-R: AGCCTTTGTCCCAGCTAAAGTCCT
ABCA1-F: ATGTGGAGTTCTTTGCCCTCCTGA
ABCA1-R: CTTTCGTTTGTTGCCGCCACTGTA
ABCG8-F: TTGGACAACCTGTGGATAGTGCCT
ABCG8-R: GGTGAAGTTGCCGATTTGTGTGGT
ABO-F: ACAGACACTGAACCATCCTGGGTT
ABO-R: AGACAAACACTGCGAAGGGAAGGA
ACTA2-F; ACTCTCTTCCAGCCATCTTTCA
ACTA2-R; ATAGGTGGTTTCGTGGATGC
ACTC1-F: ACCATGTACCCTGGTATTGCCGAT
ACTC1-R: ATGGGCCTGCCTCATCATACTCTT
ADAMTS7-F; TCATGAACATGGTGGCTGGACTCT
ADAMTS7-R; AGTCTCTTCGGCATGGTGTGTGAT
ALDH1A3-F: TCAACAAGATAGCCTTCACCGGCT
ALDH1A3-R: TTGAAGAACACTCCCTGGTGAGCA
ANKS1A-F: CAACAAGAACGTCATTGCGGAGCA
ANKS1A-R: TCAGGTTCACATCCACTGTGCTGA
ApoA1-F: TCACCCACACCCTTCAGGATGAAA
ApoA1-R: ACACATAGTCTCTGCCGCTGTCTT
APOA4-F: TTCTGACTCCGGGAAACATCCAGT
APOA4-R: CTTGGCATTGTTGCTTAGCTGGGT
APOA5-F: GCTTTGCAAACCCAGCTTCTGGTA
APOA5-R: TTAACAGGAGCCCAACTCCAGGTT
APOC3-F: TACAGGGCTACATGGAACAAGCCT
APOC3-R: AGAATCCCAGAAGCCGGTGAACTT
ATP1A2-F; ACAACCAGATCCATGAGGCTGACA
ATP1A2-R; TTGAGCAGAGCTGACTCAGAAGCA
ATP5G1-F; ACGGGAATTCCAGACCAGTGTCAT
ATP5G1-R; AGCTACCAAACACTGTGCCAATGC
B2M-F; GCAGGTTCAAATGAATCTTCAGAGCATC
B2M-R; TACGTAACACAGTTCCACCCGCCTC
CALD-F; TGCCTCAGGAACACCCAATAAGGA
CALD-R; AGAGGTTCCGCTTGCCAGATACAT
CD31-F; TGGAGTGGTCATCGCCACCTTAAT
CD31-R; AACAGAAACCCGTGGAGATGTCCA
CD45-F; ACCTCCAATGTCAGCACCACAGAT
CD45-R; ACTGACCCTCCAAGCACAACCATA
CD68-F; TACAATGTGTCCTTCCCACAGGCA
CD68-R; AGGTCAAGGTGAACAGCTGGAGAA
CDKN2A-F: ACATCGTGCGATATTTGCGTTCCG
CDKN2A-R: TTTAGCTCTGCTCTTGGGATTGGC
CDKN2B-F: TGTTTGACATTTGGGTGGGTGCAG
CDKN2B-R: ATTTCCTTGTCGAGCTGGAGGTGA
CELSR2-F: ATGAGTGTGCTGGTGTCAGATGGT
CELSR2-R: TGAATGAAGAGTCCCAGCAGTGGT
CNN1-F; GGCCAGCATGTCTTCTGCACATTT
CNN1-R; AGAATGATCCCGTCTTTGAGGCCA
CNNM2-F; GCCCACCGTGAAAGAAAGCAAGAT
CNNM2-R; ATCTGGGATGGGCTAAACGCTTCT
COL4A1-F; AGGATGCAACGGTACAAAGGGAGA
COL4A1-R; TGGCCGAGAATTTCACCAGGATCT
COL4A2-F: GCCAAACGCACTTCCTGGAATCAA
COL4A2-R: CGGTGTTGCCCATGAATCCTTGTT
CXCL12-F; TGCACGGCTGAAGAACAACAACAG
CXCL12-R; TCACACCTCTCACATCTTGAGCCT
CYP17A1-F: AAGCATATCCTTGTCACGGTGGGA
CYP17A1-R: ACGGTGTTCGACTGAAGCCTACAT
DES-F; ATGAGACCATCGCGGCTAAGAACA
DES-R; ATTGGCTGCCTGAGTCAAGTCTGA
FBN1-F; AATGCAACGATCGAAACGAGTGCC
FBN1-R; AGCCAGTGTGACAAAGGCAGTAGA
GBP2-F: AGATCCACATGTCGGAACCCATGT
GBP2-R: AGGCTGTGTAATGGCAGACAGGAT
GIP-F: TGGCTTTGAAGACCTGCTCTCTGT
GIP-R: GGGCCAGCAAATTTAGCATGGGAT
H2-AA-F: TGTGGACAACATCTTCCCTCCTGT
H2-AA-R: TGGTCTCATAAACACCGTCTGCGA
H2-AB1-F: TGTGAGTCCTGGTGACTGCCATTA
H2-AB1-R: TCGCCCATGAACTGGTACACGAAA
H2-D1-F: TGATGTTCCCTGTGAGCTTGGGTT
H2-D1-R: AGCATGGAGCTTACAGGATGCAGA
H2-EA-F: CGTGTGTGCTCTTGGGTTGTTTGT
H2-EA-R: GTCGGCGTTCTACAACATTGCGTT
HHIPL1-F; AAGCTGGGTAAATCAGTCACCGGA
HHIPL1-R; ACCTCGCTATACTTCCATTGGCCT
HMOX1-F; CAGGTGATGCTGACAGAGGA
HMOX1-R; GAGAGTGAGGACCCACTGGA
HNF1A-F;TGTCTGCGGCCTTACACCAAGTAT
HNF1A-R; AGGTAGCGAGGCCATGATAAGGTT
IIGP1-F: AAGCGGCAATTTCTGAAGCAGAGG
IIGP1-R: ATCCACTCCAAACACAGTGCGGTA
IL5-F: TCCCATGAGCACAGTGGTGAAAGA
IL5-R AGGAAGCCTCATCGTCTCATTGCT
KCNE2-F: AGGGCTTACAGGTCTCAAGCTGAA
KCNE2-R: ATTGGCTAATGTGGCCATGCTTCC
KIAA1462-F;AGAATCGCGTCTTGGTGTTCCTGA
KIAA1462-R; AGGGAAGACTGAGTGCAAAGCTGA
LDLR-F; CAACAATGGTGGCTGTTCCCACAT
LDLR-R; ACTCACACTTGTAGCTGCCTTCCA
LEP-F; TGCTGAAGTTTCAAAGGCCACCAG
LEP-R; TCATGCCTTTGGATGGGTGGTCTA
LIPA-F; TGACTGACTAGCAAGCGTCCACAA
LIPA-R; ATTACCTCCACACAAGGGCCAGAA
MIA3-F; TGAGTGCCATCGGGTTCAAGAAGA
MIA3-R; TCGGCATGCGATTTACTCCACTCT
MORF4L1-F; AATGGAGATGGTGGCAGTACCAGT
MORF4L1-R; AATGGAGATGGTGGCAGTACCAGT
MRAS-F: TCAGTGGGCCATCTTGGATGTTCT
MRAS-R: TTGGGAATGACTCCCTGTCCTTGA
MRPS6-F; TTGCTGCAGGAGGTAGAAACTGCT
MRPS6-R; AGGCTTGCAAGACAACCAAGTGTG
MTHFD1L-F; AAGCCAAAGTCCAATTGTCCCTGC
MTHFD1L-R; AGGCGAAGGAGTTGACTTTCAGGT
Myh11-F; TGAGCTCAGTGACAAGGTCCACAA
Myh11-R; AAACTGGCCAAAGATGTGGCTTCC
NT5C2-F: AAGTCAAAGAAACGGCAAGGGTGG
NT5C2-R: TGCTGTCCAGGTGCTTGTAGAGTT
PCSK9-F; ACAAGGACAGTCAACTCACAGCCA
PCSK9-R; TGCAGCAGATGAGGACATCTGGAA
PDGFD-F: ACTCCGCAGAGAGCATCCATCAAA
PDGFD-R: GGCCATTGCTTGTCACCTGAATGT
PEMT-F; TATGATGAGCCAGCCCAAGATGGA
PEMT-R; GAAGCTGGACAGCACAAACACGAA
PF4-F: TGCACTTAAGAGCCCTAGACCCAT
PF4-R: AGATCTCCATCGCTTTCTTCGGGA
PHACTR1-F; AAATCAAGAGGAGGCTGACTCGCA
PHACTR1-R; TGCCACTTCCACGTAGTCACTGAA
PIK3CG-F; TTTGTGGAAGCGAACATCCAGCAC
PIK3CG-R; ATGCCAAACTCCAGCCACACATTC
PPAP2B-F; ATGGCCTTCTACACGGGATTGTCA
PPAP2B-R; AAGAGGTCGGACACGAAGAACACT
PPARGC1A-F: AGCACTCAGAACCATGCAGCAAAC
PPARGC1A-R: TTTGGTGTGAGGAGGGTCATCGTT
PPBP-F-F: TAACCTCCAGATCTTGCTGCTGCT

Supplemental Table 1 continued

PPBP-R-R: ACTCCTGGCCTGTACACATTCACA
PSRC1-F; TCCTCAGCTAGCAACTCCCAATGT
PSRC1-R; AGAATCTGGAGCTAGGGCACCTTT
PTN-F: TTGGAGCTGAGTGCAAGTACCAGT
PTN-R: TCTTCTTTGACTCCGCTTGAGGCT
PVRL2-F: AGCTGCGGATGAGGAAGAAGAACT
PVRL2-R: TGATCAGCACAAGAGACACCAGCA
RASD1-F: AAGAGGTGCAAAGGCTCAAACAGC
RASD1-R: TTTGTTACCGCAAATGACCAGCGG
SEMA5A-F: GCATCCTTGCATGGCTGTTCTCAA
SEMA5A-R: ATCCACAGCATTCTCGGCTCTGAA
SERPINA1A-F; ACAGGCAATGGCCTCTTTGTCAAC
SERPINA1A-R; TTTCCTTGGGTTCCCTTCTCCACA
SH2B3-F: AGCCACTTTCTGCAGCTCTTCGAT
SH2B3-R: AGTTCAGCTGCTGTTCATCTCCCA
SLC17A4-F; TACGTGGTTGGTCTGGGCTTGTTA
SLC17A4-R; ATGAGCAAGGCTACTCCAGCATCA
SLC22A3-F; ATCACCCGGAAGCAAGGAGAGAAA
SLC22A3-R; GCGCTCGTGAACCAAGCAAACATA
SLC5A3-F; TATTGTGGAGATGCAAGGAGGCCA
SLC5A3-R; AAGAACAAAGCCTGCCATTCCACC
SMAD3-F: AACAACCAGGAATTTGCTGCCCTC
SMAD3-R: ACTGCAAGGGTCCATTCAGGTGTA
SMG6-F; TATCGGGAGCAAGCCAACGATACA
SMG6-R; AGGATAGGGTTGCTGGCTGCTAAA
SMTN-F; AGAATTGACTTTGGGATTGCGGGC
SMTN-R; TCTTAAAGTTGCAGCCTCCTCGGT
SNF8-F; AGAAGAAACTCGCAGAGGCCAAGT
SNF8-R; TCTTCCGGATCTCTTGCTTGTGCT
SORT1-F; ACCTGTTAGCTCTCAGCACCGAAA
SORT1-R; CAGCTTTGCAGGAGCCATTCACAT
SRR-F; AAGGAACAATTGCCCTGGAAGTGC
SRR-R; ATTCCAGCAACCATTCCTCCTCCT
TAGLN-F; TCTAATGGCTTTGGGCAGTTTGGC
TAGLN-R; TTTGAAGGCCAATGACGTGCTTCC
TCF21-F; AGATCCCACCTCAAACCCAACACA
TCF21-R; TGTTGGAGTCCACTTTCAGGGAGT
TNNT2-F; TATTCGCAATGAGCGGGAGAAGGA
TNNT2-R; AGTGCATCATGTTGGACAGAGCCT
TRIB1-F: CTTCAAGCAGATTGTTTCCGCCGT
TRIB1-R: AGGCTTTCCAGTCTAAGCTGGGTT
UBE2Z-F: AGTCTGTGACATGATGGAGGGCAA
UBE2Z-R TTGCAGGCCACCTCATAGAAGTCA

VCAM1-F; TACCAGCTCCCAAAATCCTG
VCAM1-R; TCTGCTAATTCCAGCCTCGT
vWF-F; AGACATCACAGCCAAGGTGCAGTA
vWF-R; ACACAGCTTTGCTGGCACACTTTC
WDR12-F; AACGTTTGGCATCTGGAAGCACAG
WDR12-R; AGAGACAGCGACACCAAAGAACCA
ZC3HC1-F; AGTGAGTTCCTGGACCGGTTTCAA
ZC3HC1-R; AATCAAGCTCATCCTCCAGCAGGT
ZFP259-F; TGATGATCCCTCGGGAAACAGCTT
ZFP259-R; TGCACTCTGGGCAGTTAGTGTTGA

hACTA2-F; TGACAATGGCTCTGGGCTCTGTAA
hACTA2-R; TTCGTCACCCACGTAGCTGTCTTT
hATP1A2-F; TGGAGGATGAACCATCCAACGACA
hATP1A2-R; AGGAGAAGCAGCCAGTGACAATGA
hB2M-F; GATGAGTATGCCTGCCGTGTG
hB2M-R; CAATCCAAATGCGGCATCT
hCALD-F;TGACCAACCAGAAGGCTCAGACAT
hCALD-R; TTTCTGCTTCGAGTCGCATCTCCT
hCD31; TGCACATAATTGCCATTCCCACGC
hCD31-R; GCACATTGCAGCACAATGTCCTCT
hCNN1-F; GCAACTTCATCAAGGCCATCACCA
hCNN1-R; TCGAATTTCCGCTCCTGCTTCTCT
hDES-F; AAATCCGGCACCTCAAGGATGAGA
hDES-R; TTTCTCGGAAGTTGAGGGCAGAGT
hMYH11-F; AATGGAAGACCTGGTCAGCTCCAA
hMYH11-R; CATGTTGACTTCCAGCCGCAGTTT
hSMTN-F; AGCACCATGATGCAAACCAAGACC
hSMTN-R; TCTGCGCCTTCATCAGCTCTTTCT
hTAGLN-F; TTGAAGGCAAAGACATGGCAGCAG
hTAGLN-R; TCCACGGTAGTGCCCATCATTCTT

Supplemental Table 2

Leptin (adipose)	normalized value
MAEC #8	0.000045
MAEC #9	0.000012
whole aorta #1	0.044931

CD45 (leukocyte)	normalized value
MAEC #4	not detected
MAEC #5	not detected
MAEC #6	not detected
MAEC #7	not detected
whole aorta #3	13.919402

MSR1 (macrophage)	normalized value
MAEC #1	not detected
MAEC #2	not detected
MAEC #3	not detected
whole aorta #1	0.34549
whole aorta #2	0.22967
whole aorta #3	3.99975

References

1. Kathiresan, S. and D. Srivastava, *Genetics of human cardiovascular disease.* Cell, 2012. **148**(6): p. 1242-57.
2. Libby, P., P.M. Ridker, and G.K. Hansson, *Progress and challenges in translating the biology of atherosclerosis.* Nature, 2011. **473**(7347): p. 317-25.
3. Hansson, G.K. and A. Hermansson, *The immune system in atherosclerosis.* Nature immunology, 2011. **12**(3): p. 204-12.
4. Stylianou, I.M., et al., *Genetic basis of atherosclerosis: insights from mice and humans.* Circulation research, 2012. **110**(2): p. 337-55.
5. Daugherty, A., *Mouse models of atherosclerosis.* The American journal of the medical sciences, 2002. **323**(1): p. 3-10.
6. Frid MG, K.V., Stenmark KR, *Mature vascular endothelium can give rise to smooth muscle cells via endothelial-mesenchymal transdifferentiation: in vitro analysis.* Circ Res. , 2002. **90**(11): p. 1189-96.
7. Wang, X.Q., et al., *Thioredoxin interacting protein promotes endothelial cell inflammation in response to disturbed flow by increasing leukocyte adhesion and repressing Kruppel-like factor 2.* Circulation research, 2012. **110**(4): p. 560-8.
8. Gao, J., et al., *Involvement of endoplasmic stress protein C/EBP homologous protein in arteriosclerosis acceleration with augmented biological stress responses.* Circulation, 2011. **124**(7): p. 830-9.
9. Ma, Y., et al., *Altered gene expression in early atherosclerosis is blocked by low level apolipoprotein E.* PloS one, 2008. **3**(6): p. e2503.

10. Beer, M., et al., *Laser-capture microdissection of hyperlipidemic/ApoE/ mouse aorta atherosclerosis.* Methods in molecular biology, 2011. **755**: p. 417-28.
11. Jongstra-Bilen, J., et al., *Low-grade chronic inflammation in regions of the normal mouse arterial intima predisposed to atherosclerosis.* The Journal of experimental medicine, 2006. **203**(9): p. 2073-83.
12. Schunkert, H., et al., *Large-scale association analysis identifies 13 new susceptibility loci for coronary artery disease.* Nature genetics, 2011. **43**(4): p. 333-8.
13. Kathiresan, S., et al., *Genome-wide association of early-onset myocardial infarction with single nucleotide polymorphisms and copy number variants.* Nature genetics, 2009. **41**(3): p. 334-41.
14. Samani, N.J., et al., *Genomewide association analysis of coronary artery disease.* The New England journal of medicine, 2007. **357**(5): p. 443-53.
15. *Large-scale gene-centric analysis identifies novel variants for coronary artery disease.* PLoS genetics, 2011. **7**(9): p. e1002260.
16. Erdmann, J., et al., *New susceptibility locus for coronary artery disease on chromosome 3q22.3.* Nature genetics, 2009. **41**(3): p. 280-2.
17. Wang, F., et al., *Genome-wide association identifies a susceptibility locus for coronary artery disease in the Chinese Han population.* Nature genetics, 2011. **43**(4): p. 345-9.
18. *A genome-wide association study in Europeans and South Asians identifies five new loci for coronary artery disease.* Nature genetics, 2011. **43**(4): p. 339-44.

19. Clarke, R., et al., *Genetic variants associated with Lp(a) lipoprotein level and coronary disease.* The New England journal of medicine, 2009. **361**(26): p. 2518-28.

20. Soranzo, N., et al., *A genome-wide meta-analysis identifies 22 loci associated with eight hematological parameters in the HaemGen consortium.* Nature genetics, 2009. **41**(11): p. 1182-90.

21. *Genome-wide association study of 14,000 cases of seven common diseases and 3,000 shared controls.* Nature, 2007. **447**(7145): p. 661-78.

22. Peden, J.F. and M. Farrall, *Thirty-five common variants for coronary artery disease: the fruits of much collaborative labour.* Human molecular genetics, 2011. **20**(R2): p. R198-205.

23. Watson, A.D., et al., *Structural identification by mass spectrometry of oxidized phospholipids in minimally oxidized low density lipoprotein that induce monocyte/ endothelial interactions and evidence for their presence in vivo.* The Journal of biological chemistry, 1997. **272**(21): p. 13597-607.

24. Subbanagounder, G., et al., *Determinants of bioactivity of oxidized phospholipids. Specific oxidized fatty acyl groups at the sn-2 position.* Arteriosclerosis, Thrombosis, and Vascular Biology, 2000. **20**(10): p. 2248-54.

25. Navab, M., et al., *Interaction of monocytes with cocultures of human aortic wall cells involves interleukins 1 and 6 with marked increases in connexin43 message.* The Journal of clinical investigation, 1991. **87**(5): p. 1763-72.

26. Krenek, P., et al., *A simple method for rapid separation of endothelial and smooth muscle mRNA reveals Na/K+ -ATPase alpha-subunit distribution in rat arteries.* Journal of vascular research, 2006. **43**(6): p. 502-10.

27. Romanoski, C.E., et al., *Systems genetics analysis of gene-by-environment interactions in human cells.* American journal of human genetics, 2010. **86**(3): p. 399-410.

28. Romanoski, C.E., et al., *Network for activation of human endothelial cells by oxidized phospholipids: a critical role of heme oxygenase 1.* Circulation research, 2011. **109**(5): p. e27-41.

29. Debold, E.P., et al., *Human actin mutations associated with hypertrophic and dilated cardiomyopathies demonstrate distinct thin filament regulatory properties in vitro.* Journal of molecular and cellular cardiology, 2010. **48**(2): p. 286-92.

30. Frey, N., M. Luedde, and H.A. Katus, *Mechanisms of disease: hypertrophic cardiomyopathy.* Nature reviews. Cardiology, 2012. **9**(2): p. 91-100.

31. Sadanandam, A., et al., *Semaphorin 5A promotes angiogenesis by increasing endothelial cell proliferation, migration, and decreasing apoptosis.* Microvascular research, 2010. **79**(1): p. 1-9.

32. Pitsilos, S., et al., *Platelet factor 4 localization in carotid atherosclerotic plaques: correlation with clinical parameters.* Thrombosis and haemostasis, 2003. **90**(6): p. 1112-20.

33. Yvan-Charvet, L., N. Wang, and A.R. Tall, *Role of HDL, ABCA1, and ABCG1 transporters in cholesterol efflux and immune responses.* Arteriosclerosis, Thrombosis, and Vascular Biology, 2010. **30**(2): p. 139-43.

34. Ortiz-Munoz, G., et al., *HDL antielastase activity prevents smooth muscle cell anoikis, a potential new antiatherogenic property.* FASEB journal : official publication of the Federation of American Societies for Experimental Biology, 2009. **23**(9): p. 3129-39.

35. Li, F., et al., *Pleiotrophin (PTN) is expressed in vascularized human atherosclerotic plaques: IFN-{gamma}/JAK/STAT1 signaling is critical for the expression of PTN in macrophages.* FASEB journal : official publication of the Federation of American Societies for Experimental Biology, 2010. **24**(3): p. 810-22.

36. Tahara-Hanaoka, S., et al., *Functional characterization of DNAM-1 (CD226) interaction with its ligands PVR (CD155) and nectin-2 (PRR-2/CD112).* International immunology, 2004. **16**(4): p. 533-8.

37. Lusis, A.J., J. Yu, and S.S. Wang, *The problem of passenger genes in transgenic mice.* Arteriosclerosis, Thrombosis, and Vascular Biology, 2007. **27**(10): p. 2100-3.

38. Li, A.C., et al., *Differential inhibition of macrophage foam-cell formation and atherosclerosis in mice by PPARalpha, beta/delta, and gamma.* The Journal of clinical investigation, 2004. **114**(11): p. 1564-76.

39. Alexander, I., E.R. Edelman, and H. Methe, *Function and mode of regulation of endothelial major histocompatibility complex class II.* Cell transplantation, 2009. **18**(3): p. 255-9.

40. Vaisman, B.L., et al., *Endothelial expression of human ABCA1 in mice increases plasma HDL cholesterol and reduces diet-induced atherosclerosis.* Journal of lipid research, 2012. **53**(1): p. 158-67.

41. Civelek, M., et al., *Prelesional arterial endothelial phenotypes in hypercholesterolemia: universal ABCA1 upregulation contrasts with region-specific gene expression in vivo.* American journal of physiology. Heart and circulatory physiology, 2010. **298**(1): p. H163-70.

42. Janciauskiene, S.M., et al., *The discovery of alpha1-antitrypsin and its role in health and disease.* Respiratory medicine, 2011. **105**(8): p. 1129-39.

43. Maclellan, W.R., Y. Wang, and A.J. Lusis, *Systems-based approaches to cardiovascular disease.* Nature reviews. Cardiology, 2012.

44. Akashi, M., et al., *A coronary artery disease-associated gene product, JCAD/KIAA1462, is a novel component of endothelial cell-cell junctions.* Biochemical and biophysical research communications, 2011. **413**(2): p. 224-9.

45. Arndt, S., et al., *Interactions of TANGO and leukocyte integrin CD11c/CD18 regulate the migration of human monocytes.* Journal of leukocyte biology, 2007. **82**(6): p. 1466-72.

46. Farnier, M., *The role of proprotein convertase subtilisin/kexin type 9 in hyperlipidemia: focus on therapeutic implications.* American journal of cardiovascular drugs : drugs, devices, and other interventions, 2011. **11**(3): p. 145-52.

47. Denis, M., et al., *Gene inactivation of proprotein convertase subtilisin/kexin type 9 reduces atherosclerosis in mice.* Circulation, 2012. **125**(7): p. 894-901.

48. Stein, E.A., et al., *Effect of a monoclonal antibody to PCSK9 on LDL cholesterol.* The New England journal of medicine, 2012. **366**(12): p. 1108-18.

49. Marian, A.J., *PCSK9 as a therapeutic target in atherosclerosis.* Current atherosclerosis reports, 2010. **12**(3): p. 151-4.

50. Turpeinen, H., et al., *Proprotein convertases in human atherosclerotic plaques: the overexpression of FURIN and its substrate cytokines BAFF and APRIL.* Atherosclerosis, 2011. **219**(2): p. 799-806.

51. Pei, H., et al., *Direct evidence for a crucial role of the arterial wall in control of atherosclerosis susceptibility.* Circulation, 2006. **114**(22): p. 2382-9.

Chapter 5

Concluding Remarks

In my dissertation work, I have described two main projects: one in which I develop a new procedure to identify genes that may play a role in atherosclerosis, and another in which I characterize the role of a recently-identified gene in atherogenesis. I believe that these projects contribute both valuable findings to the field of cardiovascular genetics and exciting future avenues for study.

I present evidence that Zhx2 functions as transcriptional repressor of anti-inflammatory factors. However, the direct DNA target(s) of Zhx2 and the specific mechanisms it impacts have not yet been identified. As many of the highly-perturbed genes in response to lack of Zhx2 have not been well-studied, I believe there is a potential for unraveling new immune response pathways by clarifying the individual genes involved in these regulatory networks. I am currently working on ChIP-seq experiments in RAW macrophage cell lines that will enable us to identify direct DNA targets of the Zhx2 transcription factor [1]. Coupled with the microarray data from Zhx2 null and wild-type macrophages, we can begin to form more specific hypotheses regarding the role of Zhx2 in inflammation and atherosclerosis, which can be tested using cell culture methods. I am also performing experiments on Zhx2-null Ldlr -/- mice with the liver-specific Zhx2 transgene described in Chapter 2. Once these mice have been fed a western diet, the degree of atherosclerosis in the Zhx2 Tg+ versus Tg- mice should confirm the extent to which Zhx2 acts through the liver to affect atherosclerosis. The TLR4-XBP1 hypothesis of Zhx2 regulation is also intriguing [2, 3], and can be tested in vitro using cell culture to determine if this is a pathway that results in Zhx2 activation.

In addition to our findings on the role of Zhx2 in atherosclerosis, studies have also described an involvement of Zhx2 with various types of cancer, notably those of the liver [4, 5] and lymphoma [6], and as a transcriptional repressor of developmental genes [7-9]. Based on these reports and the fact that Zhx2 is ubiquitously expressed [10], it seems possible that Zhx2 could function as a master regulator of many different processes, and studies on this transcription factor could lead to many novel findings in a variety of fields.

The MAEC RNA isolation, treatment, and isolation method I present here provides an alternative to cell culture in the study of vascular endothelial cells. This method allowed for the transcriptional profile of cells directly from vessels of pre-atherogenic mice, something that would not have been possible using cell culture. The 14 candidate genes identified provide interesting leads into the endothelial dysfunction that precedes atherosclerosis. We have a large database of HAEC expression and genotype data gathered from over 100 different donors [11], and could begin by observing differential expression of these candidates in these data. I believe this method for MAEC isolation will aid the study of endothelial cells in general, as it will be possible to assess the transcription of endothelial cells in different strains of mice under various in vivo and in vitro conditions.

In the near future, animal models of human disease will become even more important, as GWAS has provided, and will most likely continue to provide, an

abundance of disease-associated genetic loci with little additional information on the genes identified. The integration of data from human and animals will become vital as we work to understand the large sets of data made possible by recent advances in technology and computer science. The arrival of next-generation sequencing [12] has already begun to add to this explosion in data volume, and will require more efficient and careful experimental design of wet-lab and animal studies to follow up and confirm the large amounts of data gathered. Experiments such as the assessment of GWAS candidate genes in the vascular cell types involved in atherosclerosis that I present here provide information that can help interpret results of large-scale studies such as GWAS and guide future experiments. In fact, these studies are part of a LeDucq Transatlantic Networks of Excellence in Cardiovascular and Neurovascular Research grant studying the expression of GWAS candidate genes in various cells and tissues from human and mice.

During my time as a graduate student, it was necessary for me to acquire a variety of different skills in order to accomplish my research goals. Not only did I need to learn how to work with and perform surgical dissections on mice and isolate a variety of different cell types from these animals, I also needed to step outside of traditionally-defined genetics and molecular biology boundaries and learn statistics and data processing using computer programming. I found myself applying methods and ideas to my work that I had not expected when beginning the project. However, I eventually learned to be flexible and open-minded when interpreting results and planning

experiments, a quality that I believe has allowed for more comprehensive conclusions from my research and more promising future applications of my work.

This experience has taught me that as technology advances the strict classification of research fields is becoming more obsolete, and can even serve as a hindrance for investigators that may be fearful of stepping outside of their area of expertise. In order to fully take advantage of new advances and solve difficult problems, scientists must be open to the application of novel ideas to existing problems. I recall being in my high school Biology AP class in 1997 when we were introduced to the revolutionary new DNA chip that would allow for unprecedented findings in genetics and medicine. Now, just 15 years later, microarrays are considered the conservative option in comparison to next-generation sequencing technology, which bring new challenges in data analysis along with its remarkable benefits. The ever-increasing speed at which science evolves demands collaboration among labs, scientific areas, and disciplines; researchers can no longer isolate themselves in one rigidly-defined field. Scientists who embrace new concepts and collaborations will have a definite advantage in moving forward towards new discoveries.

As I was writing this dissertation, my father sent me a quote from Future Shock by the futurist Alvin Toffler. In this book about post-industrial technological society, Toffler recalls a conversation he had with another futurist, the psychologist Herbert Gerjuoy, who said: "The new education must teach the individual how to classify and reclassify information, how to evaluate its veracity, how to change categories when necessary,

how to move from the concrete to the abstract and back, how to look at problems from a new direction — how to teach himself. Tomorrow's illiterate will not be the man who can't read; he will be the man who has not learned how to learn." I found this idea to be just as relevant, if not more, in 2012 as when the book was first published in 1970. Education does not end upon receiving a diploma; successful scientists must always be aware of opportunities for learning, and not be afraid of the unfamiliar and challenging. Furthermore, the areas of business and academia, considered entirely different entities a mere generation ago, can strengthen both their individual and common goals through working together and learning about the other, rather than each shying away from the unfamiliar institution.

This concept of teaching oneself to learn extends from the arena of scientific research into our greater society as well. The internet age has allowed for the availability of unlimited amounts of information - and misinformation. For example, medical knowledge is now much more readily available to the layperson than in previous years, and companies such as 23andMe provide genotype information to anyone with $299 to spare, leaving it largely up to to consumer to interpret these results. While this knowledge can be incredibly useful, it can also be dangerous and unethical when not understood properly. There is also the frightening possibility for even basic scientific concepts to be misunderstood by the general public. This seemingly benign ignorance has a potential for negative repercussions on our society, as with the refusal to acknowledge global climate change and the bogus assertions that the birth

control pill causes death of a fetus. We should place a higher value on life-long education, critical thinking, and the scientific method for the benefit of our society.

Bibliography

1. Park, P.J., *ChIP-seq: advantages and challenges of a maturing technology.* Nature reviews. Genetics, 2009. **10**(10): p. 669-80.
2. Martinon, F., et al., *TLR activation of the transcription factor XBP1 regulates innate immune responses in macrophages.* Nature immunology, 2010. **11**(5): p. 411-8.
3. Nagel, S., et al., *Transcriptional deregulation of homeobox gene ZHX2 in Hodgkin lymphoma.* Leukemia research, 2011.
4. Peterson, M.L., C. Ma, and B.T. Spear, *Zhx2 and Zbtb20: novel regulators of postnatal alpha-fetoprotein repression and their potential role in gene reactivation during liver cancer.* Seminars in cancer biology, 2011. **21**(1): p. 21-7.
5. Yue, X., et al., *Zinc Fingers and Homeoboxes 2 Inhibits Hepatocellular Carcinoma Cell Proliferation and Represses Expression of Cyclins A and E.* Gastroenterology, 2012.
6. Nagel, S., et al., *t(4;8)(q27;q24) in Hodgkin lymphoma cells targets phosphodiesterase PDE5A and homeobox gene ZHX2.* Genes, chromosomes & cancer, 2011. **50**(12): p. 996-1009.
7. Perincheri, S., et al., *Hereditary persistence of alpha-fetoprotein and H19 expression in liver of BALB/cJ mice is due to a retrovirus insertion in the Zhx2 gene.* Proceedings of the National Academy of Sciences of the United States of America, 2005. **102**(2): p. 396-401.

8. Hystad, M.E., et al., *Characterization of early stages of human B cell development by gene expression profiling.* Journal of immunology, 2007. **179**(6): p. 3662-71.

9. Wu, C., et al., *ZHX2 Interacts with Ephrin-B and regulates neural progenitor maintenance in the developing cerebral cortex.* The Journal of neuroscience : the official journal of the Society for Neuroscience, 2009. **29**(23): p. 7404-12.

10. Kawata, H., et al., *Zinc-fingers and homeoboxes (ZHX) 2, a novel member of the ZHX family, functions as a transcriptional repressor.* The Biochemical journal, 2003. **373**(Pt 3): p. 747-57.

11. Romanoski, C.E., et al., *Systems genetics analysis of gene-by-environment interactions in human cells.* American journal of human genetics, 2010. **86**(3): p. 399-410.

12. Metzker, M.L., *Sequencing technologies - the next generation.* Nature reviews. Genetics, 2010. **11**(1): p. 31-46.